8-2014

Mechanisms of Astrocyte Contribution to Bortezomib-Induced Peripheral Neuropathy

Caleb R. Robinson

Recommended Citation

MECHANISMS OF ASTROCYTE CONTRIBUTION TO BORTEZOMIB-INDUCED

PERIPHERAL NEUROPATHY

by

Caleb Robert Robinson, B.S.

APPROVED:

_____

Patrick Dougherty, Ph.D.
Supervisory Professor

_____

Edgar Walters, Ph.D.

_____

Carmen Dessauer, Ph.D.

_____

Zhizhong Pan, Ph.D.

_____

Hongzhen Hu, Ph.D.

APPROVED:

_____

Dean, The University of Texas
Graduate School of Biomedical Sciences

MECHANISMS OF ASTROCYTE CONTRIBUTION TO BORTEZOMIB-INDUCED

PERIPHERAL NEUROPATHY

A DISSERTATION

Presented to the Faculty of
The University of Texas
Health Science Center at Houston
and
The University of Texas
M. D. Anderson Cancer Center
Graduate School of Biomedical Sciences
in Partial Fulfillment
of the Requirements
for the Degree of
DOCTOR OF PHILOSOPHY

By

Caleb Robert Robinson, B.S.

Houston, Texas

August, 2014

DEDICATION

This work is dedicated to the LORD, my God, to whom I owe everything, and to my parents and my wife, Melissa, for the unending support that they have given me.

ACKNOWLEDGEMENTS

I would like to thank my advisor, Dr. Patrick Dougherty, for taking me into his lab at a time when I had few options available to me, for his patience and guidance in training, and for both academic and financial support in the span of time that I have spent in his lab. Investigators who place such emphasis on the success and interests of their trainees are entirely too few.

I would also like to thank my committee members for their involvement and guidance in the process of my dissertation research. In addition to Dr. Dougherty, I thank Dr. Carmen Dessauer, Dr. Zhizhong Pan, Dr. Hongzhen Hu, and in particular Dr. Edgar T. Walters, who has served on each of my committees throughout my graduate studies and served as the chair of my candidacy exam.

Finally, I would like to thank my family, including both the one that I was born into and the one that I married into, and the members of the Memorial Church of Christ for all of their continued prayers throughout this process. Without all of the love and support that I have had throughout my graduate studies, I would have had an infinitely heavier load to bear.

MECHANISMS OF ASTROCYTE CONTRIBUTION TO BORTEZOMIB-INDUCED PERIPHERAL NEUROPATHY

Caleb Robert Robinson, B.S.

Advisory Professor: Patrick M. Dougherty, Ph.D.

Bortezomib is a proteasome inhibitor used in the treatment of multiple myeloma and other non-solid malignancies, alone or in combination with other chemotherapy drugs. Like other chemotherapeutic agents, bortezomib treatment is frequently accompanied by chemotherapy-induced peripheral neuropathy (CIPN) that may be dose-limiting, adversely affecting quality of life and prognosis. The mechanisms behind bortezomib-induced peripheral neuropathy (BIPN) and CIPN overall are largely unknown. Recent findings in other pain models have indicated substantial involvement of glial cells in chronic pain. Although injury models have shown activation of both astrocytes and microglia following insult, research in other CIPN models has shown astrocytic activation in the absence of microglial activation. The central hypothesis of this dissertation is that the activity of astrocytes is correlated with behavioral changes observed in a rat model of BIPN in a manner that may directly contribute to these changes in behavior. To investigate this, the work of this dissertation 1) established the multimodal changes to behavior and showed increases in spinal neuron firing in BIPN, 2) quantified activity of astrocytes and whether changes were prevented by minocycline, an anti-inflammatory drug that

prevents glial activation, and 3) quantified changes in connexin 43, GLT-1, and GLAST to assess whether astrocytic glutamate transport may be altered in BIPN. The results observed in the first aim were that the rat BIPN model is characterized by selective mechanical hypersensitivity and a significant increase in wide dynamic range (WDR) neuron firing rates and after-discharges. In the second aim, astrocytes in the BIPN model were activated in a manner that paralleled the behavioral changes. Animals co-treated with minocycline resembled saline-treated animals in both astrocytic activation and behaviors. The results in the third aim were that astrocytic gap junctions were increased and GLAST expression was decreased at the height of mechanical sensitivity. Minocycline-treated animals resembled saline-treated animals in expression of these proteins, as well. The overall conclusion was that astrocyte activity closely paralleled behaviors in the BIPN model in a manner that may be explained by their role in glutamate trafficking.

TABLE OF CONTENTS

LIST OF TABLES AND FIGURES

ABBREVIATIONS

CIPN   Chemotherapy-induced peripheral neuropathy

BIPN   Bortezomib-induced peripheral neuropathy

GFAP   Glial fibrillary acidic protein

OX-42   Clone OX-42 of cluster of differentiation molecule 11b (CD11b)

GLT-1   Glutamate transporter 1

GLAST   Glutamate aspartate transporter

Cx-43   Connexin 43

1.   GENERAL INTRODUCTION

1.1.   Neuropathic Pain

Chronic pain is a widespread and significant problem with regard to quality of life, medical care costs, and loss of productivity at work. Neuropathic pain is a phenomenon distinct from other forms of pain in that it is caused by damage or insult directly to the nerves or CNS, often without inflammation or damage to the surrounding tissue (Jay and Barkin, 2014). Instead, neuropathic pain is a condition that develops independently within nerves or lingers after tissue damage has recovered due to damage, toxicity, or other insult directly to a part of the somatosensory tract (Treede et al., 2008, Baron, Binder, and Wasner, 2010). The pain may be classified as spontaneous pain in the absence of an identifiable stimulus, increased sensitivity to painful stimuli (hyperalgesia), or painful sensations to otherwise non-noxious stimuli (allodynia) (Costigan, Scholz, and Woolf 2009; Jay and Barkin, 2014). Furthermore, neuropathic pain is not limited to one modality, but may include altered sensitivity to thermal (heat or cold) and mechanical stimuli (Baron, Binder, and Wasner, 2010). Changes in sensitivity to stimuli may also take the form of spontaneous numbness, tingling, burning, or shooting sensations that occur as a result of maladaptive persistent firing in affected neurons (Freynhagen and Bennett, 2009; Baron, Binder, and Wasner, 2010). Neuropathies may include altered sensory symptoms alone, although individuals with neuropathy may also show a degree of fine or gross motor ability impairment that may interfere with daily

living (Casellini and Vinik, 2007). However, this profile may vary depending on the type of neuropathic pain, and not all forms of sensory neuropathy also exhibit motor neuropathy. This in itself is sufficient to suggest that neuropathic pain should be treated as a class of distinct conditions that may present similar symptoms through the differing mechanisms.

Among various classes of neuropathies that may present with sensory symptoms are injury-induced neuropathy, diabetic neuropathy, alcoholic neuropathy, and chemotherapy-induced peripheral neuropathy (CIPN) (Gregory et al., 2013), although this list is not exhaustive. Injury-induced neuropathies may be induced via damage to peripheral sites, such as the primary afferent nerve or dorsal root ganglion, or central sites, such as the spinal cord. Whereas the first category presents with deficits localized to the dermatome associated with the injury, damage directly to the spinothalamic tracts in the spinal cord produces deficits starting at a level of the body and extending downward (D'Angelo et al., 2013). Systemic neuropathies may affect multiple regions of the body, but a "stocking and glove" distribution (hands and feet) is most common (Brix Finnerup, Hein Sindrup, and Staehelin Jensen, 2013). The reason behind this is not fully clear, but it could be that peripheral nerve lengths or nerve fiber densities within the skin are linked to the distribution of neuropathy. Longer nerves would be more sensitive to demyelination, axonal degradation, or changes to conduction velocity that could drive maladaptive or persistent signaling. Alternatively, dying back of intra-epidermal nerve fibers (IENFs) in skin could result in initial painful sensations at moderate levels of denervation, with numbness occurring as the region approaches complete

denervation. If there is a release of neuropeptides or other signaling molecules that could explain sensitization of neurons, then the recruitment of a greater cohort of nerve endings could produce a more pronounced response of this kind. Since the stocking-and-glove regions of the body possess relatively lower number of free nerve endings when compared with other regions of the extremities in healthy control subjects (Boyette-Davis et al., 2011b; Mancini et al., 2013), these would then be most susceptible. Indeed, not only has IENF loss been linked to multiple types of neuropathy, but the loss of IENFs has been reported to be most pronounced in those areas with the most pronounced painful symptoms (Petersen et al., 2000; Boyette-Davis et al., 2011b; Jay and Barkin, 2014). However, the reason for the stocking-and-glove distribution may vary based on the mechanisms driving the specific type of neuropathy, and evidence is still lacking to determine a cause.

Treatment options for neuropathies that present with painful symptoms are limited. Because the various causes of neuropathy are not well understood and may not act through a single common pathway, the best option currently available is simply to treat the pain symptoms, rather than to address the cause. There are currently a multitude of drugs that are being investigated for this purpose, including gabapentin, pregabalin, tricyclic antidepressants, and serotonin-norepinephrine reuptake inhibitors, but the most effective treatment option is chronic administration of strong opioids (Attal, 2012). However, this option comes with the obvious possibility of tolerance, addiction, or abuse, and there is a clear need for a better solution. Furthermore, there is emerging evidence that chronic opioid treatment may result in the development of opioid-induced hyperalgesia that could worsen

neuropathic pain sensation in the long run (Brush, 2012). It is therefore critical to try

to identify methods for reversing or preventing neuropathy, whatever the cause may

be. Unfortunately, injury-based neuropathies cannot be predicted, and preventative

treatment is thus impossible. While diabetes and alcoholism are risk factors for the

development of neuropathic pain, these conditions also do not provide a means for

pinpointing the onset of neuropathy. At best, diabetic and alcoholic neuropathy can

be identified early on, and attempts may be made to curtail worsening symptoms.

However, chemotherapy-induced peripheral neuropathy is unique among

neuropathies in that the insult that induces neuropathy is scheduled by appointment.

It is therefore a promising system for studying neuropathic pain as a whole and for

developing methods for its prevention and reversal. It is not currently known if there

are common mechanisms that govern CIPN and other forms of peripheral

neuropathy, but the prospect of finding treatments in CIPN that may translate to

other forms of neuropathy and chronic pain certainly warrants further study.

1.2.   Chemotherapy-Induced Peripheral Neuropathy

Chemotherapy-induced peripheral neuropathy is a treatment-emergent side

effect of regular chemotherapy treatment with paresthesias and neuropathic pain as

the most common symptoms (Argyriou et al. 2014). While this form of neuropathy

may also impact motor ability or autonomic function, these side effects are limited to

certain drugs and generally emerge as sensory symptoms worsen. The severity of

the neuropathy varies by patient and by total cumulative dose, but may emerge after

as little as a single cycle of treatment (Argyriou, Iconomou, and Kalofonos, 2008; Tofthagen, McAllister, and McMillan, 2011; Boyette-Davis et al., 2012). Usually the course of the neuropathy is simply monitored at Grade 1 peripheral neuropathy (mild paresthesias/partial loss of deep tendon reflexes), but progression to Grade 2 peripheral neuropathy (severe paresthesias/absent deep tendon reflexes with mild impairment of daily activity) frequently results in dose reduction, and progression to Grade 3 (disabling sensory loss/paresthesias that severely impair normal activity) or Grade 4 (permanent loss of sensory function or paralysis) peripheral neuropathy often necessitates termination of treatment altogether (Postma and Heimans, 2000; Miltenburg and Boogerd, 2014). Painful symptoms may also necessitate the termination of treatment if symptoms do not respond to conventional treatments. CIPN is therefore a concern for not only quality of life in patients receiving chemotherapy treatment, but is also a concern with regard to patient survival outcomes when patients must reduce treatment to levels below effective doses to treat cancer or cease treatment altogether.

Most studies regarding the clinical presentation of CIPN focus on patient-reported sensations in order to evaluate symptoms and severity. Although these measures are easy and convenient to obtain, they may vary widely from one patient to another, especially with regard to an individual's sensitivity to pain or biases in reporting. The development of quantitiative sensory testing measures has been instrumental in implementing objective measures for the evaluation of patient CIPN, and work has been carried out to characterize this in vincristine, taxol, and bortezomib-induced peripheral neuropathy at this time (Cata et al., 2007; Dougherty

et al., 2007; Boyette-Davis et al., 2011a; Boyette-Davis et al., 2013). The findings of these studies (summarized in Table 1) have demonstrated a trend in loss of sensation within affected areas across all of these drugs. This suggests the possibility of a central governing mechanism behind CIPN, although this cannot yet be verified. Furthermore, these studies provide a means by which preclinical experiments may be checked against the clinical presentation, as analogous behavioral measures exist within animal models for most of the same affected modalities. This may further help in translational studies moving forward to identify how preventative treatments identified in animals affect patients and whether patients show objective improvement in symptoms.

	Vincristine	**Paclitaxel**	**Bortezomib**
Most common Descriptors	Numbness, tingling, throbbing, burning, sharp	Numbness, tingling, burning	Numbness, tingling, burning
Affected regions	Hands and feet, primarily in fingers and toes	Hands and feet, primarily in fingers and toes	Hands and feet, primarily in fingers and toes, more severe in lower extremities
Affected modalities	Crude touch, sharp touch, thermal, fine motor	Crude touch, sharp touch, thermal, fine motor	Crude touch, sharp touch, thermal, cold, fine motor

Table 1. Quantitative sensory testing (QST) and patient-reported symptoms in patients treated with vincristine, paclitaxel, or bortezomib

1.3.   Rat Models of Neuropathy

Neuropathic pain can be modeled in rats in a number of ways, but the most common of these is through direct injury to the spinal cord or peripheral nerve through surgical means. The spinal cord may be directly injured via contusion from the drop of a small weight (Gruner, 1992) or by surgical section or hemisection (Vierck, Hamilton, and Thornby, 1971; Levitt and Levitt, 1981; Christensen et al., 1996). Alternative means of spinal cord injury may include laser irradiation to induce ischemic injury (Hao et al., 1991) or microinjection of quisqualic acid to induce excitotoxicity (Yezierski et al., 1993). These models produce spontaneous behaviors interpreted as painful and evoked mechanical and thermal hyperalgesia, but targeting the spinal cord is less precise than targeting a peripheral nerve, which allows localization to a single dermatome and is less likely to induce unwanted motor deficits. Injury models at the peripheral nerve are also simpler procedures and less invasive, usually being based on tying a ligature around some point of the nerve. These differ mostly in their location, with spinal nerve transection (SNT) and spinal nerve ligation (SNL) at the segmental nerve root of one or more nerves composing the sciatic nerve (Ringkamp et al., 1999; Kim and Chung, 1992), chonic constriction injury and partial nerve transection at the common sciatic nerve (Bennett and Xie, 1988; Seltzer, Dubner, and Shir, 1990), and spared nerve injury (SNI) targeting two branches of the sciatic nerve (Decosterd and Woolf, 2000). Like the models that target the spinal cord directly, these injury models also produce robust mechanical and thermal hyperalgesia.

Alcoholic neuropathy is usually modeled either through replacement of water with an ethanol solution (Juntunen et al., 1978) or through chronic administration of ethanol via oral gavage, which is beneficial for standardizing alcohol consumption between animals (Kandhare et al., 2012). Diabetic neuropathy may be modeled through genetic knockout mice (including, but not limited to knockouts for insulin 1 (Ins.Dd1) or insulin 2 (C57BL/6-Ins2Akita/J) expression) or through injection of streptozotocin, although which genes are targeted and what dose of streptozotocin is used may vary distinctly from one study to another (Sullivan et al., 2008). These neuropathies may be characterized by hyper- or hypoalgesia with regard to mechanical and/or thermal stimuli, once again varying by drug dose and genetic knockout. Chemotherapy-induced peripheral neuropathy is modeled by systemic injection of chemotherapeutic agents on schedules that may vary from one protocol to another. Affected modalities vary based on drug and are discussed in more detail later.

One drawback of modeling neuropathic pain in animals is the lack of distinction between painful sensations and non-painful sensations (e.g. tingling) when using the reflex measures commonly employed in these models. Whereas other types of pain (such as inflammatory pain) are not accompanied by these types of paresthesias, direct insults to the nerve commonly produce numbness and tingling in humans (Kim and Kim, 2012; Lau and Stavrou, 2004). It is therefore possible in any of these animal models that hyper-reflexive responses may occur in response to such sensations. However, there is currently no commonly-used method to distinguish between these sensations in animal models. This is a concern that

should be considered in the design of any experiment, and care must be taken to ensure that interpretations of observations are not dependent on the animal feeling pain instead of some form of non-painful paresthesia.

1.4.   The Proteasome and Its Inhibition by Bortezomib

Among the many drugs that may induce chemotherapy-induced peripheral neuropathy is bortezomib, a drug that targets the activity of the proteasome. It is unclear at this time whether bortezomib may have additional targets, but it was developed for its action with regard to the proteasome. The 26S proteasome is the major proteolytic structure in the majority of human somatic cells, consisting of two 19S regulatory subunits and a 20S subunit that is capable of degrading any misfolded, obsolete, or otherwise unnecessary proteins within the cell (Bhattacharyya et al., 2014). The 19S subunit of the proteasome detects poly-ubiquitylated tails that are attached to these proteins through the activity of ubiquitin ligases, then passes them into the pore of the tube-shaped 20S subunit. This 20S subunit can degrade proteins into constituent amino acids through trypsin-like, chymotrypsin-like, or peptidyl-glutamyl-peptide bond hydrolyzing activity, based on which active site the ubiquitylated protein is capable of binding (Schreiber and Peter, 2014). Because these sites are located on the interior of the 20S subunit pore, only proteins recognized by the 19S subunit come into contact with them. Once the protein is digested by the activity of these catalytic sites, the constituent amino acids are then available for protein synthesis within the cell once more.

In addition to maintaining functionality of the cell by degrading inappropriate proteins, the proteasome is also important for maintaining the balance of proteins related to regular cell function. Progression of the cell cycle requires the activity of the proteasome to degrade certain proteins that keep the cell in its current growth phase. For example, the anaphase promoting complex (APC), a type of ubiquitin ligase, is responsible for ubiquitylating a host of substrates that appear to be necessary for anaphase to occur during cell division (Merbl and Kirschner, 2009). It is not fully understood which of these substrates are necessary for mitosis to proceed, as the substrates of the APC include a diverse array of cellular proteins. However, the necessity of a ubiquitin ligase in the progression of the cell cycle is also sufficient to implicate the proteasome as necessary for it to occur. This may not be a contributing factor in the context of CIPN, but is thought to be one possible mechanism for bortezomib's anti-tumor activity. The APC is not the only ubiquitin ligase involved in the cell cycle, but many types of E1, E2, and E3 ubiquitin ligases are needed in order for the cell cycle to progress, with only a handful that have been identified at this time in tumor progression out of several hundred ubiquitin ligases (Mattern, Wu, and Nicholson, 2012). The proteasome is therefore vital in all of these cases, governing many stages in the life of a cell and serving as a common ground to target a multitude of diverse and poorly-understood mechanisms simultaneously.

It is based largely on this role in driving the cell cycle that the proteasome was identified as a target for chemotherapy, and this is one of the means by which bortezomib is thought to affect tumor progression. Most somatic cells in adults do not require frequent cell cycle turnover, but cancer cells are highly proliferative.

However, the developers of bortezomib also recognized several other means by which it may act to sensitize or kill cancer cells. Bortezomib may have a greater effect on cancer cells in part simply because of the very high metabolic demand in malignant tissue. In support of this, bortezomib has been shown to inhibit angiogenesis by downregulating associated genes (e.g. VEGF and IL-6), stunting tumor growth and progression (Roccaro et al., 2006). Another possible explanation for bortezomib's activity is through the accumulation of the tumor suppression protein p53. Upregulation of this protein in response to potentially tumorigenic mutations results in apoptosis, and successfully proliferating tumors continually ubiquitylate p53 in order to prevent this from occurring (Melvin et al., 2013). The inhibition of the proteasome therefore may result in the accumulation of p53 and subsequent apoptosis of cancer cells. Inhibition of the proteasome also stabilizes IκB, the inhibited form of NF-κB, which must normally be degraded before NF-κB can become active (Richardson, Hideshima, and Anderson, 2003). The activity of this transcription factor is diverse, but it promotes the expression of inhibitors of apoptosis such as Bcl-2, XIAP, and suvivin and downregulates pro-apoptotic signaling from Bax (Mitsiades et al., 2002). NF-κB is constitutively upregulated in multiple myeloma cells to promote tumor survival in a manner that was prevented by bortezomib (Berenson, Ma, and Vescio, 2001; Ma et al., 2003). Endoplasmic reticulum-mediated apoptosis is another possible mechanism by which bortezomib may trigger cell death in malignant cells. While the ER may be affected by Bcl-2 signaling and therefore be tied to NF-κB regulation, it may also trigger apoptosis on its own. Accumulation of misfolded proteins at low levels triggers a pro-survival

response in the endoplasmic reticulum of cells, but when this progresses beyond a point that is manageable, the ER then triggers a pro-apoptotic signal cascade via increases in intracellular calcium (Ferri and Kroemer, 2001; Landowski et al., 2005). It seems unlikely that any one of these possibilities is the sole answer for how bortezomib acts as a chemotherapy drug. Instead, a combination of these mechanisms may work in tandem in order to induce cancer cell apoptosis or slow metastasis of the malignancy.

Bortezomib was one of several proteasome inhibitors developed with the intent of chemotherapeutic use, but it was the first to gain FDA approval for use in cancer treatment (Cavo 2006). Bortezomib targets the chymotrypsin-like activity of the 20S proteasome subunit and binds competitively to this site (Lightcap et al., 2000; Cavo 2006). It has a half-life lasting 24 hours, and proteasomal activity returns to basal levels between 72 and 96 hours following administration of bortezomib (Adams 2001). Bortezomib cannot cross the blood brain barrier and does not penetrate into the brain, spinal cord, testes, or eyes (Adams et al., 1999; Adams 2001).Bortezomib is usually administered at 1.3mg/m² or 1.0mg/m² either intravenously or subcutaneously (with equal efficacy) in cycles of 4 doses over 2 weeks, followed by a week without treatment (Arnulf et al.,2012; Zeng, Lin, and Chen, 2013). Number of cycles may then vary. Bortezomib has been proven effective in patients who are refractory and no longer responding to other forms of treatment (Richardson et al., 2003). It may be given alone in non-solid malignancies such as multiple myeloma, and single-agent treatment of bortezomib has resulted in partial responses or better in 41% of patients (Richardson et al., 2009). However, it

is also effective in increasing positive responses when used in combination with other chemotherapy drugs such as thalidomide, dexamethasone, melphalan, or prednisone (San Miguel et al., 2008; Jagganath et al., 2009; Cavo et al., 2010; Mateos et al., 2010; Arnulf et al.,2012; Zeng, Lin, and Chen, 2013). These studies have demonstrated that response rates are greater when bortezomib is employed alongside these drugs, but the incidence and severity of adverse events also increases. The most common side effects observed in bortezomib treatment include chemotherapy-induced peripheral neuropathy, neutropenia, thrombocytopenia, anemia, and diarrhea (Reece et al., 2006).

1.5.   Clinical Presentation of Bortezomib-Induced Peripheral Neuropathy

Bortezomib-induced peripheral neuropathy follows closely with the aforementioned trend of CIPN as a whole in patients: a stocking and glove distribution, poor response to pain medication, and symptoms that may necessitate reduction or cessation of treatment. However, BIPN does vary somewhat in how it presents in patients versus other forms of CIPN. Total incidence of BIPN was 35% of patients in the CREST and SUMMIT trials, with 12% of patients experiencing grade 3 or higher peripheral neuropathy (Jagannath et al., 2006). Another study reported BIPN in 40% of treated patients, with 15% of patients experiencing grade 3 or higher peripheral neuropathy (Bang et al., 2006). This was the second most common adverse event in this study, with thrombocytopenia reported at 45% of patients (38% in the first study). However, while the thrombocytopenia was transient in both

studies, returning to near-baseline levels at the end of each cycle, sensory neuropathy induced by bortezomib lingers after cessation of treatment. Some studies report a higher incidence of peripheral neuropathy, but this may be in part due to pre-existing levels of peripheral neuropathy from other forms of treatment that predispose patients to worsening treatment-emergent neuropathy (Richardson et al., 2009). The intensity of BIPN is very pronounced, even in the presence of daily pain medication, with patients reporting daily maximum pain at a mean rating of 7.8 out of 10 (Cata et al., 2007). However, incidence of painful peripheral neuropathy is generally not noted separately from that of peripheral neuropathy presenting with sensory loss or paresthesias. Regardless, dose modification guidelines do seem to have a positive impact on management peripheral neuropathy symptoms, and patients with BIPN have been reported as experiencing improvement or recovery from sensory neuropathy at a median time of 110 days (Richardson et al., 2009).

Of the studies conducted in human subjects with BIPN, few have been published relating to mechanistic studies or preventative treatment strategies. Many of these have focused on the identification of genetic factors associated with BIPN. Targets of interest to follow up on in these studies include altered expression of genes related to general immune function, TNFα, caspases, and general mitochondrial function (Broyl et al., 2010; Favis et al., 2011; Corthals et al., 2011). However, since samples were obtained from patient blood samples, it cannot be said for sure whether these changes would also be observed in nervous tissue, especially since the blood is taken from individuals treated for a hematologic malignancy. Nevertheless, these are potential targets for future research. Apart from

genetic studies, investigators have identified potential contributing factors to BIPN, including increased axonal depolarization prior to full onset and reduced levels of soluble BDNF in blood (Nasu et al., 2014; Azoulay et al., 2014), but these findings have not yet been validated.

Comparatively little is known about BIPN in patients for several reasons. First of all, the drug has only been on the market for about 10 years. Taken together with the fact that it is the first proteasome inhibitor approved for use in the treatment of cancer, there has been less time for research into the causes and effective treatment of BIPN versus the CIPN induced by other drugs. Second, the survival times for multiple myeloma patients are poor, even with bortezomib treatment. This makes it difficult for investigators to follow up on long-term effects and recovery in clinical trials. Furthermore, there is still little to no standardization of the evaluation of CIPN as a whole. Whereas the bulk of studies and clinical assessments rely on patient-reported symptoms and questionnaires that may be biased, a mere handful of researchers have attempted objective quantifications in BIPN (Richardson et al., 2006; Cata et al., 2007; Boyette-Davis et al., 2011a). Apart from these studies, there is little reliability in identifying and assessing the severity of BIPN from one patient to the next. Preclinical animal studies in a BIPN model would be an attractive means of studying BIPN not only because of the greater potential for controlled mechanistic studies, but also because of widely-implemented objective behavioral measures that allow for reliability in replicating and following up on findings from other studies.

1.6.   Current Findings in Animal Models of Bortezomib-Induced Peripheral Neuropathy

Animal studies in BIPN have been relatively few when compared against other classes of chemotherapy drugs. Part of this is no doubt due to the relative novelty of proteasome inhibitors as chemotherapeutic agents. The single most prolific contributor to what research currently exists is the Cavaletti lab. The first major study in animals by this group did not include any behavioral measures, but reported decreases in tail nerve conduction velocity and damage to Schwann cells and DRG (Cavaletti et al., 2007). However, the doses used in this study were much higher than those given to patients. It is therefore uncertain how much of the reported damage is directly linked to BIPN and how much may be due to excessive toxicity. Furthermore, a follow-up study examining the myelin within these Schwann cells found that bortezomib produced no difference in myelination and a great deal of variability between individuals (Gilardini et al., 2012). This should also call into question whether or not the purported axonopathy and changes to nerve conduction velocity are valid. A recent paper published by the Cavaletti lab demonstrated increased mechanical sensitivity and firing rates of WDR neurons in the absence of changes in response to thermal or cold stimuli (Carozzi et al., 2013). This study also claimed to demonstrate changes in nerve conduction velocity and axonal degeneration, but the changes observed were not robust in the former and were completely absent of any quantification in the latter. Nevertheless, the other findings are in agreement with what has been found in our own lab in a rat model. Another recent study from this lab has investigated potential molecular changes in the

bortezomib model in spinal cord and dorsal root ganglia (Quartu et al., 2014). The study showed increases in levels of TRPV1, CGRP, and substance P, but there were several concerns present within the data. First, this study included only a single behavioral time point apart from baseline which showed an elevation of threshold in control animals, rather than an increase in sensitivity in bortezomib-treated animals. The difference between the two groups was modest, at best, and adding additional time points may have abolished this effect. There was also a reciprocal down-regulation of mRNA expression for proteins that showed greater expression in other measures that was explained as a possible effect of the proteasome. It is unclear whether or not this would be the case without further study. Also, representative Western blots showed inconsistency in GADPH control bands, as well as several GADPH bands which clearly came from different blots than the accompanying bands for TRPV1. RT-PCR had similar issues. Finally, the quantification of immunohistochemistry showed modest changes with overlapping error bars in every case, making the claims of significance using t-tests possible, but suspicious. This should not suggest that the changes observed do not occur, but that the major issues within the data necessitate follow-up research to verify the findings of this study.

An earlier study from Bennett's lab using rats differs in its results from Cavaletti's work in that no axonal degradation was observed, but cold hyperalgesia was reported (Zheng, Xiao, and Bennett, 2012). This study also reported mitotoxicity in primary afferents and used this as the proposed mechanism driving BIPN. However, patients often report neuropathic pain symptoms in BIPN without any

muscular weakness, and other mitochondria-dense regions such as the eyes are unaffected. Another group has reported cold sensitivity after a single dose of bortezomib treatment, as well as a prevention of both mechanical and cold sensitization in TRPA1 knockout mice (Trevisan et al., 2013). However, the paper also reported that bortezomib does not directly activate or alter expression of TRPA1 receptors, and how mechanosensation would be affected by a TRPA1 knockout is unclear.

Surprisingly, only a few preventative treatments have been investigated for the treatment of BIPN in animals. However, one study of interest identified TNF-α and IL-6 as potential therapeutic targets within the dorsal root ganglion (Alé et al., 2014). Levels of TNF-α and IL-6 were reported to be higher in the DRG of bortezomib-treated animals than controls, and antibodies against these were successful in preventing the development of a change in behavior and preventing their upregulation. This finding provides evidence in support of a mounting theory in neuropathy as a whole, that proinflammatory signals are necessary and possibly even sufficient to drive peripheral neuropathy. Furthermore, a signal cascade beginning with a proinflammatory signal in the dorsal root ganglion could be sufficient to induce changes observed in the spinal cord, as it has been established that bortezomib cannot cross the blood-brain barrier (for further discussion, see Conclusion). However, the fact remains that there is at this time a general paucity of research in animal models of bortezomib-induced peripheral neuropathy, and there is little agreement between researchers as to what may drive the observed condition that is modeled.

1.7.   Glial Involvement in Neurotransmission

Glia are commonly thought to contribute to neuronal cell function in ways that do not directly involve them in neuronal synaptic transmission. This should not suggest, however, that they do not play an important role in this process. Taking into consideration their role as modulators of inflammatory immune function, microglia are prevalent in many situations of insult, injury, or otherwise negatively altered function (Graeber, 2010; Smith, 2013; Eyo and Dailey, 2013). Astrocytes, the glial cells responsible for neurotransmitter recycling and metabolite production for nearby nerve terminals, have a clear role synaptic sensitization. First of all, astrocytes express multiple types of neurotransmitter receptors, including many that are relevant to neuropathic pain, such as substance P receptors, NMDA receptors, and metabotropic glutamate receptors (Porter and McCarthy, 1997). These are sufficient to drive astrocyte activation in response to high levels of synaptic neurotransmitters. Astrocyte activation is characterized by changes such as increased GFAP surface marker expression, increased connexin 43 expression, and decreased expression or function of the glutamate transporters GLT-1 and GLAST. GLT-1 and GLAST are responsible for clearing neurotransmitter from the synapse following a synaptic event, and loss of function in these may have stark effects on synaptic transmission (Samuelsson et al., 2000; Vandenberg and Ryan, 2013; Nicholson, Gilliland, and Winkelstein, 2014). Decreased glutamate transporter function results in lingering amounts of glutamate within the synapse. This increases the probability of an action potential, and greater levels of glutamate transporter dysfunction can even result in persistent firing of the postsynaptic cell (Campbell and Hablitz, 2004). There is even

some recent evidence concerning a greater role for astrocytes with regard to synaptic events: the binding of glutamate onto astrocyte glutamate receptors results in elevated intracellular Ca^{2+}, which may be followed by subsequent release of glutamate from the astrocyte itself (Parpura et al., 1994; Haydon, 2001; Nie, Zhang, and Weng, 2010). It is furthermore possible for this glutamate release into the synaptic cleft to be sufficient to create an excitatory postsynaptic potential (Parpura and Zorec, 2010). This has been termed "gliotransmission," but the concept is still relatively new and not widely accepted. Even so, it is apparent that sensitization of synapses such as may be the case in chronic pain may be due in part to a positive feedback loop between astrocytes and neurons. Increased signaling may drive astrocyte activation, which may result in decreased glutamate transport and therefore foster greater signaling.

The importance of glutamate transport with regard to regular synaptic events is clear. Furthermore, it indicates a possible role for astrocytes with specific regard to chronic pain sensitization. There is evidence within the spinal cord that a type of central sensitization which could be induced by these glutamate transporters occurs in dorsal horn neurons. Spinal cord wide dynamic range (WDR) neurons show increased firing rates and persistent after-discharges in both injury and chemotherapy-based neuropathic pain models in response to both noxious and non-noxious stimuli (Yakhnitsa, Linderoth, and Meyerson 1999; Sotgiu and Biella 2000; Weng, Cordella, and Dougherty, 2003; Cata, Weng, and Dougherty 2006). The increased firing in response to non-noxious stimuli provides a strong argument for central sensitization occurring, and the persistent after-discharges likely indicates

20

persistent synaptic glutamate. Importantly, the same types of stimuli that show altered behavioral responses in these studies evoked these kinds of enhanced and persistent responses from WDR neurons, indicating a link between the two.

Although microglia are not usually thought of as directly impacting synaptic transmission, their inflammatory activity may play a role in sensitization of neurons. However, it seems that this is not a unique aspect of microglia, but something that astrocytes may contribute to, as well. Following activation of astrocytes or microglia, either of these cell types will increase transcription of proinflammatory cytokines and chemokines via p38, JNK, or ERK MAPK signal cascades (Milligan and Watkins, 2009). The transcription and subsequent release of cytokines and chemokines such as IL-1β, IL-6, TNFα, CCL2, CCL7, and PGE$_2$ from astrocytes and microglia serve not only to induce further glial activation, but also bind to receptors on nearby neurons to sensitize neurons directly (Watkins, Milligan, and Maier, 2001; Marchand, Perretti, and McMahon, 2005; Gao and Ji, 2010a; Huang et al., 2014; Zhu et al., 2014).

Any effect that astrocytes may have on synaptic transmission, neuronal sensitization, or inflammatory activity may be further exacerbated by communication between astrocytes. In order for astrocytes to communicate in a unified network, they form a functional syncytium with the other astrocytes around them via gap junctions composed of connexin 43 (Cx43) in gray and white matter and connexin 30 (Cx30) in the gray matter alone (Nagy and Rash, 2000). This allows for the propagation of signals between astrocytes, such as the conduction of intracellular Ca^{2+} that allows for direct release of glutamate (Giaume and Venance, 1998). In

circumstances of insult or injury, the permeability of these gap junctions increases, and the connexins themselves become upregulated (Chew et al., 2010; Wu et al., 2012). Not only does this increase transmission of Ca^{2+} between astrocytes, but it is also accompanied by the propagation of prostaglandins and other inflammatory mediators that result in a vasodilatory response (Wu et al., 2012). The combined potential for increased glutamate release and inflammatory responses that could sensitize neurons or induce cytotoxicity make Cx43 an attractive target in the context of neuropathic pain. Inhibition of Cx43 has correlated with the prevention of the development of pain and neuronal cell death in multiple models, including CCI, sciatic inflammatory neuropathy, mustard oil-induced inflammatory pain, focal cerebral ischemia, and SCI (Spataro et al., 2004; Chew et al., 2010; Chiang et al., 2011; Wu et al., 2011; Wu et al., 2012). Although these findings have largely been restricted to injury-based models, our own lab has been successful in preventing oxaliplatin-induced peripheral neuropathy using the gap junction decoupler carbenoxolone (Yoon et al., 2013). Not only does the implication of astrocytic gap junctions in neuropathic pain provide a degree of mechanistic understanding, but it suggests a necessary role for astrocytes in the development of a neuropathic pain condition. Whether or not the findings in glutamate transporters and connexins are generalizable to all forms of neuropathy has not yet been firmly established, but the involvement of glia in neuropathic pain is becoming increasingly clear.

1.8.   Minocycline as an Anti-Inflammatory Drug

Minocycline is a tetracycline derivative that was originally developed for its use as an antimicrobial drug, but it soon became clear that minocycline had potential for a broad spectrum of therapeutic uses apart from its use as an antibiotic (Garrido-Mesa, Zarzuelo, and Gálvez, 2013). Animal studies have shown positive effects resulting from minocycline treatment in multiple sclerosis, ALS, Parkinson's disease, Huntington's disease, spinal cord injury, schizophrenia, and mood disorders, although transitions into clinical trials have not been universally successful (Yong et al., 2004; Plane et al., 2010; Dodd et al., 2013). Beneficial effects were observed in brain ischemia, spinal cord injury, multiple sclerosis, and schizophrenia in clinical trials. ALS, Huntington's disease, and Parkinson's disease trials were unsuccessful. The mechanisms by which minocycline affects such a diverse array of conditions is still uncertain, but a generalized anti-inflammatory mechanism would explain its efficacy in most of these disorders. Indeed, minocycline has been shown to downregulate levels of proinflammatory cytokines such as CCL2, IL-6, and IL-1β independently of its antibiotic activity (Kielian et al., 2007; Henry et al., 2008).

The regulation of inflammatory mediators has made minocycline a subject of interest in neurodegenerative and neuropathic pain models, as inappropriate levels of inflammation contribute to neuronal cell death following injury, ischemia, infection, or other forms of insult (Beattie 2004; Hailer, 2008; Ramesh, MacLean, and Phillipp, 2013; Shastri, Bonifati, and Kishore, 2013). To this end, treatment with minocycline in both animals and patients with spinal cord injury shows promise, improving both motor function and sensory scores over time (Festoff et al., 2006; Casha et al.,

2012). Infiltrating microglial cells are a potential locus of this kind of damage, and minocycline treatment has been shown to be effective in reducing this kind of infiltration and glial activation (Zemke and Majid, 2004; Beattie 2004; Hailer, 2008). It is partly because of this activity that minocycline has gained a reputation in glial research as a selective inhibitor of microglia. However, it is important to note that the production of cytokines and chemokines targeted by minocycline includes some that are also produced by cells other than microglia, including the expression of IL-6 and CCL2 by astrocytes (Thompson and Van Eldik, 2009; Ramesh, MacLean, and Phillipp, 2013; Zhu et al., 2014). Minocycline may therefore prove effective in the treatment of disorders driven by any cell type expressing proinflammatory mediators, even in cases where there is not any observed activation of microglia. Furthermore, there is also the possibility that minocycline exerts its neuroprotective and antinociceptive effects by acting on neurons directly. It has been observed that cultured neurons treated with minocycline show depressed glutamatergic currents (Gonzalez et al., 2007), which could reduce excitotoxicity in neurodegenerative models or persistent firing observed in neuropathic pain models.

1.9. Summary

Neuropathic pain can refer to many types of maladaptive chronic pain conditions brought about by damage or insult to the nerves or the CNS. These neuropathies may occur through traumatic injury to affect a localized region, or they may be systemic, resulting in a more widespread effect. Chemotherapy-induced

peripheral neuropathy is any neuropathy that occurs as a result of chemotherapy treatment. Like other systemic neuropathies, symptoms may include a combination of painful and non-painful symptoms that are usually in a stocking-and-glove distribution. Sensory symptoms can become so severe in CIPN as to limit effective treatment. Treatments to manage these symptoms are usually not very effective. Because treatment is scheduled in advance, it may be possible to develop preventative strategies pending a better mechanistic understanding of CIPN. Bortezomib, a proteasome inhibitor drug, is one chemotherapeutic agent that can cause CIPN. Its anti-tumor activity is poorly understood, but it may exert its effects through cell cycle arrest, ER-mediated apoptosis, or several other mechanisms. Even less is known about how it may induce CIPN.

Bortezomib-induced peripheral neuropathy (BIPN) usually occurs within the first 3-5 cycles of treatment and may affect about 37% of bortezomib-treated individuals. Patients experiencing BIPN may show spontaneous numbness and tingling sensations and altered sensitivity or painful sensation to mechanical, thermal, and cold stimuli. These symptoms occur in both the hands and feet, usually with the greater effects occurring in the feet.

Recent findings in animal models suggest that there may be a correlation between CIPN and astrocyte activation. There are several means by which astrocytes may contribute to observed symptoms in CIPN, including altered activity of cytokines, gap junctions, and glutamate transporters. Such changes have been shown in other animal models of CIPN, but it is unknown if these occur in the bortezomib model, as well. One or more of these may contribute to BIPN, possibly

through modulation of signaling in the dorsal horn. Cytokines may directly sensitize

neurons or exert many other possible effects. Increases in astrocytic gap junctions

may result in increased calcium flow between cells. This may result in release of

glutamate directly from astrocytes. Decreases in glutamate transporter expression or

function could inhibit glutamate reuptake. This would foster increased or persistent

signaling within synapses. Any or all of these could create enhanced or spontaneous

sensations such as those seen in patients (Cata et al., 2007). Astrocytes therefore

have multiple potential means by which they may contribute to the BIPN model and

CIPN as a whole. Thus, the central hypothesis of the present work is that astrocyte

activation is correlated with behavioral changes in CIPN in a manner that may

contribute to these changes in behavior.

2.   CHANGES IN BEHAVIORAL RESPONSES AND WDR NEURON ELECTROPHYSIOLOGY IN BIPN

Content in this chapter is based on the following publication with permission from the publisher:

Robinson CR, Zhang H, Dougherty PM (2014) Altered discharges of spinal neurons parallel the behavioral changes shown in rats with Bortezomib related chemotherapy induced peripheral neuropathy. Brain Res pii: S0006-8993(14)00816-6.

License No.: 3414340341956

2.1.   INTRODUCTION

In order to determine whether astrocyte activity is correlated with behavioral changes in the animal model of BIPN, it was first necessary to characterize how the responses to stimuli in behavioral tests may be altered in this model. At the time that this research was conducted, it was unknown whether bortezomib treatment would produce a condition like those seen in another drug model of CIPN, or whether it would instead affect a different set of behaviors. The hypothesis of this work was therefore that treatment with bortezomib in a rat model would produce behavioral changes indicating a condition similar to the CIPN symptoms observed in patients. This was tested by conducting multiple behavioral tests representing reflexive responses to multiple types of stimuli and a test of motor ability, then verifying whether observed behaviors were supported by a corresponding alteration in stimulus-evoked neuronal responses. While behavioral changes did not match exactly with patient symptoms, bortezomib treatment in rats did produce robust

mechanical hypersensitivity that was accompanied by increased firing and after-discharges in spinal wide dynamic range neurons.

Bortezomib is a drug that was originally developed for the treatment of multiple myeloma. It was developed for its activity as a proteasome inhibitor, and it is the first such drug to be approved for use as a chemotherapeutic agent. Bortezomib treatment may occur in single-agent therapy, but it is more frequently used in combination with other drugs for increased efficacy (San Miguel et al., 2008; Kaufman et al., 2010). Although the side effects of bortezomib treatment may be diverse, chemotherapy-induced peripheral neuropathy (CIPN) is a side effect of particular concern (Aghajanian et al., 2002; Kane et al., 2006). The distribution of bortezomib-induced peripheral neuropathy (BIPN) is in what is referred to as a "stocking and glove" distribution, with greatest severity localized to fingers and toes (Cata et al., 2007). As BIPN progresses in severity, physicians may opt for dose-reduction strategies or cessation of treatment (Cata et al., 2007; Broyl , Jongen, Sonneveld., 2012). This strategy is a sub-optimal solution, as it limits the efficacy of a patient's treatment when doses are reduced. It is therefore of critical importance to obtain a greater mechanistic understanding of BIPN. Doing so would allow for the development of appropriate treatment strategies or for the prevention of BIPN altogether.

The efficacy of bortezomib as an anti-neoplastic drug was quickly apparent, and the FDA granted it fast-track approval. Bortezomib binds selectively to the proteasome, which is responsible for digesting misfolded or obsolete proteins within the cell. The proteasome consists of two subunits: a regulatory 19S subunit for

detecting ubiquitylated proteins and a 20S subunit for digesting them. Bortezomib

binds competitively to the latter of the two at its chymotrypsin-like catalytic site,

thereby preventing the normal degradation of proteins (Adams et al., 1999; Adams,

2002; Adams and Kauffman, 2004). Malignant cells are subject to a greater impact

from this inhibition from healthy cells due to a higher metabolic demand and

increased proliferative tendencies. Potential downstream effects of proteasomal

inhibition are diverse, and it is therefore unclear how exactly bortezomib exerts its

effects. One of the favored explanations is that proteasomal inhibition stabilizes

NFκB into its inactive form, IκB (Hideshima et al., 2001; Voorhees et al., 2003). The

effect of this is a blockade in cell cycle progression, preventing cancer cell

proliferation. However, it is also possible that proteasomal inhibition may trigger

apoptosis directly. Inappropriate proteins in excessive amounts put undue stress on

the endoplasmic reticulum. The ER may then trigger a cascade that results in

caspase-mediated apoptosis (Landowski et al., 2005). Bortezomib also has been

shown to directly affect p53 activity. This may then trigger cytochrome *c*-mediated

apoptosis in the mitochondria (Hideshima et al., 2003; Voorhees et al., 2003).

Furthermore, it is possible that proteasomal inhibition simply disrupts the balancing

act between pro-survival and pro-apoptotic signals in cancer cells. There are even

more possible explanations than those listed here, but any one of these would be a

plausible mechanism. A more likely explanation is that a combination of these

pathways work in concert with one another for bortezomib to produce its effects.

Judging by the diversity of proposed anti-neoplastic mechanisms in

bortezomib, it should come as no surprise that the mechanisms responsible for BIPN

are also poorly understood. Unfortunately, this also means that direct treatment strategies are severely hampered. Different chemotherapy drugs may produce differing neuropathic conditions with modality specificity. Numbness and tingling are common symptoms, but patient-reported descriptors and objective sensitivity to different types of stimuli vary between drugs (Cata et al., 2007; Dougherty et al., 2007; Boyette-Davis et al., 2012). Preclinical data across multiple modalities is therefore important before a mechanistic understanding can be reached in animal models of BIPN. The studies in animal models have been few and necessitate further study (see introduction).

It is uncertain where along the somatosensory tract BIPN originates, but it is clear that bortezomib cannot cross the blood-brain barrier (Adams, 2002). However, findings in other CIPN models have shown clear changes in spinal wide dynamic range (WDR) neuron activity (Cata et al., 2006a; Cata, Weng, and Dougherty, 2008a). Such findings indicate a possibility that some combination of glutamate transporter dysfunction and central sensitization may contribute to CIPN. If such findings are also seen in the present model, then this would explain enhanced and persistent sensations that are observed in patients with BIPN (Cata et al., 2007; Boyette-Davis et al., 2011a). Thus, the focus of the present study was twofold: first, to identify a behavioral profile of affected modalities associated with BIPN in the rat model, and second, to assess whether there is an accompanying change in spinal wide dynamic range neurons.

2.2   METHODS

2.2.1. Animals

A total of 61 male Sprague Dawley rats (Harlan) were used. Animals were housed on a 12hr/12hr light cycle and provided food and water ad libitum throughout the testing period. All efforts were taken to minimize pain and discomfort in animals, and all handling and procedures were approved by the institutional review board and in accordance with institutional ethical standards.

2.2.2. Drugs

All agents were administered by intraperitoneal (i.p.) injection at in equivalent volumes (0.7mL per injection). Pharmaceutical grade bortezomib (Velcade®, Millennium Pharmaceuticals) was diluted in saline to the desired concentration. Dosages of 0.05mg/kg, 0.10mg/kg, 0.15mg/kg, and 0.20mg/kg per injection were used in the initial behavioral characterization studies. A total of four injections of each dose were administered on days 1, 3, 5, and 7 of each study resulting in cumulative doses of 0.20mg/kg, 0.40mg/kg, 0.60mg/kg, and 0.80mg/kg per treatment. The 0.15mg/kg dose was subsequently defined as the optimal dose in producing the behavioral changes that was used in the follow-up neurophysiology studies. Control groups of rats were treated with saline vehicle alone at the same time intervals.

2.2.3. Mechanical Sensitivity Testing

Sensitivity to mechanical stimuli was assessed using Von Frey filaments as previously described (Boyette-Davis and Dougherty, 2011; Yoon et al., 2013). A range of filaments calibrated to 1g, 4g, 10g, 15g, and 26g of bending force were used for testing. Filaments were applied to the mid-plantar surface of the hindpaw until a bend was observed in the filament and held for approximately 1 second. After a half-hour habituation period, each animal had its mechanical withdrawal threshold for each foot assessed as the lowest filament in the ascending series at which the animal responded to at least 50% of six applications. Animals were tested for baseline response just prior to their first injection of drug (day 1) and the days after each injection (days 2, 4, 6, and 8). Following this, rats were tested for mechanical threshold twice weekly for one month, then once weekly until recovery from the hypersensitivity behaviors, assessed as a return to baseline withdrawal threshold.

2.2.4. Heat Sensitivity Testing

Heat sensitivity in rats was tested using a Hargreaves testing apparatus (Ugo Basile). An infrared beam was directed to the mid-plantar surface of each hindpaw, and the latency to withdrawal was measured. This was repeated for three trials per paw with a 20 second cutoff to prevent tissue damage. Baseline beam intensity was set to evoke a baseline response between 10-12 seconds. Rats were tested at time points corresponding to those of dose response testing until day 30.

2.2.5. Cold Sensitivity Testing

Rats were tested for cold sensitivity via scored responses to application of acetone. For each trial, 50µL of acetone was applied to the mid-plantar surface of each hindpaw using a calibrated pipette. The behavior of the rat was observed and scored for 20 seconds following this application. A score of 1 was assigned for each rapid withdrawal or flicking of the foot. A score of 2 indicated prolonged (>1 second) withdrawal, and a score of 3 indicated licking of the hindpaw. Trials were conducted three times per hindpaw, for a total of six trials per testing period. Cold sensitivity testing was conducted at the same time points as thermal testing.

2.2.6. Motor Impairment Testing

The potential for motor impairment due to chemotherapy treatment was assessed by rotarod assay as previously described (Cata, Weng, and Dougherty, 2008b). A rotating wheel was set to increase over time from a speed of 4rpm to 40rpm. Each animal was placed on this accelerating wheel and allowed to walk for 120 seconds or until it fell off of the wheel, at which point the rotating wheel would shut off automatically. Three trials were recorded per animal per time point with a 5 minute resting period between trials. Time points corresponded to those of thermal testing.

2.2.7. *In vivo* Electrophysiology

All rats used for *in vivo* electrophysiology treated with bortezomib had confirmed behavioral hypersensitivity to chemotherapy and were compared to saline-treated controls. Rats were anesthetized using urethane (1.5g/kg i.p.) and anesthetic depth was verified by toe pinch for loss of nociceptive reflexes with supplemental anesthetic given as needed. The L5-6 spinal cord was exposed via laminectomy and the animal then mounted into a stereotactic frame. The spinal cord was covered with agar with an opening to allow electrode access that was kept filled with saline. A parylene-coated tungsten filament electrode (resistance 1.4-1.8MΩ, Microprobes Inc.) was advanced into the spinal cord using a hydraulic Microdrive. Cells were isolated using mechanical stimulation of the paw. Wide dynamic range (WDR) neurons responding in graded fashion to innocuous and noxious stimuli achieving a signal to noise ratio greater than 5 were selected for study.

Assessment of neuronal activity began with recording of 60 seconds spontaneous activity. Mechanical stimuli were then applied for 10 seconds each with 30 second inter-stimulus intervals. The stimuli included camel hair brush (1 application/second), 0.07g von Frey filament (1 application/second), 1.4g von Frey filament (1 application/second), 60g von Frey filament (1 application/second), venous clip (continual application), and arterial clip (continual application). Spike2 software was used to capture spikes and for off-line analysis of stimulus response frequencies and afterdischarge rates. The 5 seconds following each stimulus were used for analysis of afterdischarges.

2.2.8. Statistics

For all measurements in both behavior testing and electrophysiology, each representative data point was calculated as the mean value for a given group at the time point represented. Error bars were then calculated as standard error of the mean, and significance was determined using a Mann-Whitney test (α = 0.05, 0.025, 0.01). Additionally, a one-way ANOVA with a post-hoc Tukey test was used in mechanical behavior testing across doses to determine whether the observed behavior differed versus control and between other doses (P = 0.05, 0.01).

2.3. RESULTS

2.3.1. Mechanical Sensitivity

2.3.1.1   0.05mg/kg Bortezomib

Rats treated at the 0.05mg/kg dose of bortezomib had a gradual and slight onset of mechanical hypersensitivity versus baseline behavior that was determined in ANOVA to not differ significantly versus controls (Fig. 1A). Nevertheless, this group was significantly lower versus control at day 19 (naïve: 17.2±2.49g, bortezomib: 10.4±1.10g), as well as at days 23, 26, and 34. After this point, rats began to recover from changes in mechanical sensitivity. Although the average withdrawal threshold was higher for this group at later time points than in saline-treated rats, this difference was not statistically significant, and these rats started with a higher baseline threshold than the saline-treated group.

2.3.1.2.   0.10mg/kg Bortezomib

Rats treated at the 0.10mg/kg dose of bortezomib showed a significantly reduced mechanical withdrawal threshold than the saline-treated and 0.05mg/kg treated groups (P<0.01), but not different from the 0.15mg/kg or 0.20mg/kg groups. This group first showed statistically significant mechanical hyperalgesia versus controls at day 6 (naïve: 19.3±2.56g, bortezomib: 13.9±1.54g), after the third injection of bortezomib (Fig. 1B). Significant differences were also observed at every

following time point until day 54. Peak severity was observed from day 16 to day 34 (approx. 7.5g). Recovery from changes in mechanical sensitivity was gradual after this point, with statistically equivalent behavior versus saline-treated rats at days 63 and 69.

2.3.1.3.   0.15mg/kg Bortezomib

Rats treated at the 0.15mg/kg dose of bortezomib showed significantly lowered withdrawal threshold from the saline-treated and 0.05mg/kg group ($P<0.01$), but not from the 0.10mg/kg or 0.20mg/kg groups. This group first showed statistically significant mechanical hyperalgesia versus controls at day 8 (naïve: 17.3±2.48g, bortezomib: 11.1±2.41g), after the final injection of bortezomib (Fig. 1C). Significant differences were also observed at days 12, 19 through 41, and 54. Peak severity was observed from day 19 to day 34 (approx. 7.5g). Animals began to recover from mechanical hypersensitivity following this point, with statistically equivalent behavior versus saline-treated rats at days 47, 63, and 69.

2.3.1.4.   0.20mg/kg Bortezomib

Rats treated at the 0.20mg/kg dose of bortezomib showed significantly lowered withdrawal threshold from the saline-treated and 0.05mg/kg group ($P<0.01$), but not from the 0.10mg/kg or 0.15mg/kg groups. This group first showed statistically significant mechanical hyperalgesia versus controls at day 19 (naïve: 17.2±2.49g,

bortezomib: 9.75±1.36g), after the 0.10mg/kg and 0.15mg/kg doses showed similar

differences (Fig. 1D). However, because of a larger error at the day 12 and 16 time

points, the 0.20mg/kg group could not be determined to be significantly different

from either saline-treated rats or rats treated with other doses of bortezomib.

Significant differences versus saline-treated rats were also observed at days 23, 26,

34, 47, and 54. Peak severity was observed at days 23 and 26 (7.25 and 7.36g).

Animals showed highly variable mechanical sensitivity in the time points that

followed, but did not show consistent recovery with statistically equivalent behavior

versus saline-treated rats until days 63 and 69.

Mechanical Sensitivity
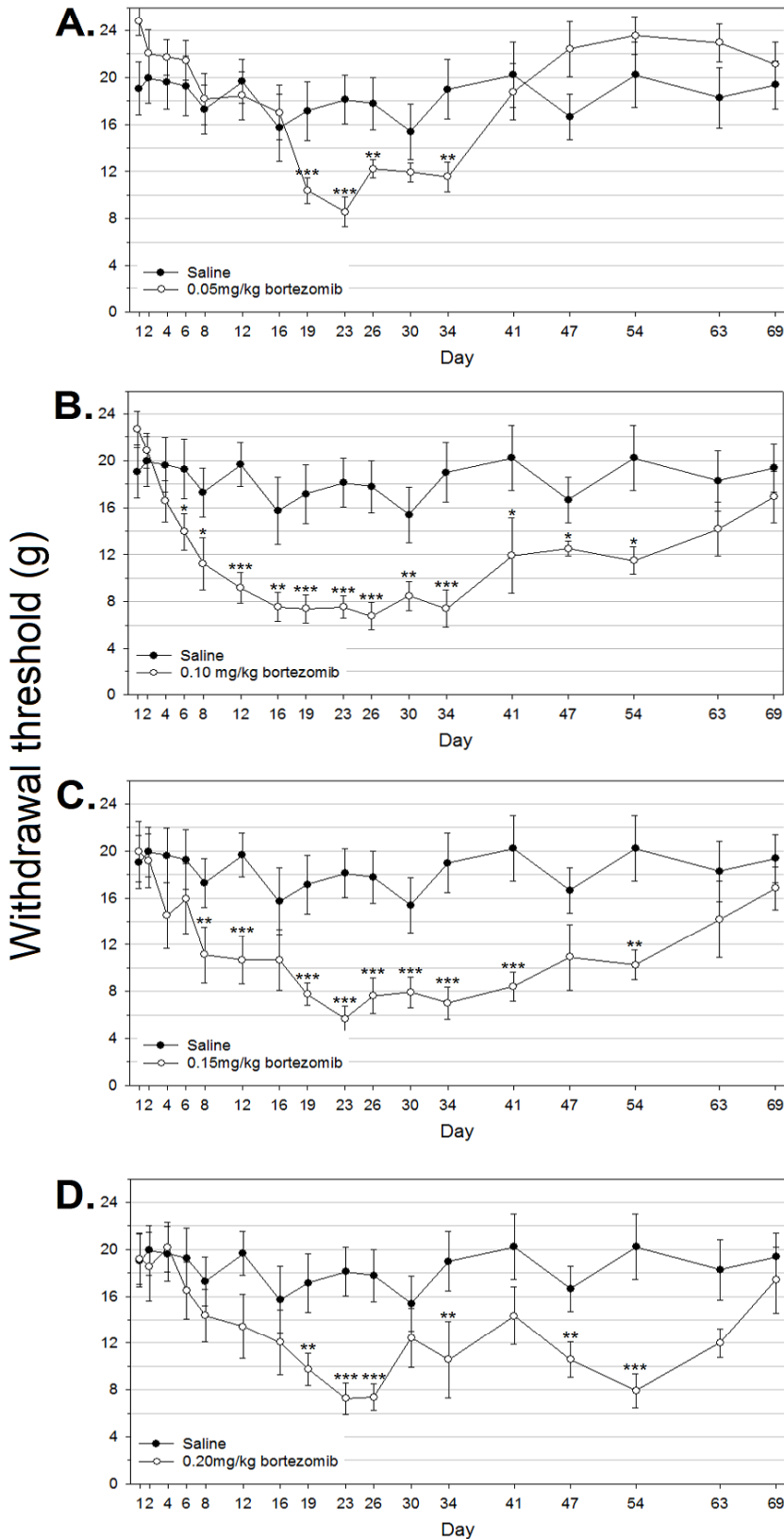
Figure 1. Bortezomib produces mechanical hypersensitivity in rats. Mechanical sensitivity was assessed by responses to mid-plantar application of von Frey filaments over time. **A)** Saline treated control group vs. rats treated with 0.05mg/kg bortezomib **B)** Saline treated control group vs. rats treated with 0.10mg/kg bortezomib **C)** Saline treated control group vs. rats treated with 0.15mg/kg bortezomib **D)** Saline treated control group vs. rats treated with 0.20mg/kg bortezomib.

2.3.2. Heat, Cold, and Motor Behavior

In thermal testing, both saline and bortezomib -treated groups remained at baseline levels throughout testing until they were sacrificed at day 30, long after significant differences appeared in rats tested for mechanical hyperalgesia (Fig. 2). Similarly, bortezomib-treated animals remained in line with saline-treated counterparts when tested for cold sensitivity throughout the period of testing (Fig. 3). There was one time point in which bortezomib-treated rats scored significantly higher than saline-treated rats, but this score was less than 0.5, indicating on average less than one withdrawal event per test. Peak scores never rose far beyond a score of 1.0. Rotarod testing showed a lack of motor impairment in animals treated with bortezomib, as well (Fig. 4). Although some time points showed average walking times less than the 120 second cutoff time, none of these data points were significant.
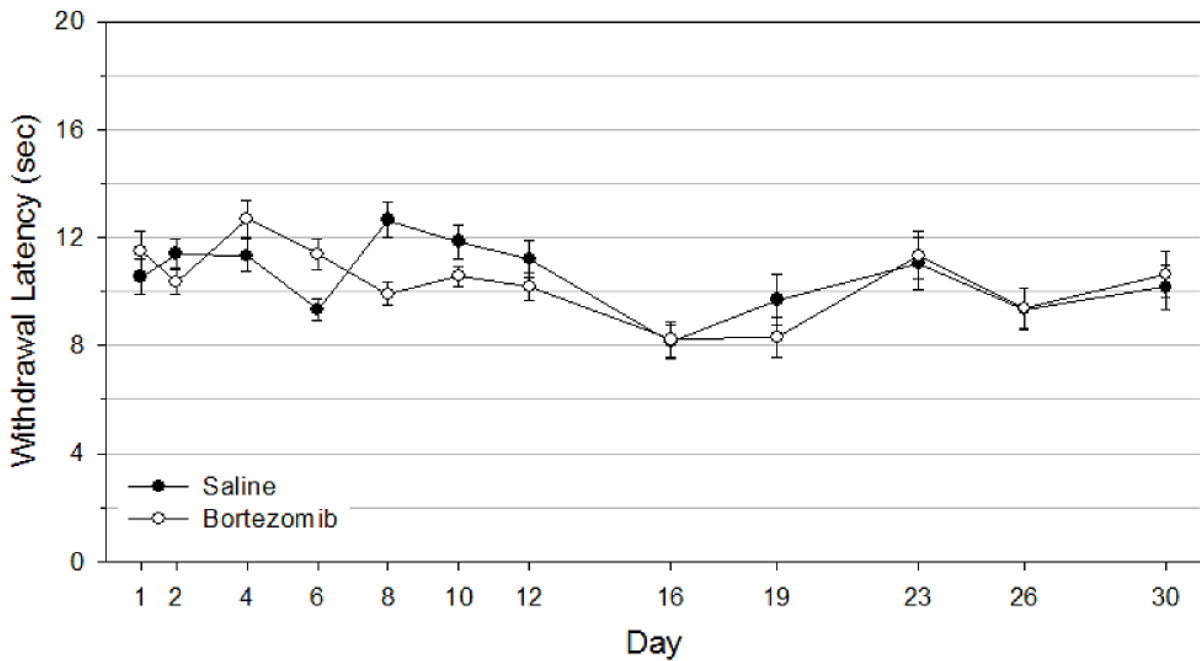
Figure 2. Bortezomib does not produce thermal hypersensitivity in rats. Thermal sensitivity was assessed via Hargreaves test, using a focused infrared beam with an automatic cutoff when interrupted by movement of the rat's foot. Infrared intensity was calibrated such that animals would respond on average after 10-12 seconds of continuous exposure at baseline, and this intensity was maintained throughout testing. Withdrawal latencies were obtained three times per foot per rat per time point. Neither saline-treated nor bortezomib-treated rats consistently showed an average withdrawal latency significantly below 10 seconds throughout testing, which falls within baseline range.

Cold Sensitivity
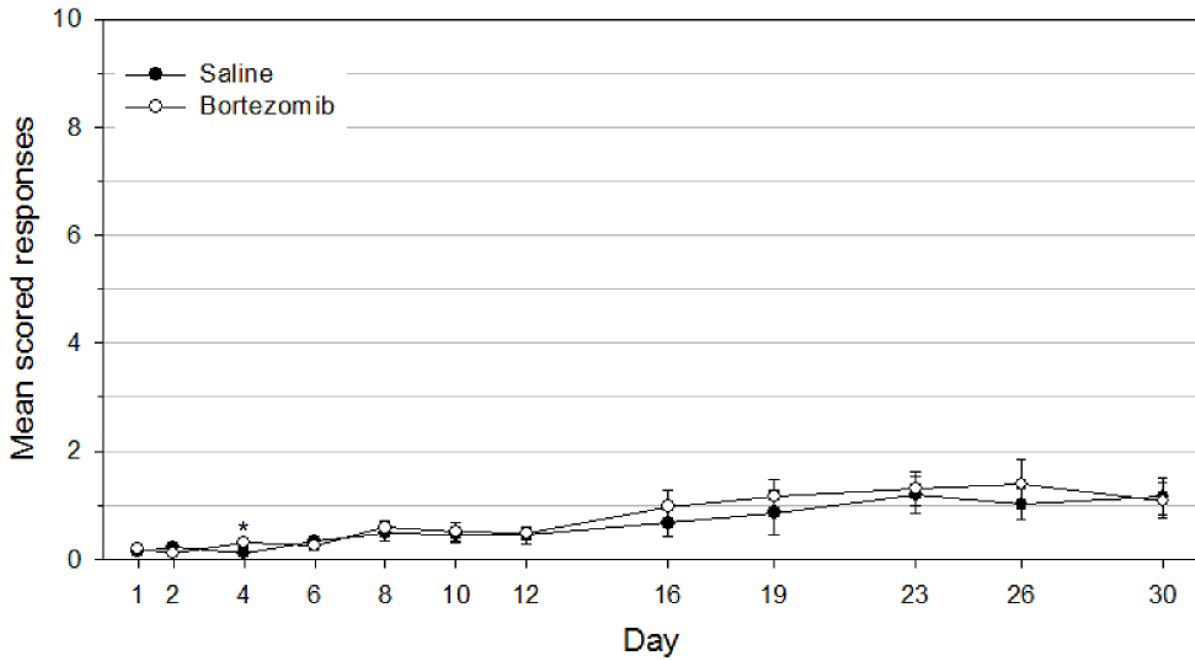
Figure 3. Bortezomib-treated rats did not develop cold hypersensitivity. Cold stimuli were simulated by applying acetone to the mid-plantar surface of each hindpaw. Responses were scored for each of three trials per foot per rat per time point. Scores were based on behavior in the 20 seconds following application of acetone.
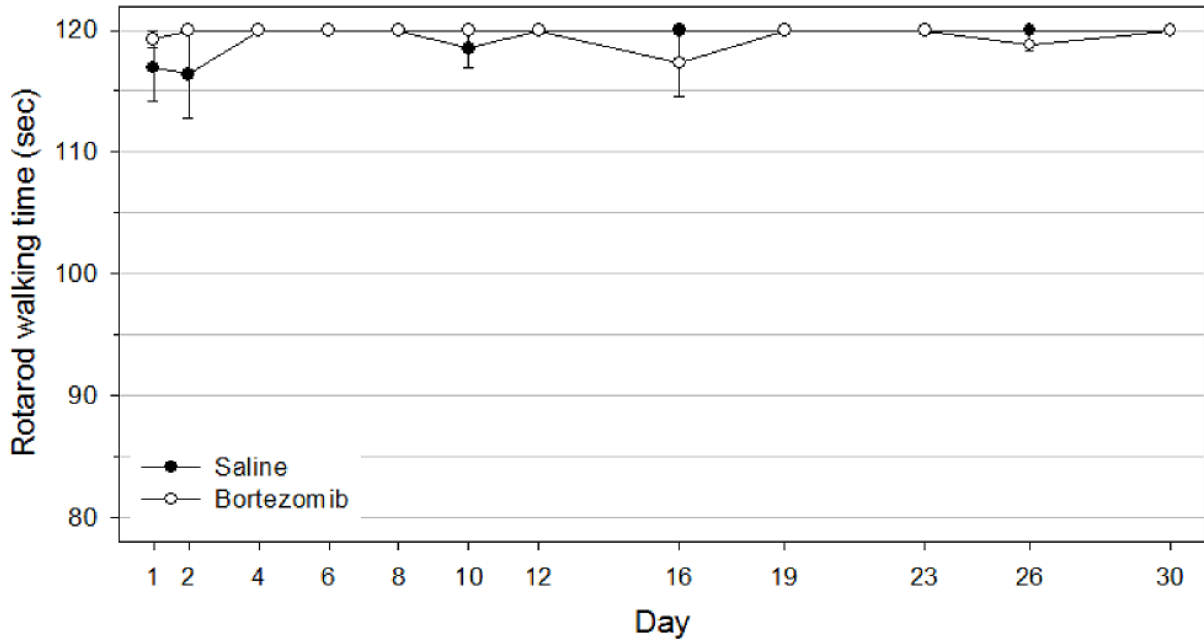
Figure 4. Bortezomib-treated rats did not develop motor impairment. Rats were allowed to walk on a rotarod that slowly accelerated from 4-40rpm. Walking time was recorded either until the rat fell from the wheel or until a 120 second cutoff was reached.

2.3.3. Electrophysiology

WDR neurons in bortezomib-treated rats (n=30) showed higher acute responses and afterdischarges to mechanical stimuli compared against neurons in control rats (n=22) (Fig. 5). Spontaneous firing of neurons was negligible in both groups (naïve: 0.036±0.016 spikes/s, bortezomib: 0.13±0.053 spikes/s). Both acute responses to Brush (naïve: 3.6±0.30 spikes/s, bortezomib: 9.1±0.93 spikes/s) and afterdischarges (naïve: 0.090±0.052 spikes/s, bortezomib: 1.6±0.32 spikes/s) were significantly elevated in bortezomib rats. The acute responses to the 0.07g von Frey stimulus were not significantly different in bortezomib rats (naïve: 1.3±0.16 spikes/s, bortezomib: 9.2±0.93 spikes/s), but the afterdischarges to this stimulus were significantly higher (naïve: 0.036±0.036 spikes/s, bortezomib: 0.43±0.16 spikes/s). Neither the acute response to the 1.4g von Frey filament (naïve: 2.7±0.32 spikes/s, bortezomib: 3.5±0.42 spikes/s) nor the afterdischarges (naïve: 0.13±0.056 spikes/s, bortezomib: 0.57±0.15 spikes/s) were significantly different from control rats. The responses to the 60g von Frey filament were significantly higher in bortezomib (naïve: 4.7±0.40 spikes/s, bortezomib: 7.5±0.73 spikes/s), as were the afterdischarges (naïve: 0.20±0.13 spikes/s, bortezomib: 1.2±0.29 spikes/s). Venous clip (light skin compression) responses were significantly higher in bortezomib (naïve: 5.3±0.77 spikes/s, bortezomib: 9.6±0.67 spikes/s), as were the afterdischarges (naïve: 0.65±0.26 spikes/s, bortezomib: 3.5±0.62 spikes/s). Arterial clip (painful skin compression) responses were significantly higher in bortezomib (naïve: 7.5±0.98 spikes/s, bortezomib: 14±1.2 spikes/s), as were the afterdischarges (naïve: 1.0±0.31 spikes/s, bortezomib: 5.9±0.80 spikes/s).

In vivo Electrophysiology
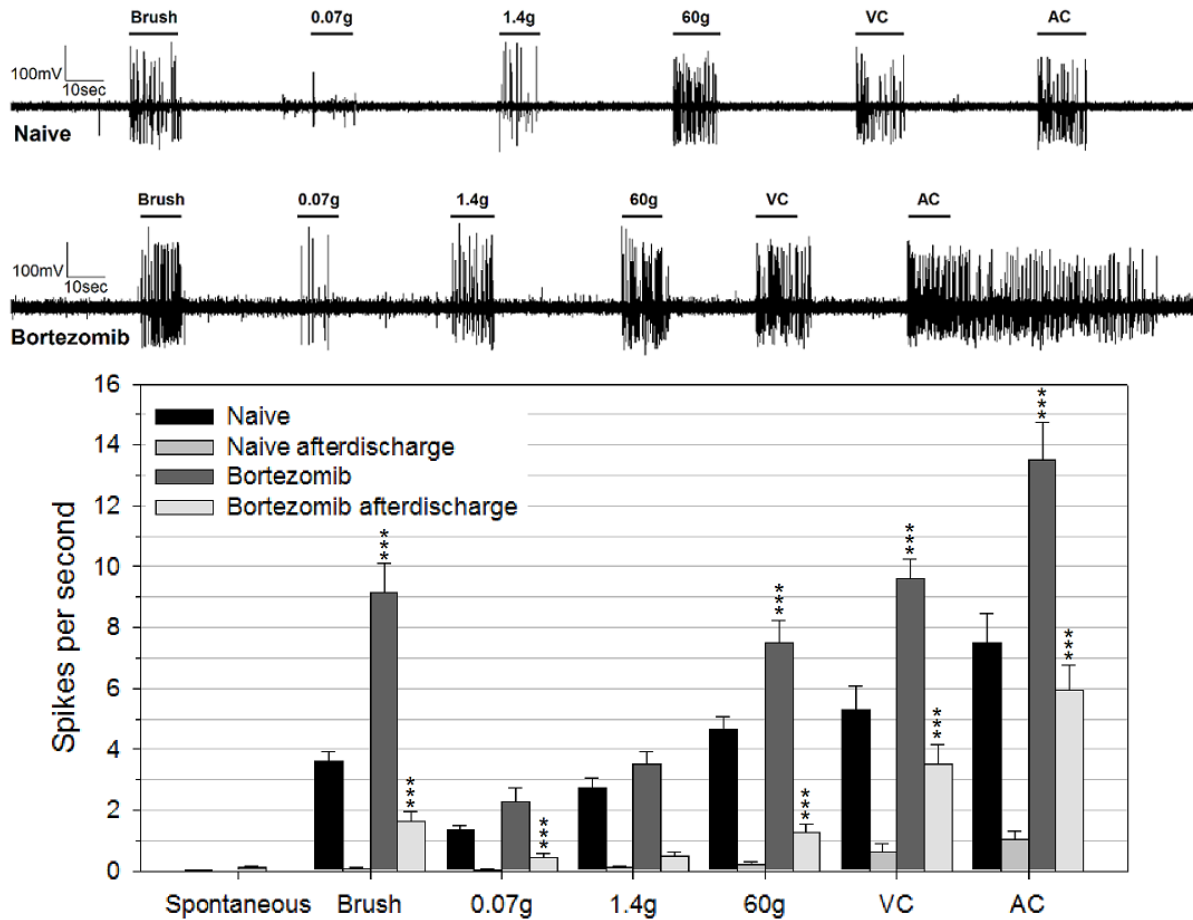
Figure 5. Bortezomib-treated rats developed enhanced firing responses in *in vivo* spinal WDR neuron electrophysiology. Spikes during and after stimulus application were quantified for spontaneous activity, brush application, three sizes of von Frey filament (0.07g, 1.4g, and 60g), venous clip (VC), and arterial clip (AC).

2.4. DISCUSSION

The dose-response data generated in the present study indicate that even doses below those used for chemotherapy in patients are sufficient to induce the BIPN model. However, doses approximating the therapeutic dose were more effective in generating this condition. Exceeding therapeutic doses did not increase the sensitivity further. A similar trend is observed in patients. 37% of patients will develop BIPN within 5 cycles of treatment, but those that do not develop BIPN by this time are unlikely to develop it at all (Kane et al., 2006; Richardson et al., 2006; Cavaletti and Jakubowiak, 2010; Broyl, Jongen, Sonneveld, 2012). It is therefore possible that bortezomib exerts its neuropathic effects based on whether a threshold is reached, rather than in a manner that directly correlates with dosage. However, dose reduction was reported to be effective in reducing all BIPN symptoms if implemented at the first signs (Richardson et al., 2006). This may be a matter of addressing emergent BIPN before the threshold is fully reached, as the present data show a lesser effect at the lowest dose that resolves more quickly.

Bortezomib-treated animals were similar to animals treated with paclitaxel in the time course of neuropathic symptoms, which also showed a recovery at approximately 60 days (Cata, Weng, and Dougherty, 2008b). Animals treated with oxaliplatin followed a similar trend and took over two months to recover (Xiao, Zheng, and Bennett, 2012). This trend is not at all surprising, considering that it may take months for patients to recover by even one grade of neuropathy (Cavaletti and Jakubowiak, 2010; Broyl, Jongen, Sonneveld, 2012). The genetic homogeneity of the strain of rat used may be a contributing factor to the time course and relatively

stable recovery time in the current study. On the other hand, the pharmacokinetics of bortezomib show a full return of proteasomal function in 48-72 hours (Adams, 2002). It is therefore important in future studies to consider the possibility of a long-lasting signal cascade maintaining BIPN that is not dependent on continued proteasomal inhibition.

The present data show a clear change in mechanical sensitivity in the BIPN model. However, there were no changes to other modalities observed. Bortezomib therefore differs from other drugs in the profile of affected behaviors, as paclitaxel induces thermal sensitivity in rats (Dina et al., 2001; Cata, Weng, and Dougherty, 2008b), and oxaliplatin is capable of inducing sensitivity to thermal and cold stimuli (Joseph and Levine, 2009; Xiao, Zheng, and Bennett, 2012). Patients with BIPN showed a different profile than what was observed in rats in the present study, with decreased sensitivity to thermal stimuli, increased sensitivity to cold stimuli, and some degree of fine motor impairment (Cata et al., 2007). It is unclear whether these discrepancies are due to differences between the tests used in humans versus rats, or perhaps if there are differences in how the species respond to the drug. However, it is important to note that the tests used to assess changes in the present study have been successful in other models. It is therefore unknown what causes the mechanical sensitivity to be the sole form of behavior affected in the present study, but nevertheless important to note that this distinguishes bortezomib from other agents.

The alterations observed in WDR neurons were robust, but the fact remains that bortezomib cannot cross the blood-brain barrier. This finding strongly suggests

that bortezomib initiates damage to primary afferents that then act on the spinal

cord. This could occur through increased presynaptic signaling, as continual firing of

these primary afferents could result in spinal central sensitization (Rygh et al., 1999;

Ji et al., 2003). The present electrophysiological data would suggest something akin

to central sensitization, although it cannot be said with certainty that it results from

increased presynaptic signaling. The same effect could also occur due to

downregulation of astrocytic glutamate transporters or by increases in sensitivity at

the postsynaptic cell if there is input from outside of the blood-brain barrier. The

glutamate transporter hypothesis in particular could account for the persistent after-

discharges because of the persistence of synaptic glutamate. However, there must

still be some signal from outside of the spinal cord to initiate such a change. The

activity of spinal glial cells may also contribute to the changes observed in the

present study through the release of proinflammatory cytokines. This has been of

particular interest in similar models, and the diverse role of these cytokines may

contribute to pain in multiple ways (Clark, Old, and Malcangio, 2013; Ji, Berta, and

Nedergaard, 2013). Our lab has previously shown alterations of glutamate

transporters in other models of CIPN in models that show similar changes in WDR

responses, and ongoing work is investigating this possibility of a cytokine cascade

(Cata et al., 2006a; Cata, Weng, and Dougherty, 2008a; Zhang et al., 2012).

Bortezomib clearly possesses some mechanistic differences from other drugs

in order to produce a distinct neuropathic condition, but how this occurs is unknown.

In summary of the present study's findings, bortezomib induced hypersensitivity to

mechanical stimuli and increases to WDR neuron firing and after-discharges. Other

modalities investigated were not affected. Precisely how bortezomib induces the

BIPN model will require a significant amount of future study, but there may be some

overlap in this model with other models of CIPN. The similarity in WDR neuronal

responses suggest a degree of overlap, and future studies involving glial

mechanisms seen in other models would suggest further similarities. The findings in

the present study now provide a foundation for mechanistic studies, as proposed

mechanisms can be compared for their effects on the modalities presently identified.

3. SPINAL CORD GLIAL ACTIVATION PROFILE IN BIPN

Content in this chapter is based on the following publication with permission from the publisher:

Robinson CR, Zhang H, Dougherty PM (2014) Astrocytes, but not microglia, are activated in oxaliplatin and bortezomib-induced peripheral neuropathy in the rat. Neuroscience pii: S0306-4522(14)00459-X.

License No.: 3413230352490

3.1. INTRODUCTION

In order to show a correlation between observed changes in behavior and the activity of astrocytes, it was important to track the course of reactive gliosis in the bortezomib model. To truly establish a connection between these two phenomena, it is necessary for the data to support three conclusions: astrocytes are activated in animals that display appropriate behavioral changes, astrocytes are not activated in controls that do not develop behavioral changes, and the prevention of behavioral changes also prevents astrocyte activation. The hypothesis in this chapter was therefore that astrocytes are activated in chemotherapy-treated animals that develop mechanical sensitivity and that both phenomena are prevented by co-treatment with an inhibitor of glial activation. The data were in support of this hypothesis, and it was also verified that microglia were not similarly activated at observed time points. This further suggests that the astrogliosis occurs as its own phenomenon, rather than as an extension of other glial functions.

Current research on neuropathic pain is hampered by a limited mechanistic understanding regarding both its induction and maintenance. However, emerging evidence suggests a role for a glial-driven release of proinflammatory cytokines that may drive sensitization of spinal neurons (Graeber, 2010; Sivilotti and Woolf, 1994; Ji and Suter, 2007; Miller et al., 2009). Microglia have become particularly popular in this regard due to a prominent role in immune and inflammatory function (Graeber, 2010; Ji and Suter, 2007). In spite of this popularity of microglia, it is important to note that astrocytes have been known to play a role in injury models for decades now (Garrison et al., 1991). To note a common activation profile across multiple models of pain may suggest common mechanisms in neuropathic pain, even in spite of the vastly different forms of insult that may contribute to such a disorder.

Like many other forms of small-fiber neuropathies, chemotherapy-induced peripheral neuropathy (CIPN) presents with a spectrum of dysesthesias and paresthesias that include increased pain sensitivity, spontaneous pain, tingling, burning sensations, and numbness, among other descriptors (Dougherty et al., 2007). The exact presentation of CIPN in patients may vary from one drug to another, with some modalities affected more or unaffected entirely (Cata et al., 2006b; Cavaletti and Marmiroli, 2010). Thus, effective development of therapeutic strategies requires a more exact understanding of CIPN and how it may be distinct from other forms of pain. One such distinction was recently discovered when it was found that microglia are not activated in animal models of CIPN as they are in nerve injury models (Zheng, Xiao, and Bennett, 2011; Zhang et al. 2012). Such a finding is

somewhat controversial, considering that popular theory holds that microglia play a pivotal role across all types of chronic pain. This assumption may not be entirely accurate, as there is some evidence that astrocytes may be both necessary and sufficient to induce neuropathy in some models (Gao and Ji, 2010b; Hald, 2009). In fact, our own work has reported astrocyte activation in paclitaxel without any apparent activation of microglia (Zhang et al., 2012). The aim of the current study is to determine whether a similar trend is also seen in other CIPN models, suggesting a centralized role for glia in CIPN as a whole.

Minocycline is an antibiotic and anti-inflammatory drug that has previously produced an abrogation of sensitivity behaviors in some models (Hua et al., 2005; Ledeboer et al., 2005; Guasti et al., 2009). Although this was previously assumed to be a result of microglial inhibition, additional work has shown an effect following minocycline treatment in models that show no activation of microglia (Boyette-Davis and Dougherty, 2011; Boyette-Davis et al., 2011b; Cata, Weng, and Dougherty, 2008b; Zheng, Xiao, and Bennett, 2011). These findings point to a generalized anti-inflammatory role for minocycline, rather than a selective microglial inhibitory effect. This would explain why minocycline produces an effect in microglia, but it could also potentially affect any inflammatory mechanisms in astrocytes in a similar manner. The current study therefore also used minocycline in co-treatment with bortezomib and oxaliplatin to test whether these animals differed from those treated with their respective vehicles. If minocycline successfully impacts both behavioral and glial changes in the animal CIPN model, then it is possible that there is a direct connection between the two observed effects. Although this has not been

investigated in the bortezomib model, minocycline was previously shown to be successful in preventing mechanical sensitivity in oxaliplatin-treated animals (Boyette-Davis and Dougherty, 2011). The present study therefore has two major goals: first, to ascertain whether astrocytes are selectively activated in oxaliplatin and bortezomib treatment, and second, to determine whether co-administration of minocycline has an effect on behaviors and glial activation in bortezomib-treated animals.

3.2. METHODS

3.2.1. Animals

All procedures were reviewed and approved by the M.D. Anderson Institutional Animal Care and Use Committee and were in accordance with the guidelines established by the NIH and the International Association for the Study of Pain. 111 Male Sprague-Dawley rats between 60 and 75 days of age upon beginning of treatment (300-350 g) were used for all experiments. Rats were housed in a facility with a 12-h light/dark cycle and were given food and water *ad libitum.* All efforts were taken at each stage of the experiments to limit the numbers of animals used and any discomfort to which they might be exposed.

3.2.2. Drugs

All drugs were administered by intraperitoneal injection in a volume of 0.5 ml. Oxaliplatin (Tocris Bioscience) was administered in dextrose vehicle at a dose of 2mg/kg on days 1, 3, 5, and 7 of experimentation for a cumulative dose of 8mg/kg as previously described (Boyette-Davis and Dougherty, 2011). Bortezomib (Millennium Pharmaceuticals) was administered in saline vehicle at a dose of 0.15 mg/kg on days 1, 3, 5, and 7 of experimentation for a cumulative dose of 0.60 mg/kg. Groups treated with minocycline hydrochloride (Sigma Aldrich) were injected daily with 25.0 mg/kg minocycline in saline vehicle beginning at day 0 and continuing daily through day 8 (one day past chemotherapy treatment) of experimentation for a cumulative

dose of 225mg/kg. Control groups were injected with an equivalent volume of appropriate vehicles (saline for bortezomib or dextrose for oxaliplatin).

3.2.3. Surgery

As a positive control for activation of both astrocytes and microglia, 6 rats received spinal nerve ligation (SNL) surgery (Kim and Chung, 1992). The rats were anesthetized using inhaled isoflurane (3-4%) to an adequate depth, verified by loss of nociceptive and blink reflexes. The L5 spinal nerve was exposed immediately distal to the dorsal root ganglion and then ligated with 6-0 silk suture. The wound was then closed in layers using vicryl suture and the skin closed with wound clips. The animal was monitored during recovery until it resumed normal activity. Another 6 rats received sham surgery, in which the L5 nerve was exposed, but not ligated.

3.2.4. Behavior Testing

Sensitivity to mechanical stimuli was assessed in all animals using von Frey filaments (Boyette-Davis and Dougherty, 2011; Boyette-Davis et al., 2011b). Filaments calibrated to 4g, 10g, 15g, and 26g bending force were applied 6 times each to the mid-plantar surface of each hindpaw in order to determine the filament corresponding to the animal's response threshold. Animal identifiers were concealed prior to testing to ensure blinding of the tester. Application of filaments began following a half-hour habituation period with the lowest (4g) filament. This was

followed by other filaments of increasing bending force until a withdrawal threshold was obtained. Rats were allowed a resting period of 5 to 10 minutes between filaments in order to minimize the possibility of responses due to anxiety during testing. Filaments were applied with steady force until bending of the filament was observed and held for approximately 1second. A response was evaluated as a rapid withdrawal of the paw. The threshold for sensitivity to mechanical stimuli was recorded as the bending force of the filament for which at least 50% of applications elicited a response. The mean of this threshold was reported for each treatment group at each time point. Error was reported as standard error of the mean (SEM), and significance was tested at critical time points (those in which the errors of the two groups did not overlap or in which there was minimal overlap of errors) using Mann-Whitney tests.

The persistence of sensation was also measured based on von Frey responses that evoked exaggerated behaviors such as prolonged lifting, shaking, or licking of the paw. Out of the responses used to determine the 50% withdrawal threshold, the number of these that evoked an exaggerated response was recorded and expressed as percent of total responses. Error was reported as standard error of the mean (SEM), and significance was tested in bortezomib and bortezomib + minocycline groups versus saline-treated controls using Mann-Whitney tests.

3.2.5. Tissue Collection

At the conclusion of the behavioral testing, animals with confirmed CIPN or SNL mechanical hyper-responsiveness were overdosed with sodium pentobarbital (150mg), then perfused intracardially with room temperature heparinized saline, followed by cold 4% paraformaldehyde in 0.1M phosphate buffer. Spinal cords were removed and post-fixed in 4% paraformaldehyde at $4^{o}C$ overnight, then moved to 15% sucrose the following day. Tissue was then moved after 24h to 30% sucrose for a minimum of 48h as a cryoprotectant. The lumbar enlargement was mounted and the L5 segment cut in a cryostat at a thickness of 30μm.

3.2.6. Immunohistochemistry

Spinal cord slices were washed in phosphate-buffered saline (PBS) for 6 washes lasting 15 minutes each and then blocked in normal donkey serum (5% NDS and 0.2% triton X in PBS). Slices were incubated overnight at $4^{o}C$ with primary antibodies against GFAP (mouse anti-rat 1:1000, Cell Signaling Technology) or OX-42 (mouse anti-rat 1:1000, AbD Serotec). Slices were washed the following day in PBS for 6 washes lasting 15 minutes each, then incubated with either FITC-conjugated donkey anti-mouse secondary antibody for the GFAP primary antibody (1:500, Jackson Immunoresearch) or Cy-3-conjugated donkey anti-mouse secondary antibody for the OX-42 primary antibody (1:500, Jackson Immunoresearch) for 2 hours at room temperature. Slices were washed for a final

course of 6 washes lasting 15 minutes each, then mounted onto glass slides using

Vectamount medium.

3.2.7. Quantification of Immunohistochemistry

Slices were viewed and images captured using light and fluorescent

illumination at 10X using a Nikon Eclipse E600 microscope. These images were

layered with both a fluorescent and bright field image to allow toggling between

filters to draw a region of interest limited to but containing the full dorsal horn. The

region of interest was drawn using the light image to avoid bias from fluorescent

imaging. The filter was then changed to fluorescence imaging, maintaining the

location of the region of interest. A region containing only background signal was

selected within the slice, and the corresponding level of fluorescence intensity was

analyzed using NIS Elements software (Nikon, USA). Background was subtracted

and the resulting signal was then expressed as intensity within the region of interest

in pixels/μm^2. For each treatment group, the mean of these values was calculated

and expressed as a percent versus the control group of the same time point. Error

was expressed as the combined standard error of the mean (SEM) for treatment and

control groups to account for variability within controls. Significance was determined

via Mann-Whitney test (α = 0.05, 0.025, 0.01).

3.3. RESULTS

3.3.1. Behavior

Mechanical sensitivity as described by von Frey filament testing was taken for rats treated with bortezomib, bortezomib + minocycline, saline, oxaliplatin, oxaliplatin + minocycline, dextrose, SNL (ipsilateral and contralateral to surgery), and sham surgery (ipsilateral and contralateral to surgery). Baseline von Frey withdrawal thresholds were not significantly different between groups treated with bortezomib (21.2 ± 1.5g), saline (21.2 ±1.4g), or bortezomib + minocycline (23.3 ± 1.7g). Rats treated with bortezomib showed a steady decrease in withdrawal thresholds to von Frey stimuli starting at day 6 that became significantly different from vehicle-treated controls at day 12 (bortezomib = 10.3 ± 1.2g/ saline = 19.8 ± 2.1g) and reached peak severity at days 20 (bortezomib = 11.0 ± 2.6g/ saline = 19.4 ± 2.3g), 24 (bortezomib = 5.7 ± 1.1g/ saline = 18.6 ± 3.2g) through day 28 (bortezomib = 9.4 ± 1.3g/ saline = 18.3 ± 2.7g) (Fig. 6A). The rats showed a gradual recovery in withdrawal threshold after day 41 until a complete recovery was observed at day 69 (bortezomib = 15 ± 0g/ saline = 17.8 ± 3.8g). Rats co-treated with minocycline showed no difference in withdrawal threshold versus saline-treated controls at any time point.

Baseline von Frey filament thresholds were not significantly different between groups that were treated with oxaliplatin (20.5 ± 1.6g), dextrose (22.3 ± 1.5), or oxaliplatin + minocycline (20.5 ± 2.3g). Oxaliplatin-treated rats showed a significant decrease in threshold following treatment at day 14 (oxaliplatin = 12.0 ± 1.4g/

dextrose = 20.6 ± 2.8g) (Fig. 6B), but were not observed for recovery. As with

bortezomib, co-treatment with minocycline in oxaliplatin-treated rats prevented this

change (Boyette-Davis and Dougherty, 2011).

SNL rats showed a sharp decrease in response threshold in the paw

ipsilateral to surgery on day 3, the first day of testing following surgery (6.0 ± 1.3g

ipsilateral/ 16.0 ± 2.2g contralateral) (Fig. 6C). This increased sensitivity was

maintained a week following surgery (3.5 ± 0.5g ipsilateral/ 17.0 ± 3.0g contralateral)

until animals were sacrificed on day 14 (5.0 ± 1.0g ipsilateral/ 19.6 ± 2.9g

contralateral). There was no change in sensitivity between ipsilateral or contralateral

paws in sham surgery rats.

The percent of persistent withdrawal responses during von Frey testing was

exaggerated by chemotherapy treatment, with bortezomib-treated rats showing a

significantly higher percentage of exaggerated withdrawals at days 7 and 28 versus

saline-treated controls (Fig. 6D). Bortezomib animals co-treated with minocycline did

not differ significantly from saline-treated controls at any time point.

In summary, animals treated with bortezomib or oxaliplatin, as well as those

with SNL surgeries, developed marked increases in sensitivity to von Frey filament

stimulation as an assay of mechanical sensitivity. The bortezomib-treated rats were

tested until the behaviors recovered to baseline, as this model has not been

described in as much detail. Animals treated with minocycline in both bortezomib

and oxaliplatin models did not differ in mechanical sensitivity from vehicle-treated

animals.
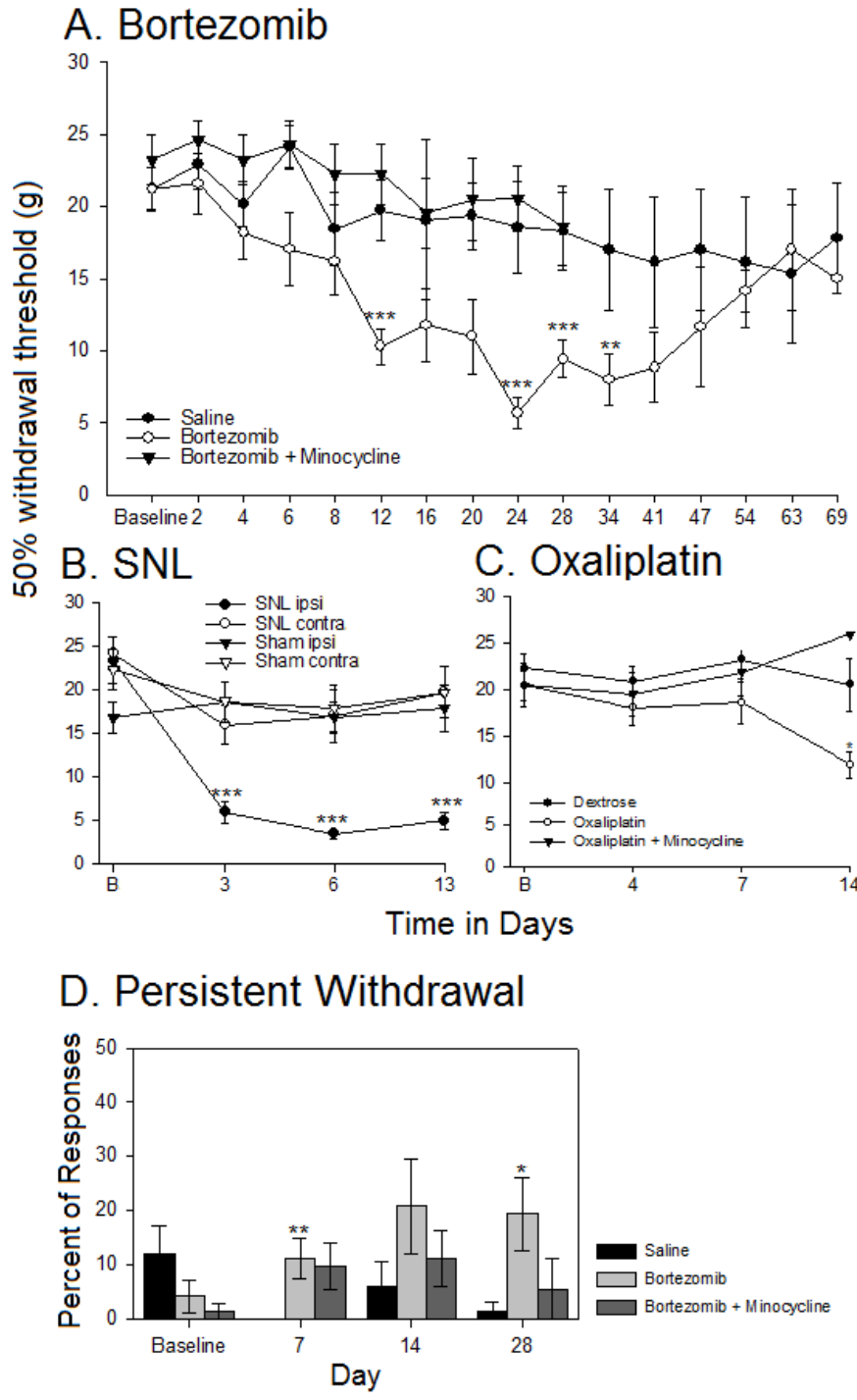
Figure 6. Verification of changes in mechanical sensitivity using von Frey filament withdrawal thresholds. **(A)** Bortezomib-treated rats (n=16) showed an decrease in withdrawal thresholds compared to saline-treated controls (n=15), that was not observed in rats co-treated with minocycline (n=8). **(B)** Rats treated with spinal nerve ligation (SNL) (n=6) showed a marked decrease in withdrawal thresholds in feet ipsilateral to ligation versus contralateral, and sham surgery rats (n=6) showed no such change. **(C)** Oxaliplatin-treated rats (n=12) showed an decrease in withdrawal thresholds compared to dextrose-treated controls (n=12) that was not observed in rats co-treated with minocycline (n=6). **(D)** Bortezomib-treated rats (n=12) showed increases in the percent of persistent withdrawals during von Frey stimulation versus saline-treated rats (n=11) that were not observed in animals co-treated with minocycline (n=12).

61

3.3.2. Qualitative Changes in Glial Morphology and Distribution

Although measures used in the present study were limited to overall expression of glia, several qualitative changes in spinal glial morphology were also noted. Activated astrocytes and microglia showed increased surface marker expression, as well as an observed increase in density and number of processes and swollen cell bodies when viewed under high magnification (Fig. 7). These changes were not restricted to the dorsal horn, where GFAP and OX-42 expression were quantified, but activation was distributed in an apparently homogenous manner throughout the ventral horn and other spinal cord gray matter, as well (Fig. 8-10). The observed changes in morphology are notable as a trend that is not restricted to a single model, but as generalized trends in all models that showed increases in GFAP or OX-42 markers. These changes observed in astrocytes applied to all three models, whereas the changes in microglia morphology only applied to the SNL model in which they showed increases in OX-42 expression.
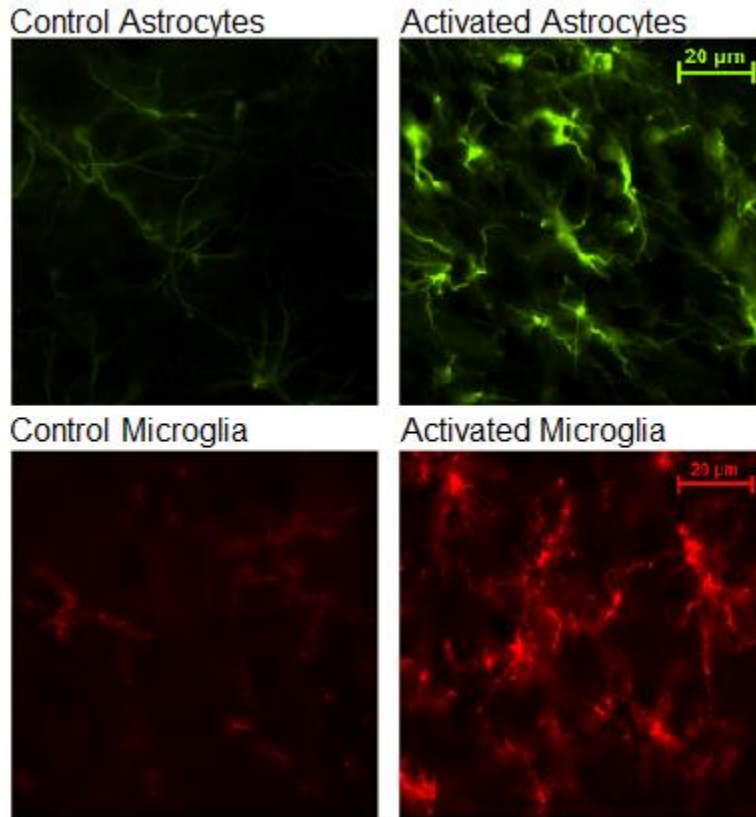
Figure 7. Activated astrocytes and microglia are marked with greater arborization and hypertrophy versus inactive counterparts. Astrocytes shown are from day 30 saline treated (left) and bortezomib-treated (right) dorsal horn. Microglia shown are from sham surgery (left) and SNL surgery (right) dorsal horn ipsilateral to surgery.

3.3.3. Astrocyte Activation Following Bortezomib Treatment

Fluorescent intensity of GFAP immunohistochemistry in bortezomib-treated rats was found to be significantly higher versus saline-treated controls at multiple time points. Staining intensity for GFAP showed statistically significant increases at day 7 (111 ± 3.9% of control), day 14 (113 ± 5.1% of control), and day 30 (162 ± 11.5% of control) (Fig. 7 and Fig. 11A). GFAP staining intensity was not statistically significant in bortezomib at day 69 (94 ± 9.5% of control). Co-treatment of minocycline with bortezomib produced a significantly lower activation of astrocytes versus saline-treated controls at day 30 (76 ± 3.0% of control), in contrast to the astrocyte activation observed in rats treated with bortezomib alone. In short, bortezomib-treated animals showed higher GFAP staining intensity at days7, 14, and 30, with peak intensity at day 30.

Figure 8. GFAP staining intensity as represented in day 30 saline, bortezomib + minocycline, and bortezomib-treated spinal cord tissue.

3.3.4 Astrocyte Activation Following Oxaliplatin Treatment

Oxaliplatin-treated animals showed significantly higher GFAP fluorescence intensity versus controls. Staining intensity for GFAP showed statistically significant increases at day 7 (131 ± 9.4% of control) and day 14 (122 ± 4.7% of control) (Fig. 8 and Fig. 11B). Groups co-treated with minocycline showed an increase at day 7 (115 ± 13.5% of control) and decrease at day 14 (91 ± 20.2% of control), but neither of these findings were statistically significant. There was a decrease of GFAP intensity versus control at day 40 (87 ± 7.8% of control), but this was not found to be statistically significant. Because the increase in astrocyte activation from earlier time points is fully reversed by this time, and because other studies have shown that sensitivity to mechanical stimuli is abolished by this time, further time points were not examined.
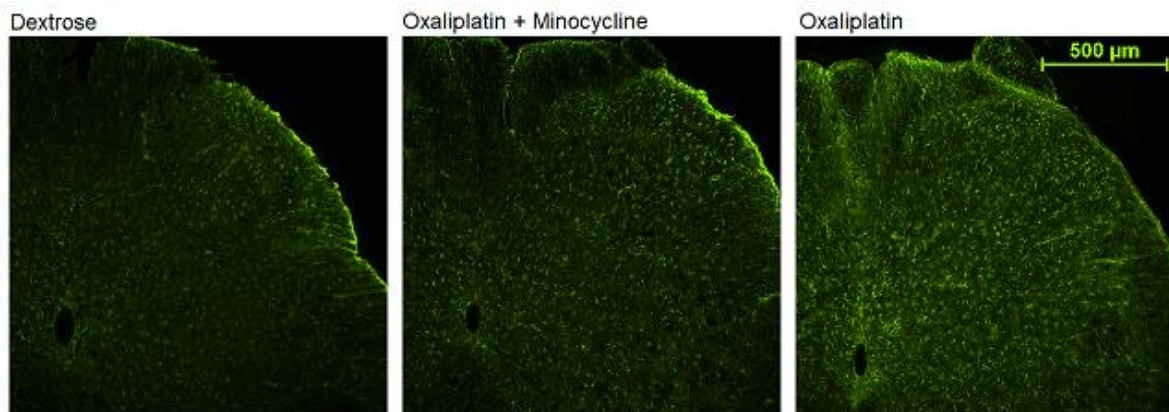
Figure 9. GFAP staining intensity as represented in day 7 dextrose, oxaliplatin + minocycline, and oxaliplatin-treated spinal cord tissue.

3.3.5 Astrocyte Activation Following Spinal Nerve Ligation

Astrocyte activation indicated by GFAP staining was significantly higher in SNL rats on the ipsilateral side of the spinal cord versus the contralateral side (126 ± 9.28%) (Fig. 11C). Sham surgery rats showed no significant difference between halves of the spinal cord ipsilateral or contralateral to surgery (100 ± 10.3%). The overall finding was therefore in line with this model as a positive control, that there was a marked activation of astrocytes only in those animals that received the actual surgery, and this activation was significantly higher on the side ipsilateral to the ligation.

3.3.6 Microglial Activation Following Spinal Nerve Ligation

Microglial expression of OX-42 was markedly higher in day 14 SNL rats ipsilateral to surgery versus contralateral spinal cord (130 ± 12.3%), whereas sham surgery rats showed statistically equivalent microglial expression on ipsilateral versus contralateral spinal cord (98 ± 10.4%) (Fig. 9 and Fig. 11C). This was therefore a trend in line with that of the SNL astrocyte data: the microglial activation occurred only in SNL rats and primarily on the side of the spinal cord ipsilateral to the ligation.

3.3.7 Microglial Activation Following Bortezomib Treatment

The staining intensity of OX-42 as a marker for microglial activation was slightly, though significantly, lower in bortezomib versus control at day 7 ($95 \pm 5.2\%$), 14 ($96 \pm 8.6\%$), and 30 ($93 \pm 4.6\%$) (Fig. 11D). The finding that bortezomib does not activate microglia at any of the time points observed is in line with other models of chemotherapy treatment.
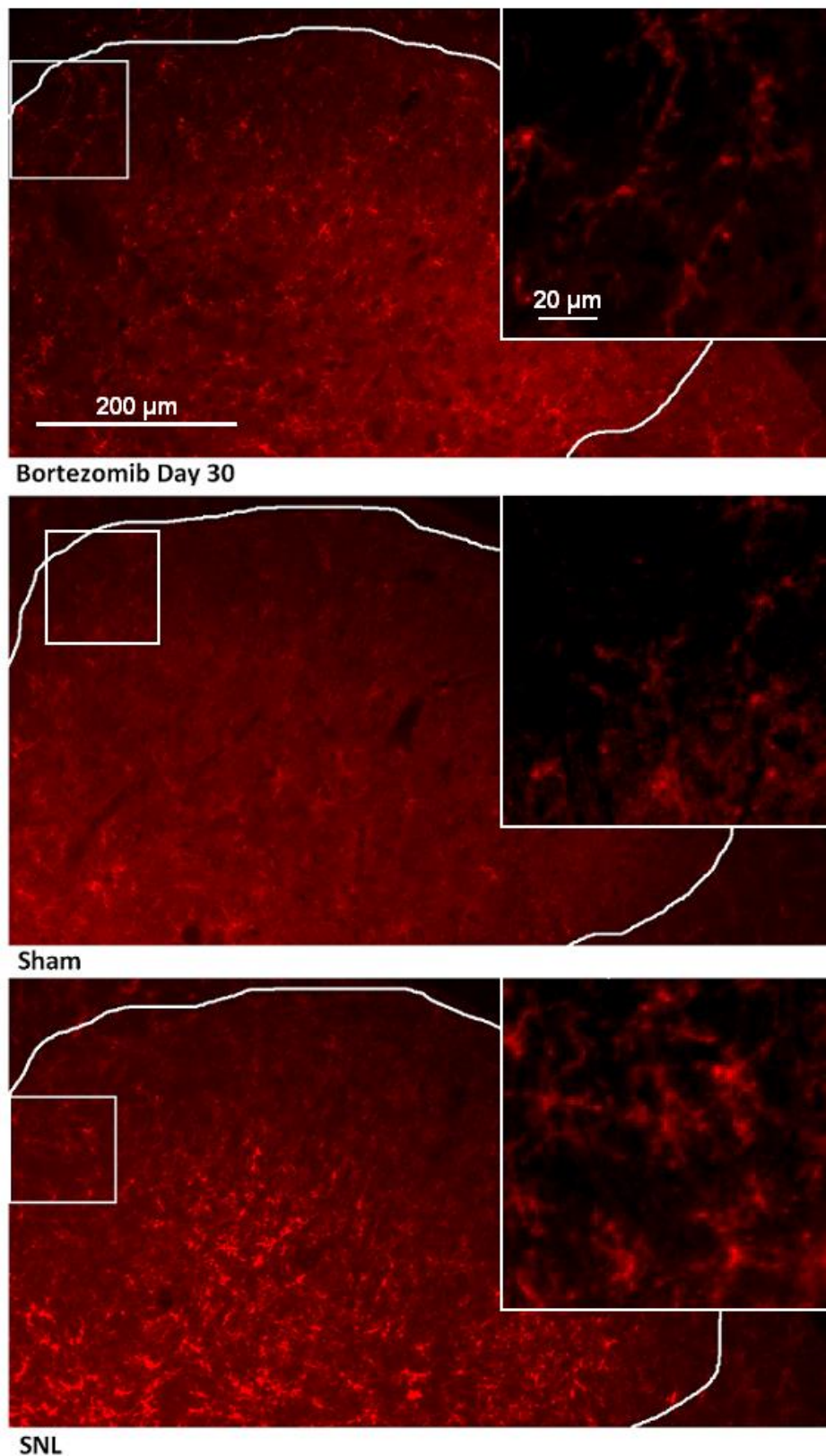
Figure 10. OX-42 staining intensity in bortezomib and SNL. Staining is increased following spinal nerve ligation (bottom) but not 30 days following bortezomib treatment (top), or following sham surgery (middle). Inserts at show increased magnification with background subtracted to highlight microglial cell morphology in each condition.
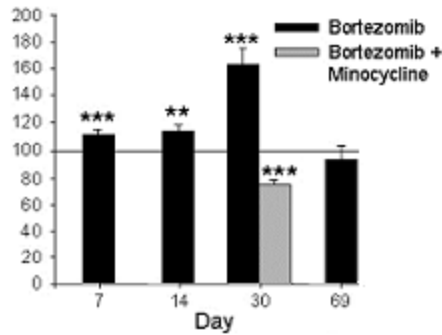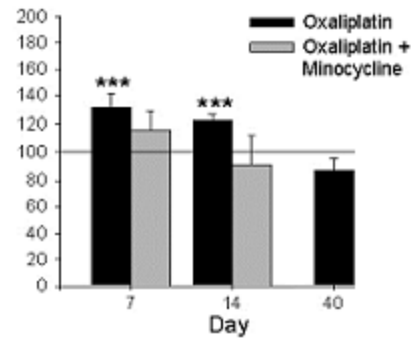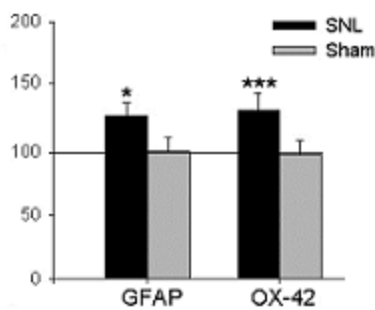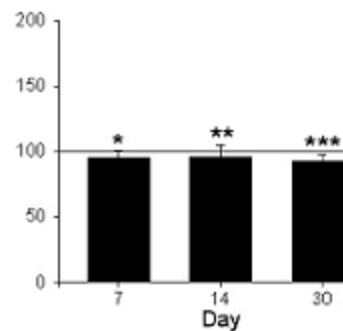
Figure 11. Glial marker expresion was quantified in bortezomib, oxaliplatin, and SNL. Staining intensity in treated animals was expressed as a percentage of intensity versus respective controls. **(A)** GFAP staining in bortezomib-treated rats was significantly higher at days 7 (n=6 vs. n=5), 14 (n=7 vs. n=5), and 30 (n=6 vs. n=6), but not at day 69 (n=3 vs. n=3). Co-treatment with minocycline resulted in siginificantly lower GFAP staining at day 30 (n=3). **(B)** GFAP staining in oxaliplatin-treated rats was significantly higher at days 7 (n=9 vs. n=8) and 14 (n=9 vs. n=9), but not at day 40 (n=4 vs. n=4). Co-treatment with minocycline resulted in GFAP staining equivalent to control at day 7 (n=6) and 14 (n=6). **(C)** Both GFAP and OX-42 staining were higher in ipsilateral spinal cord in SNL rats (n=6) versus contralateral cord. Neither GFAP nor OX-42 were higher in ipsilateral cord in sham-treated rats (n=6) versus contralateral cord. **(D)** OX-42 staining intensity in bortezomib-treated rats was significantly lower versus control at days 7 (n=6 vs. n=5), 14 (n=7 vs. n=5), and 30 (n=8 vs. n=9).

3.4. DISCUSSION

The present study aimed to establish whether or not astrocytes play an active role in oxaliplatin- or bortezomib-driven CIPN. The reported increases in GFAP were indicative of this kind of trend, but it is uncertain what the downstream effects of this activation may be. However, it is possible that astrocytes may have a bigger part in pain as a whole than previously thought. One group recently reported that microglia were not activated in a model of bone cancer pain (Ducourneau et al. 2014). It is therefore possible that microglia are an important part of some, but not all, types of pain. Astrocyte activation may be a far more universal form of reactive gliosis. It is possible that the production of proinflammatory cytokines by astrocytes may contribute to pain sensitization (Hald, 2009; Gao and Ji, 2010a; Bradesi, 2010). It is well-known that excessive levels of these cytokines may result in sensitization of neurons (Miller et al., 2009; Bradesi, 2010). The lack of a change in astroglial activation in response to minocycline certainly seems to suggest that this activation is mediated by inflammatory mechanisms. The case for proinflammatory cytokines is further supported by the fact that minocycline has prevented their upregulation in other models (Ledeboer et al., 2005; Mao-Ying et al., 2012). Many of the original studies using minocycline to affect glia report effects on microglia without impacting astrocytes (Yrjänheikki et al., 1999), but many other groups have reported that minocycline exerts a robust effect on both types of glia (Ledeboer et al., 2005; Ryu et al., 2004; Sung et al., 2012; Teng et al., 2004). These findings may very well depend on that model is used, but the data of the present study suggest a

mechanism for minocycline that does affect astrocytes. Co-treatment with both bortezomib and minocycline was showed mechanical sensitivity and GFAP expression resembling that of saline-treated controls. There was no concomitant activation of microglia to suggest that minocycline was targeting these cells, rather than astrocytes. Activation of either cell type may result in the production of proinflammatory messengers, so this suggests that minocycline's anti-inflammatory activity is at work in the present model. Although tetracyclines like these are usually classified as atibiotics, minocycline is usually prescribed for the treatment of inflammatory acne (Garner et al., 2012). Its clinical use would therefore also suggest a generalized anti-inflammatory mechanism. Additional research may benefit from quantifying cytokines like IL-1β and TNF-α (Sung et al., 2012; Mao-Ying et al., 2012). While these are largely expressed by microglia and neurons, these may also appear in astrocytes and could be targets of interest for future study.

There are a number of directions that future research may take in order to explain the apparently astrocyte-specific activation profile of the present study. Firstly, it is possible that astrocytes possess specific receptors that respond to extracellular damage or signals from outside the spinal cord altogether. Alternatively, it is possible that propagation of this CIPN model depends on inter-astrocyte signaling. Previous work has shown upregulation of astrocytic gap junctions following oxaliplatin treatment (Yoon et al., 2013), but it is still unknown whether this also occurs following treatment with other chemotherapeutic agents.

In addition to effects from cytokine expression, astrocytes may also contribute to a maladaptive condition through regulation of glutamate transporters (Liaw et al.,

2005; Cata et al., 2006a; Araque and Navarrete, 2010). Decreases in these glutamate transporters have been reported in both injury and chemotherapy models of neuropathy (Sung, Lim, and Mao, 2003; Weng et al., 2005; Cata et al., 2006a; Xin, Weng, and Dougherty, 2009; Zhang, Xin, and Dougherty, 2009) and may account for many of the maladaptive and pronounced symptoms that are reported clinically (Cata et al., 2007; Dougherty et al., 2007; Boyette-Davis et al., 2013). The persistent behaviors reported in the present study seem to suggest the possibility of glutamate transporter dysfunction (Fig. 6B). Based on the time course and intensity of glial activation and mechanical sensitivity, there is a strong possibility that the two are correlated, but this has not been examined in the present study with regard to other types of behavioral stimuli. Furthermore, other chemotherapy models have shown decreases in peripheral nerve fibers in the skin, but it is unknown at this time whether a similar effect is seen in bortezomib-treated animals. However, biopsies taken from human patients have indicated that this may be the case. This effect was likewise prevented by minocycline in animal models corresponding to other drugs. It is certainly likely that the initial damage driving bortezomib-induced peripheral neuropathy occurs outside of the spinal cord, but this warrants further study. Understanding where the insults induced by bortezomib treatmen exert their primary effects would be of particular interest in a clinical context in order to develop treatments with maximal therapeutic efficacy. The Cavaletti lab has indicated potential sites along the peripheral nerve upon which bortezomib may act, but there are several issues with these studies that warrant follow-up research (see introduction).

Unlike bortezomib-treated rats, the animals treated with oxaliplatin did not show a direct correlation in the time course of their mechanical sensitivity and astroglial activation. Instead, the astrocytes in these animals were activated at earlier time points, and activation decreased over time once treatment had ended. This suggests differential mechanisms between the two. It may be that astrocytes are activated in oxaliplatin-treated animals in an induction-dependent manner and that they are activated in bortezomib-treated animals in a maintenance-dependent manner. As with bortezomib-treated animals, however, oxaliplatin-treated animals co-treated with minocycline showed behavior and glial activity resembling controls.

Microglial activation was not observed at any time point in either of the chemotherapy models used in this study. The spinal nerve ligation animals used as positive controls, on the other hand, developed a robust microgliosis, even at the observed two-week time point. Many would argue that the microglia may still be active at early time points, as there are reports suggesting that these cells are responsible for the activation of astrocytes (Zhang et al., 2010). A follow-up investigation was therefore conducted to help rule out this possibility (Appendix) In conflict with our data, a recently-published study reported activation of microglia in oxaliplatin-treated animals at day 7 (Di Cesare Mannelli et al., 2013). However, this conflicts not only with the present data, but with earlier work that showed no microgliosis in chemotherapy-treated animals in general (Zheng, Xiao, and Bennett, 2011). It should be noted that the conflicting study used a far greater dose of drug than what was used in the present study, which may account for excess toxicity or

damage that may have recruited microglia. On the other hand, this is the second

such study in which our group has reported no sign of microglial activation in a

chemotherapy model of neuropathy (Zhang et al., 2012). This is similar to the lack of

observed microgliosis in other cancer models (Ducourneau et al. 2014). There may

therefore be a common pathway for glial cell activation in these models, even though

they are markedly different.

Another possibility is that using the OX-42 antibody alone may not fully

characterize the activation of microglia. The use of the antibodies OX-42 and Iba1

has been well documented for the measure of overall activity and proliferation of

microglia. However, microglia also present with different activation states with

markedly different purposes. The M2 state is a quiescent, pro-survival state that aids

in maintaining neuronal health, but the M1 state is a reactive, inflammatory state that

may be detrimental to survival of neurons (Guerrero et al., 2012; Hu et al., 2012;

Boche, Perry, and Nicoll, 2013). There may be a possibility that microglia may shift

from one state to another without proliferating or recruiting other microglia. In such a

case as this, an antibody like OX-42 would not detect this kind of change. However,

the proliferative tendencies of microglia in neuropathic conditions are well-

established.

Proinflammatory cytokines may indeed contribute to the CIPN state, but this

is generally thought of as primarily the territory of microglia (Ji and Suter, 2007;

Zhuang et al., 2007). For astrocytes to have this activity selectively, it may be

necessary to first identify some form of activation that is specific to astrocytes, such

as a receptor not found on microglia that triggers cytokine release. This should be

taken into account when designing future studies. Furthermore, previous data in other CIPN models suggests that the dysfunction of glutamate transporters is likely to be found in the present model, as well (Zhang, Xin, and Dougherty, 2009; Nie, Zhang, and Weng, 2010). At the very least, the present study has established that the observed behavioral and astrocytic changes are related, and this has provided ample direction for future research.

4.   GLUTAMATE TRANSPORTERS AND CONNEXINS IN BIPN

4.1.   INTRODUCTION

The former two studies focused on establishing altered behaviors corresponding neuronal function in the bortezomib CIPN model in rats and the correlated changes in persistent behaviors and astrocyte activation, respectively. From these two, it is possible to establish a correlation, but not a causal relationship. The goal of the third study was then to investigate a possible means by which astrocytes may directly contribute to BIPN. It is important to note that this is by no means exhaustive. Furthermore, the course of a single study is sufficient to strengthen this kind of case, but is not sufficient to conclusively determine how BIPN is induced or maintained. Nevertheless, this study was designed to show whether dysfunction of glutamate transporters and gap junctions in astrocytes occurs at the time point corresponding to the peak of mechanical sensitivity. These were selected as astrocyte-specific molecules which could contribute to changes observed in behavior and neuronal function if disrupted. These changes had been previously observed in other CIPN models, as well. The time point was selected in order to match any changes to the behavioral and electrophysiological data previously obtained. The hypothesis of this study was that increases in connexin 43 expression and decreases in GLT-1 and GLAST expression correspond with behavioral changes and astrocyte activation in the rat model of BIPN. The expression of

connexin 43 verified this, but data from the expression of glutamate transporters provided mixed results.

Bortezomib is a first-generation proteasome inhibitor chemotherapy drug used primarily for the treatment of multiple myeloma. Among its multiple side effects, bortezomib is known to produce chemotherapy-induced peripheral neuropathy (CIPN) that may be dose-limiting (Argyriou et al., 2012; Ferrier et al., 2013; Argyriou et al., 2014; Miltenburg and Boogerd, 2014). This neuropathy may extend long after the cessation of treatment, and current treatment options to manage CIPN symptoms are few and limited in their efficacy.

Among other forms of neuropathic pain, there is emerging evidence that spinal astrocytes and microglia may contribute to the model's development and maintenance. However, it is becoming apparent that astrocytes are activated in the absence of microglia in CIPN models. Our own lab has now demonstrated this in paclitaxel, oxaliplatin, and bortezomib models of CIPN (Zhang et al., 2012; Robinson, Zhang, and Dougherty, 2014a). However, there is currently limited evidence demonstrating precisely how astrocytes may contribute to CIPN. Potential candidate mechanisms have been identified, including the downregulation of glutamate transporters in paclitaxel (Zhang et al., 2012) and the upregulation of astrocytic gap junctions in oxaliplatin (Yoon et al., 2013). These provide promising explanations for observed behavioral changes, but these findings had not yet been replicated in other models of CIPN.

The investigation of glutamate transporter dysfunction as a possible mechanism for CIPN may be justified by observations of behavior and neuronal activity in the spinal dorsal horn. Downregulation of glutamate transporters leads to persistent synaptic glutamate, which is sufficient to potentiate action potentials, drive persistent after-discharges, and even generate spontaneous ectopic activity (Matute, Domercq, and Sánchez-Gómez, 2006; Yi and Hazell, 2006; López-Bayghen and Ortega, 2011). Downregulation of glutamate transporters through pharmacological means may even be sufficient to drive spontaneous nociceptive behaviors (Nakagawa and Kaneko, 2010). Previous work from our lab has demonstrated altered activity in spinal wide dynamic range neurons and downregulation of glutamate transporters in support of such a model in animals treated with vincristine or paclitaxel (Weng, Cordella, and Dougherty, 2003; Cata et al., 2006a). Work within the bortezomib model has demonstrated behaviors indicating persistent sensation and *in vivo* recordings showing potentiated responses and persistent after-discharges in spinal wide dynamic range neurons (Robinson et al., 2014). Taken together, it is possible that the changes observed in glutamate transporters in paclitaxel may also carry over to the bortezomib model, as well.

The activity of connexin 43 is another point of interest in CIPN. Connexin 43 is the protein in astrocytes that composes gap junction hemichannels that connect astrocytes together in a functional syncytium (Giaume and Liu, 2012; Theis and Giaume, 2012). The openings that are formed by astrocytic gap junctions are small, allowing only ions and molecules smaller than 1.2 kDa to pass. This is too small for the majority of signaling molecules, but astrocytic gap junctions permit the flow of

78

such messengers as calcium ions and glutamate between cells (Tabernero, Medina, and Giaume, 2006; Theis and Giaume, 2012; Pannasch and Rouach, 2013). Hemichannel-forming proteins are upregulated in conjunction with astrocyte activation in multiple models of insult or injury, suggesting an increase in intercellular communication in these reactive astrocytes (Homkajorn, Sims, and Muyderman, 2010; Chen et al., 2013; Chen et al., 2014). The potential downstream effects of this increased hemichannel expression are of great interest in CIPN. Increases in intracellular calcium in astrocytes may lead to decreased glutamate uptake or even direct release of glutamate from astrocytes (Malarkey and Parpura, 2008; Devinsky et al., 2013; Hansen and Malcangio, 2013; Aguirre et al., 2013). Thus, increases in connexin 43 potentially indicate a parallel means by which astrocytes decrease glutamate uptake at the tripartite synapse.

The focus of the present study is to assess the activity of the astrocytic glutamate transporters GLT-1 and GLAST and the activity of connexin 43 in bortezomib-treated animals. Data in support of previous findings in other models would explain behaviors and electrophysiological data seen in bortezomib-treated animals. The present work also includes minocycline in treatment groups, since this has been shown to prevent behavioral changes in bortezomib-treated animals. Therefore a direct role for connexins and glutamate transporters in bortezomib-induced peripheral neuropathy may only be established if (1) these proteins are altered in accordance with an observed change of behavior, and (2) if prevention of changes to behavior also prevent changes in these proteins. Carbenoxolone was included in additional treatment groups for behavioral data as a gap junction

decoupler (Juszczak and Swiergiel, 2009; Yoon et al., 2013), and ceftriaxone was included as an upregulator of glutamate transporter expression (Lee et al., 2008; Kim et al., 2011). The inclusion of these treatment groups was to establish whether pharmacological strategies to directly counteract possible changes would also prevent the development of behavioral changes. Positive data would indicate that changes to these proteins are sufficient to drive the bortezomib model of CIPN in animals.

4.2. METHODS

4.2.1. Animals

All procedures were reviewed and approved by the M.D. Anderson Institutional Animal Care and Use Committee and were in accordance with the guidelines established by the NIH and the International Association for the Study of Pain. 94 Male Sprague-Dawley rats between 60-75 days of age upon beginning treatment (300-350 g) were used for all experiments. Of these rats, all 94 were used for behavioral testing, but 21 of these were used for immunohistochemistry. Another 14 of these were used for Western blotting. Rats were housed in a facility with a 12h light/dark cycle and were given food and water *ad libitum.* All efforts were taken at each stage of the experiments to limit the numbers of animals used and any discomfort to which they might be exposed.

4.2.2. Drugs

Saline, minocycline, and bortezomib were administered by intraperitoneal injection, and volumes were calculated based on body mass to approximate a volume of 0.5 ml. The gap junction decoupler ceftriaxone (Sigma Aldrich) and the glutamate transporter upregulator carbenoxolone (Sigma Aldrich) were administered intrathecally at a volume of 10µL. Animals were divided into eight treatment groups: saline alone (n=11), saline + minocycline (n=11), saline + carbenoxolone (n=12), saline + ceftriaxone (n=12), bortezomib alone (n=12), bortezomib + minocycline (n=12), bortezomib + carbenoxolone (n=12), and bortezomib + ceftriaxone (n=12).

81

Bortezomib (Millennium Pharmaceuticals) was administered in saline vehicle at a dose of 0.15 mg/kg on days 1, 3, 5, and 7 of experimentation for a cumulative dose of 0.60 mg/kg. Equivolume saline was administered to rats not treated with bortezomib. Animals treated with minocycline hydrochloride (Sigma Aldrich) were injected daily with 25.0 mg/kg minocycline in saline vehicle beginning at day 0 and continuing daily through day 8 (one day past chemotherapy treatment) of experimentation for a cumulative dose of 225mg/kg. Carbenoxolone (25µg/day) and ceftriaxone (150µg/day) were administered on the same schedule as minocycline for cumulative intrathecal doses of 225µg and 1350 µg, respectively. Animals not injected with carbenoxolone or ceftriaxone were administered an equivalent volume of saline intrathecally on the same dosing schedule.

4.2.3. Behavior Testing

Von Frey filament testing was used to assess mechanical sensitivity over time as previously described (Boyette-Davis and Dougherty, 2011; Boyette-Davis et al., 2011b; Robinson, Zhang, and Dougherty, 2014a). Briefly, filaments calibrated to a bending force equal to 4g, 10g, 15g, and 26g were applied 6 times each to the mid-plantar surface of each hindpaw. Animals were allowed a half-hour to habituate to the testing apparatus prior to application of filaments. Testing began with the lowest (4g) filament and escalated in filament size until a withdrawal threshold was reached. 5 to 10 minutes was allowed between filaments in order to minimize responses due to anxiety or sensitization. Filaments were applied with steady force

until bending of the filament was observed and held for approximately 1second. Responses were classified as a rapid withdrawal of the paw immediately followed by a return of the paw to the mesh. The threshold for sensitivity to mechanical stimuli was recorded as the bending force of the filament for which at least 50% of applications elicited a response. The mean was reported for each treatment group at each time point. Error was reported as standard error of the mean (SEM), and significance was tested at each time point using Mann-Whitney tests.

4.2.4. Tissue Collection

On day 30, following the final time point of behavioral testing, animals were sacrificed for tissue collection. Rats were overdosed with sodium pentobarbital (150mg), then perfused intracardially with room temperature heparinized saline, followed by cold 4% paraformaldehyde in 0.1M phosphate buffer. After tissue fixation was verified by rigidity of the rat's extremities, spinal cords were removed and post-fixed in 4% paraformaldehyde at 4°C overnight. Spinal cords were then moved to 15% sucrose the following day, then moved after another 24h to 30% sucrose for a minimum of 48h. The lumbar enlargement was mounted and the L5 segment cut in a cryostat at a thickness of 30μm.

For Western blotting, fresh tissue was collected from a different group of animals. Animals were overdosed with sodium pentobarbital (150mg). Each animal was then sacrificed via decapitation, and the spinal cord was quickly removed. The dorsal horns of the spinal cord were taken and frozen rapidly using liquid nitrogen.

All samples were then kept at -80°C until tissue could be processed. Following this, tissue was homogenized in lysis buffer and centrifuged. The supernatant was taken and had protein concentration quantified via Lowry assay. Protein concentration was then adjusted to 1μg/μL for all samples and heated at 70°C for 10 minutes.

4.2.5   Immunohistochemistry

Spinal cord slices were washed in phosphate buffered saline (PBS) for 6 washes lasting 15 minutes each and then blocked in normal donkey serum (5% NDS and 0.2% triton X in PBS). Slices were incubated overnight at 4°C with primary antibodies against GFAP (mouse anti-rat 1:1000, Cell Signaling Technology), connexin 43 (rabbit anti-rat 1:1000, Invitrogen), GLT-1 (guinea pig anti-rat 1:2000, Chemicon), or GLAST (rabbit anti-rat 1:250, Abcam). Slices were washed the following day in PBS for 6 washes lasting 15 minutes each, then incubated with secondary antibodies. For one set of tissue, slices were incubated with FITC-conjugated donkey anti-mouse secondary antibody for GFAP detection (1:500, Jackson Immunoresearch) and Cy-3-conjugated donkey anti-rabbit secondary antibody for Cx43 detection (1:500, Jackson Immunoresearch). A second set of tissue was incubated with FITC-conjugated donkey anti-guinea pig secondary antibody for GLT-1 detection (1:500, Jackson Immunoresearch) and Cy-3-conjugated donkey anti-rabbit secondary antibody for GLAST detection (1:500, Jackson Immunoresearch). All tissue was incubated with secondary antibodies for 2

hours at room temperature. Slices were washed for a final course of 6 washes

lasting 15 minutes each, then mounted onto glass slides using Vectamount medium.

4.2.6. Quantification of Immunohistochemistry

Slices were viewed and images captured using fluorescent illumination at 20X

magnification using a Nikon Eclipse E600 microscope. Captured images were

analyzed using NIS Elements software (Nikon, USA). A region of interest was drawn

within the dorsal horn containing lamina I and II for quantification purposes. A region

outside of the tissue slice was selected as background, and its signal was subtracted

from the entire image. The signal within the dorsal horn region of interest was then

expressed as intensity in pixels/μm^2. For each treatment group, the mean of these

values was calculated and expressed as a percent versus the mean values of the

saline-treated group. Error was expressed as the combined standard error of the

mean (SEM) for the corresponding treatment and saline-treated groups to account

for variability within controls. Significance was determined via t-test (P = 0.05, 0.01).

4.2.7. Western Blotting

For each Western blot, 20μL of each sample (20μg protein) was separated

via gel electrophoresis and transferred to polyvynilidene (PVDF) membranes. After

transferring, membranes were washed three times for 10 minutes each in Tris-

buffered saline with Tween-20 (TBST). Membranes were then blocked in a solution

of 5% powdered nonfat milk in TBST for 1 hour at room temperature. Primary

antibodies were added, and membranes were incubated overnight at 4°C. The membranes were then washed three times for 10 minutes each in TBST. These were then incubated with secondary antibodies conjugated against horseradish protein (HRP) in 5% nonfat milk/TBST solution for 30 minutes at room temperature and washed a final three times at 10 minutes each in TBST. Target proteins on membranes were then visualized using an enhanced chemiluminescence system (Amersham Pharmacia Biotech, Little Chalfont, UK). Primary antibodies were selected in order to verify changes observed in immunohistochemistry. The primary antibodies used for Western blotting were the same as those used for immunohistochemistry, incubated at a 1:1000 concentration. Mouse anti-rat beta-actin (1:10,000, Sigma) was also included as a control for basal protein expression. Secondary antibodies were either goat anti-rabbit or goat anti-mouse HRP-conjugated antibodies (1:10,000, Calbiochem).

Band intensity was quantified using ImageJ software, available from the NIH website. A region of interest containing the full band was taken, and background was subtracted. The expression of a protein was then quantified as the ratio of the expression of that protein over the expression of beta-actin in the same lane. The average of these values was taken for saline treated controls. The other treatment groups were then normalized as a percentage of this value. Error bars were calculated as the SEM, and significance was determined via t-test (p = 0.05, 0.01). For the connexin 43 antibody, which detects three bands for different phosphorylation states, this calculation was performed for total amount of connexin 43 and for each phosphorylation state.

4.3. RESULTS

4.3.1. Mechanical Withdrawal Thresholds

Mean withdrawal thresholds across groups were not significantly different at baseline (Fig. 12). Animals treated with saline alone or saline with minocycline, carbenoxolone, or ceftriaxone (not shown) did not change over time versus baseline withdrawal threshold. Bortezomib-treated animals first showed a significant difference in withdrawal thresholds versus saline-treated controls at day 14 (19.5 ± 1.9g saline/ 11.2 ± 0.9g bortezomib). Thresholds continued to decrease and showed significant differences at day 21 (18.1 ± 2.4g saline/ 6.5 ± 0.9g bortezomib) and day 28 (20.6 ± 2.1g saline/ 7.1 ± 1.2g bortezomib). Animals co-treatmed with minocycline, ceftriaxone, or carbenoxolone did not differ significantly from saline-treated controls at any time point that was tested.
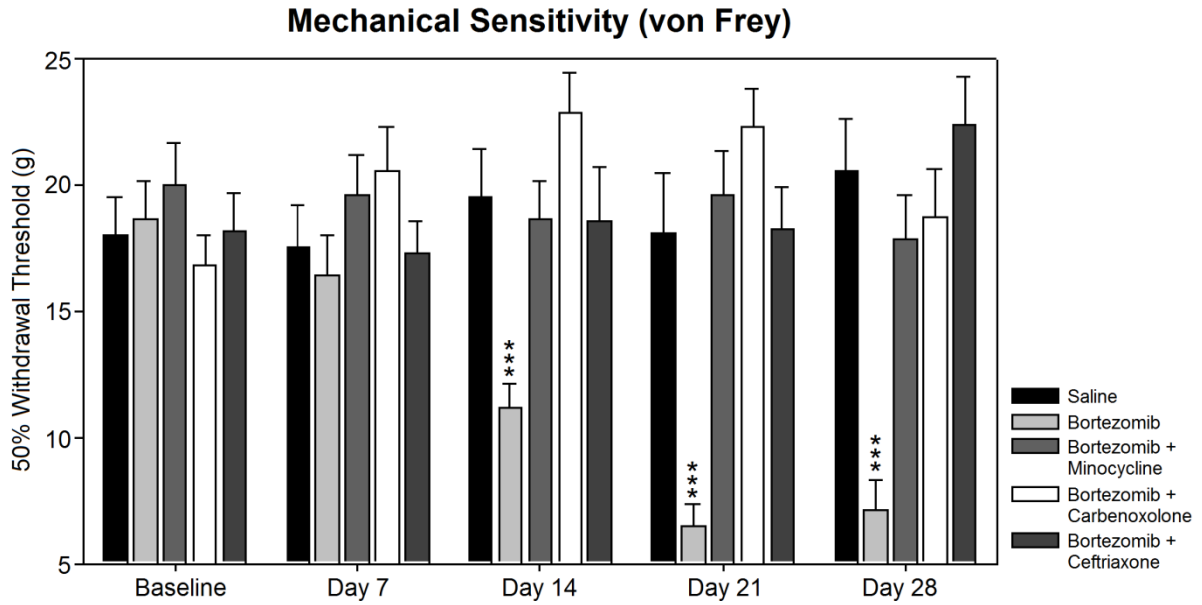
Figure 12. Mechanical sensitivity was assessed in bortezomib-treated animals versus preventative treatment groups. Treatment of animals with bortezomib (n=12) induced mechanical hypersensitivity versus saline-treated controls (n=11) that was not observed in rats co-treated with minocycline (n=12), carbenoxolone (n=12), or ceftriaxone (n=12). Rats treated with minocycline (n=11), carbenoxolone (n=12), or ceftriaxone (n=12) alone did not develop mechanical hypersensitivity (not shown).

4.3.2. Astrocyte Activation

GFAP staining for astrocytes showed no difference in minocycline-treated rats versus saline-treated controls (104.9 ± 13.6% of control) (Fig. 13). Astrocytes from these groups showed thin arbors and uniform distribution throughout the dorsal horn gray matter (top-left and bottom-left panels). Bortezomib-treated rats showed significantly higher GFAP activation versus controls (132.1 ± 16.9% of control). Astrocytes from this group showed brighter staining, hypertrophy, and increased arborization (top-right panel). Distribution of astrocytes was uniform throughout the dorsal horn in this group, as well. Minocycline co-treatment animals were not significantly different from controls (113.1 ± 16.2% of control). Qualitative observations of cell size, brightness, arborization, and distribution indicated no apparent difference in the astrocytes in this tissue versus saline-treated controls (bottom-right panel). These findings are in line with previous data from our lab showing the same profile of activation (Robinson, Zhang, and Dougherty, 2014a).

GFAP Expression

Figure 13. Activation of GFAP was expressed as percent fluorescence intensity versus mean fluorescence intensity of control. Treatment of animals with bortezomib (n=5) induced a significantly increased expression of GFAP in astrocytes versus saline-treated controls (n=6). Animals co-treated with minocycline (n=5) did not differ from saline-treated controls. Minocyline alone (n=5) did not affect GFAP activity.

4.3.3. Connexin 43 Expression

Staining for connexin 43 activation was equivalent in minocycline-treated rats versus saline-treated controls (97.3 ± 17.6% of control) (Fig. 14). Connexin 43 staining was distributed evenly throughout the dorsal horn (top-left and bottom-left panels). The staining was granular in appearance, indicating staining of gap junctions apart from background levels of staining. Bortezomib-treated rats showed a significant upregulation of connexin 43 expression (131.3 ± 19.3% of control). The dorsal horn staining appeared brighter in this tissue than in saline-treated controls (top-right panel). This could indicate either increases in the brightness of individual gap junctions or an increase in the number of gap junctions. Rats that were also treated with minocycline did not differ from controls (111.7 ± 19.9% of control). Levels of connexin 43 in these animals were higher than in saline-treated controls, but the difference was not significant (bottom-right panel). Staining was slightly brighter in this tissue than in saline-treated controls, but it maintained an even distribution and granular appearance. This would indicate a significant abrogation by minocycline of the connexin increases induced by bortezomib.

Connexin 43 Expression

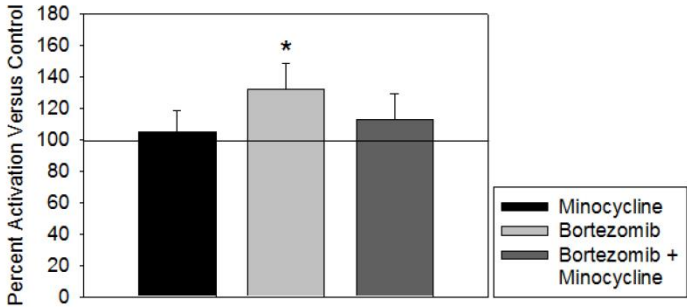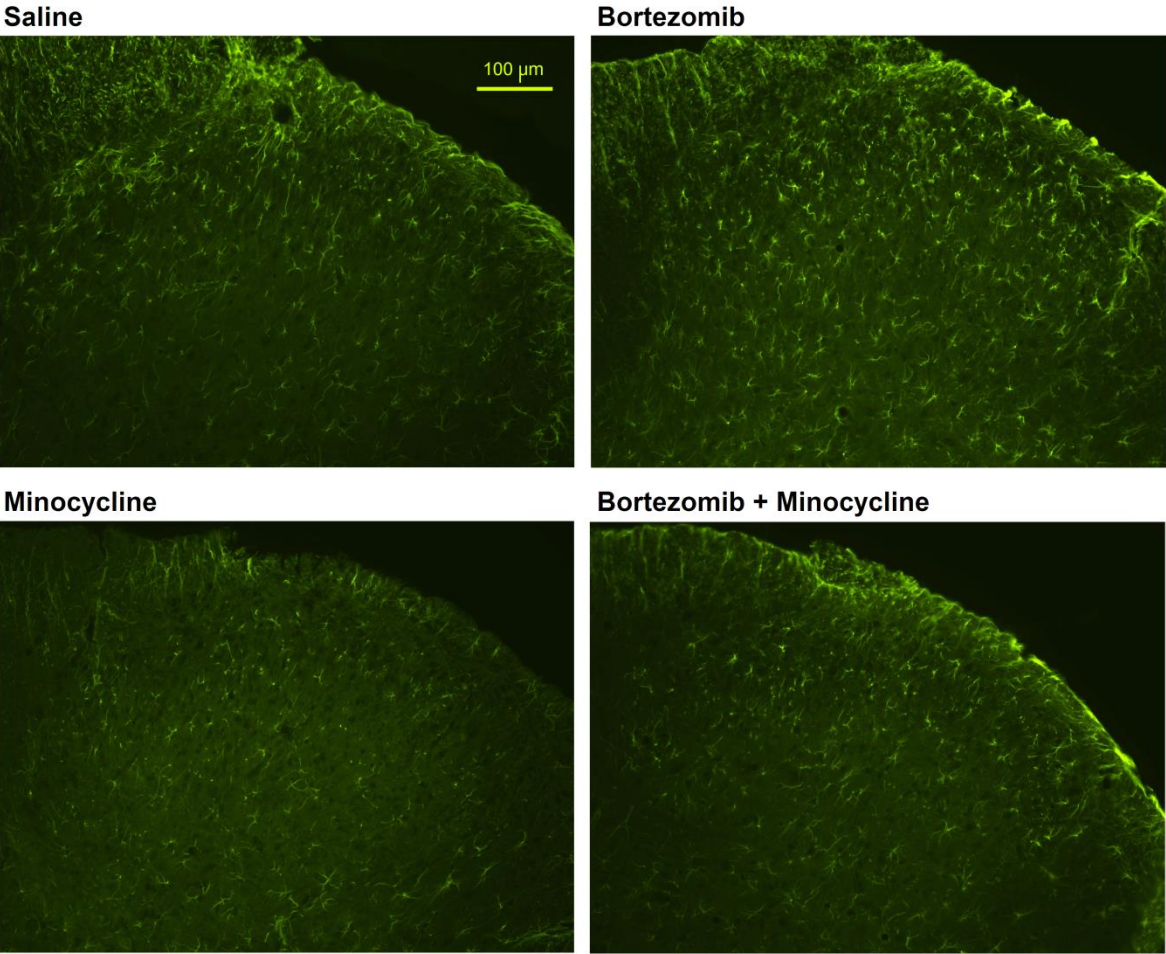**Figure 14.** Expression of connexin 43 was represented as percent fluorescence intensity versus mean fluorescence intensity of control. Treatment of animals with bortezomib (n=5) induced a significantly increased expression of connexin 43 in the spinal dorsal horn versus saline-treated controls (n=6) Animals co-treated with minocycline (n=5) did not differ from saline-treated controls. Minocyline alone (n=5) did not affect connexin 43 activity.

4.3.4. GLT-1 Expression

Staining for GLT-1 activation did not differ significantly between minocycline-treated and saline-treated groups (111.7 ± 8.1% of control) (Fig. 15). There was also no change detected in rats treated with bortezomib (102.9 ± 10.5% of control) or bortezomib and minocycline (98.4 ± 12.3% of control). GLT-1 staining was not localized to any one region of the spinal cord gray matter. There was minimal staining within the white matter, which reflects the paucity of synapses in these regions. Furthermore, staining was granular in appearance, but difficult to distinguish in appearance from background staining. The difficulty in distinguishing background from signal could potentially mask smaller changes, but the current data did not indicate any difference between treatment groups with this staining.

GLT-1 Expression
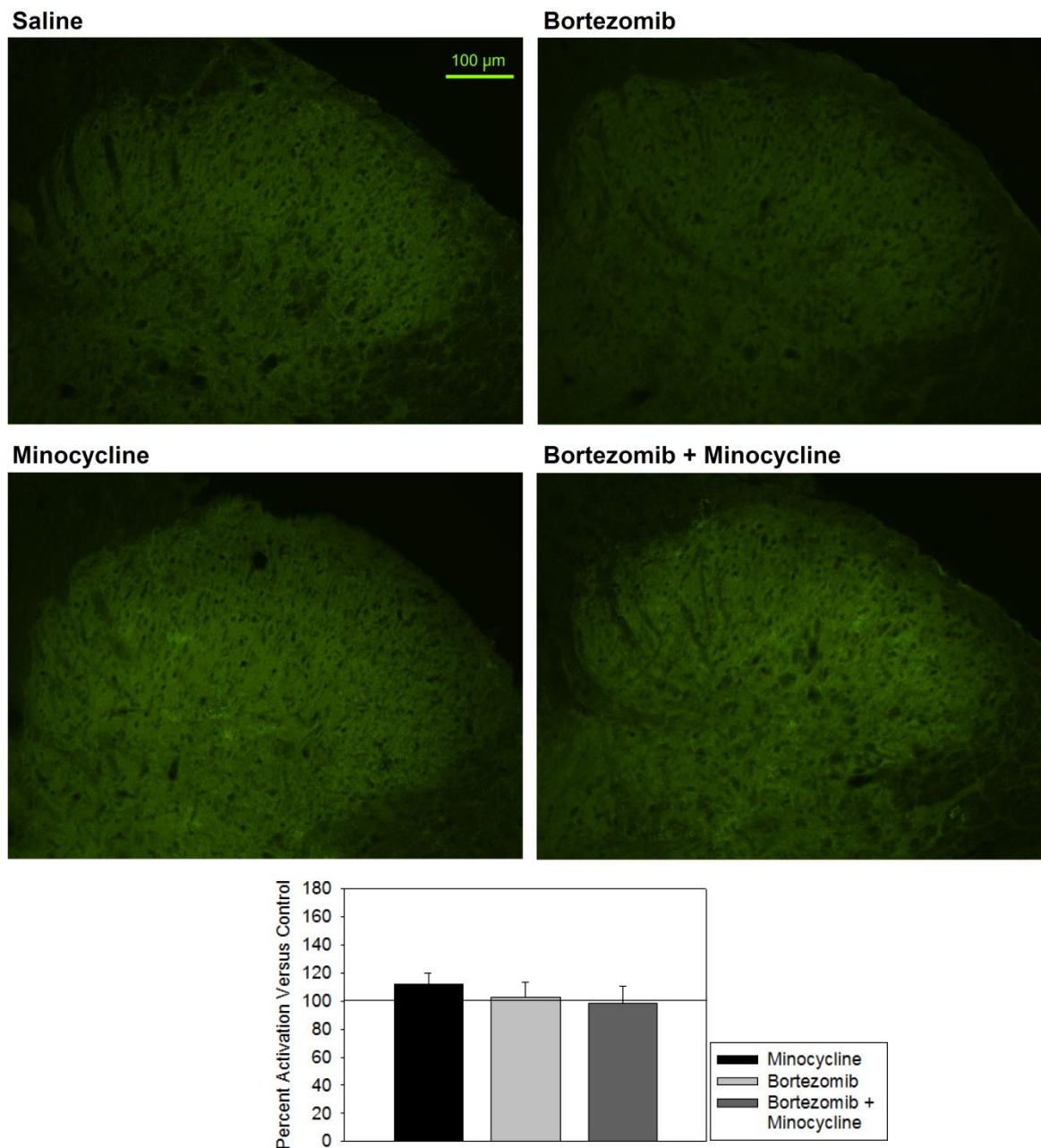
Figure 15. Expression of GLT-1 was represented as percent fluorescence intensity versus mean fluorescence intensity of control. Treatment of animals with bortezomib (n=5), minocycline alone (n=5), or bortezomib + minocycline (n=5) showed no change in GLT-1 expression in the spinal dorsal horn versus saline-treated controls (n=6).

4.3.5. GLAST Expression

Expression of GLAST was not significantly different in minocycline-treated rats versus saline-treated rats (106.7 ± 10.5% of control) (Fig. 16). Staining was most densely localized to the first two laminae of the dorsal horn, which is where nociceptive neurons synapse (top-left and bottom-left panels). Staining was granular in appearance. Bortezomib-treated rats showed significantly lower expression of GLAST (81.5 ± 8.5% of control), as did animals co-treated with minocycline, although to a lesser extent (top-right and bottom-right panels). However, there did not appear to be analogous differences in staining in regions outside of the quantified region. It is difficult to say whether this is truly the case, considering that the far greater brightness in the first two laminae could overshadow lesser changes. Animals treated with both bortezomib and minocycline still showed significantly lower expression of GLAST versus saline-treated animals (87.0 ± 7.9% of control), although this change showed a lower degree of significance versus animals treated with bortezomib alone.
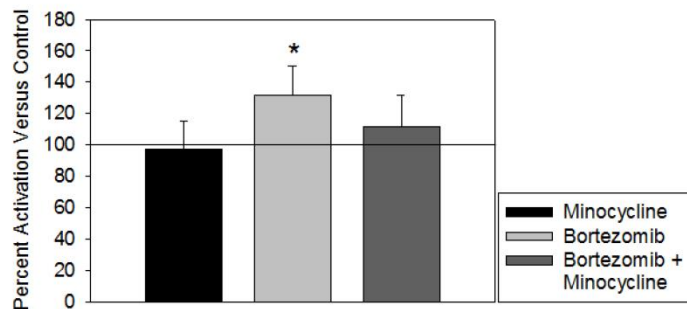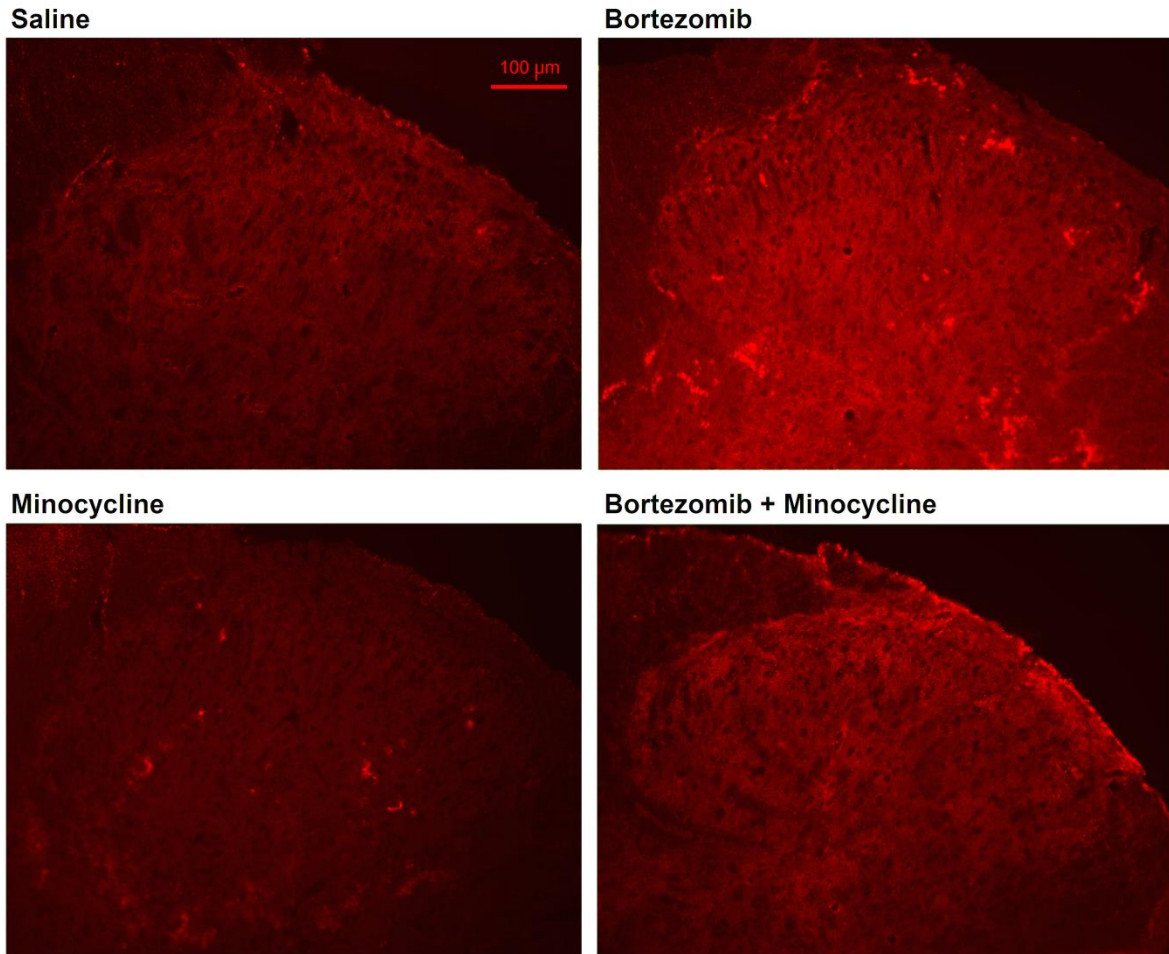
GLAST Expression
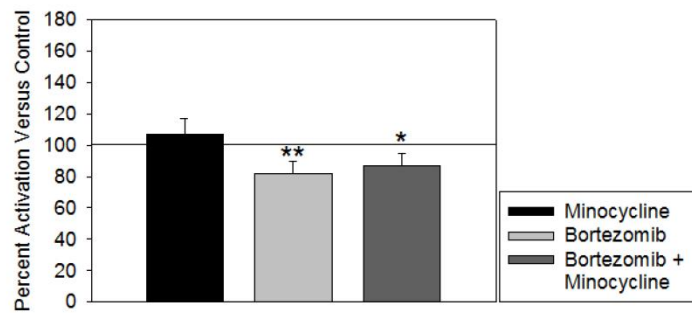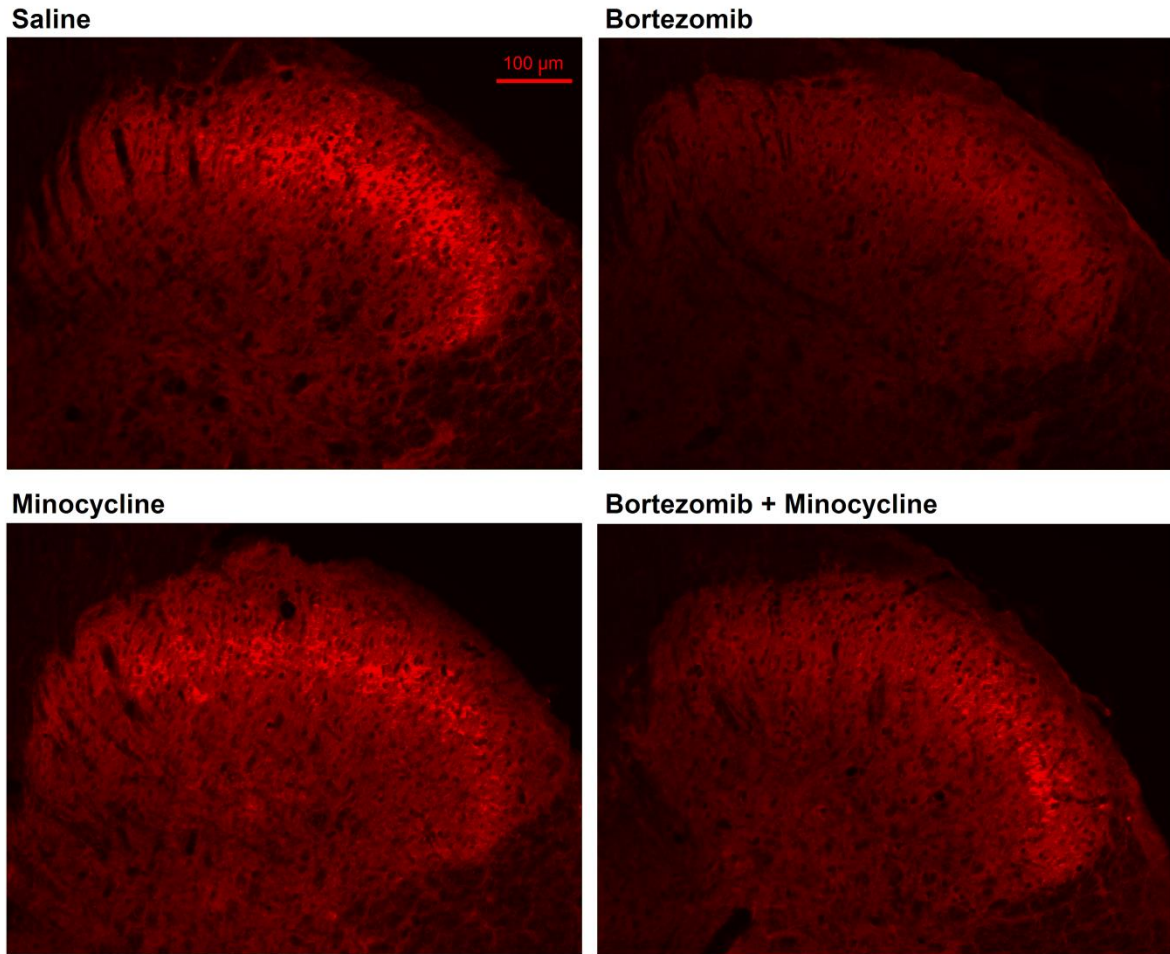
Figure 16. Expression of GLAST was represented as percent fluorescence intensity versus mean fluorescence intensity of control. Treatment of animals with bortezomib (n=5) significantly decreased expression of GLAST in the spinal dorsal horn versus saline-treated controls (n=6). Animals co-treated with minocycline (n=5) differed from saline-treated controls, but decrease of GLAST was not as pronounced. Minocyline alone (n=5) did not affect GLAST activity.

4.3.6. Western Blotting

Western blotting data for the GLAST antibody yielded no significant differences between any of the treatment groups (Fig. 17). Tissue from animals treated with minocycline alone showed slightly lower staining than saline-treated animals, but these differences were not significant. However, connexin 43 expression showed significant changes in the expression of its different phosphorylation states (Fig. 18). The different bands detected by the connexin 43 antibody corresponded to non-phosphorylated (NP), phosphorylated (P1), and phosphorylated (P2) forms of connexin 43. There was no significant difference between groups in the NP bands or the P2 bands. There was, however, a significantly higher expression of phosphorylated (P1) connexin 43 in both the groups treated with bortezomib alone (494.7 ± 103.7% of control) and those treated with both bortezomib and minocycline (308.0 ± 85.3% of control). The antibody used was for the detection of overall connexin 43 expression, rather than phosphorylated connexin 43 selectively. It is therefore unlikely that the observed effects are a result of preferential staining of one state over another. The tissue corresponding to bortezomib-treated animals also appeared to have greater overall staining, but this was not compared quantitatively.
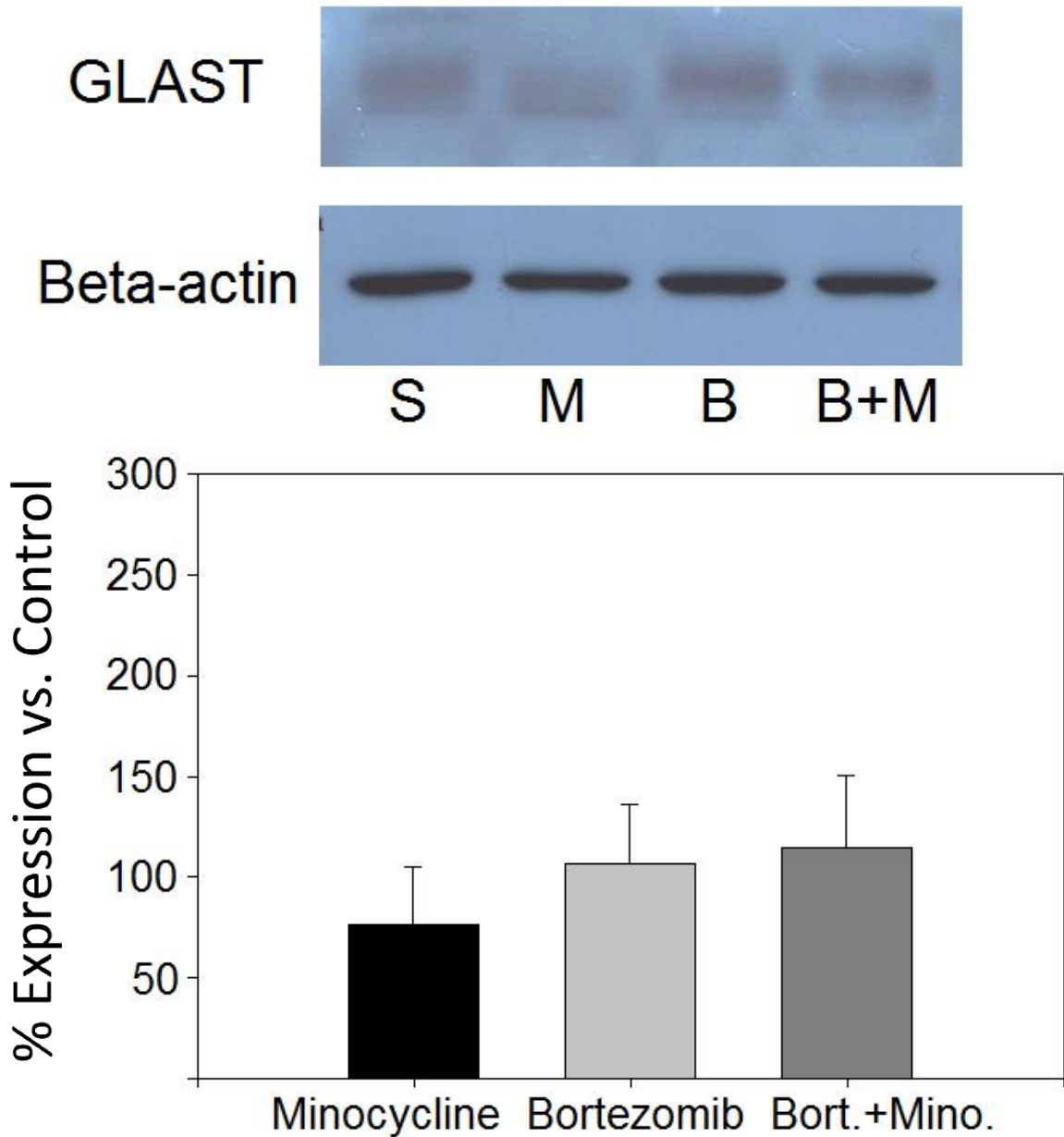
Figure 17. Western blotting data for GLAST did not indicate significant differences between treatment groups. Treatment groups included saline (n=4), minocycline (n=4), bortezomib (n=4), and bortezomib + minocycline (n=4). Ratios for each band were calculated as GLAST intensity over beta-actin intensity within the same lane. Band intensity was expressed as a percent increase of the average ratio for a treatment group versus the average ratio of saline-treated controls.
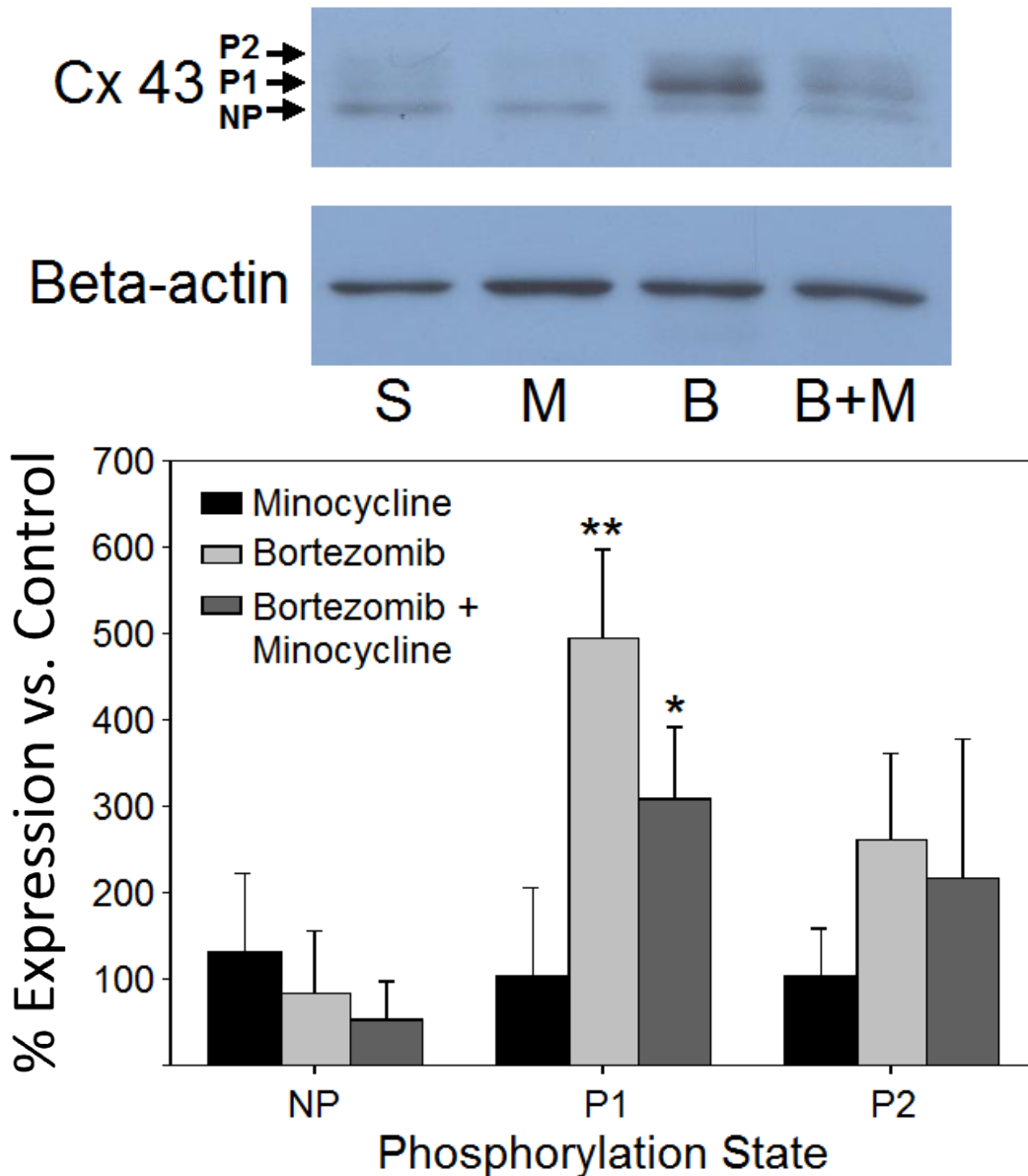
Figure 18. Western blotting data for connexin 43 indicated significant differences between treatment groups. Treatment groups included saline (n=3), minocycline (n=4), bortezomib (n=3), and bortezomib + minocycline (n=4). Bands for individual phosphorylation states indicated an increase in the P1 phosphorylation state of connexin 43 in animals treated with bortezomib or bortezomib + minocycline. Ratios for each band were calculated as connexin 43 intensity over beta-actin intensity within the same lane. Band intensity was expressed as a percent increase of the average ratio for a treatment group versus the average ratio of saline-treated controls.

4.4.   DISCUSSION

The data in the present study show alterations in astrocytic connexins and glutamate transporters in animals treated with bortezomib. Previous work in our lab has shown a clear involvement of astrocytes in various forms of CIPN, and these changes provide a possible means by which astrocytes may contribute to these models. First, GFAP staining and von Frey mechanical sensitivity were used to verify the bortezomib-induced behavioral changes. Development of mechanical hypersensitivity and astrocyte activation were in line with previous data from our lab (Robinson, Zhang, and Dougherty, 2014a; Robinson, Zhang, and Dougherty, 2014b).

For immunohistochemistry, the 30-day time point in this model was selected because it corresponds to peak behavioral sensitivity. In addition to the activation of GFAP, increased expression of connexin 43 was observed. The changes in the levels of these two markers were nearly identical. This increase in connexin 43 expression suggests possible increased flow of calcium ions between astrocytes that may result in glutamate release. A possible point of interest for future experimentation would be to verify whether this glutamate release occurs *in vitro*. Alternatively, *in vivo* electrophysiology in rats treated with gap junction decouplers like carbenoxolone could be employed to see whether this inhibition of connexin 43 prevents potentiated responses to stimuli. However, it is possible that the connexins are responsible for the transport of other intercellular signal molecules. What exactly they may contribute in the context of this model is currently unknown, but the data in

the present study show a clear correlation between peak hyperalgesia and connexin activity.

The involvement of glutamate transporters in the present study was less clear-cut than that of connexin 43. While GLAST was downregulated in the immunohistochemistry data in this model, no change was observed in GLT-1 expression. It is unknown why one form of astrocytic glutamate transporter would be depressed without another. However, the decreased levels of at least one form of glutamate transporter at the peak of the behavioral changes suggests a mechanism for persistent sensations and persistent after-discharges observed in other studies from our lab (Robinson, Zhang, and Dougherty, 2014a; Robinson, Zhang, and Dougherty, 2014b). One possibility for the disparity between GLT-1 and GLAST is that GLT-1 activity may be involved at a different time point. The possibility of early and late forms of glutamate transporter downregulation has not been explored to the knowledge of the author, but another study from our lab has shown GLT-1 and GLAST downregulation at earlier time points that returns to baseline at later time points (Zhang et al., 2012). The successful use of ceftriaxone, which is generally considered to be specific to GLT-1 upregulation (Lee et al., 2008), would suggest that early GLT-1 changes are a strong possibility. It is therefore possible that a follow-up study examining earlier time points in bortezomib-treated rats would yield a similar result of early downregulation of GLT-1. The early downregulation of glutamate transporters would then suggest the induction of central sensitization that persists long after the changed expression resolves.

The Western blotting data both validated and contradicted the changes observed in immunohistochemistry. The lack of any change observed in GLAST is difficult to explain, but it is possible that the means of processing the tissue for Western blotting washed out any changes that may have occurred. Considering that the change in expression observed in immunohistochemistry was less than 20% and surveyed only in the first two laminae of the dorsal horn within the gray matter, it is possible that inclusion of the entire dorsal half of the spinal cord for Western blotting diluted any changes that may have occurred in a much smaller region.

The changes observed in connexin 43 Western blotting, on the other hand, were of particular interest. There was a clear shift in phosphorylation of connexin 43 in bortezomib-treated animals. The P1 phosphorylation state of connexin 43 corresponds to increased trafficking of connexin 43 from the cytoplasm to the membrane (Solan and Lampe, 2007). This would indicate that there is not only an apparent increase in overall expression of the protein, but that it is also being transported for use within a greater number of gap junctions, as well.

The activity of minocycline co-treatment in the present study showed more similarity to controls versus the changes induced by bortezomib. Behavior, GFAP expression, and connexin 43 expression did not differ significantly from controls, and the changes observed in GLAST were not as significant as the changes observed in animals treated with bortezomib alone. Furthermore, the phosphorylation states of connexin 43 in animals treated with both bortezomib and minocycline indicate that minocycline exerted its effects on connexin 43 activity by affecting the increase in

expression, rather than by altering its post-translational modification. This suggests that minocycline acts on a target upstream of the regulation of connexin 43.

The behavioral data obtained from animals co-treated with carbenoxolone or ceftriaxone showed that these animals did not differ in behavior from saline-treated controls. Further studies using these three agents may provide important information on the mechanisms of CIPN as well as potential therapeutic strategies for its prevention.

Previous studies from our lab have clearly demonstrated a correlation between astrocytes and animal models of CIPN. The changes to connexin and glutamate transporter expression observed now in bortezomib-treated animals provide mechanistic support for direct astrocytic involvement. In conjunction with similar studies in oxaliplatin and paclitaxel, there is increasing evidence for a unified pathway for the development of CIPN. However, upstream mechanisms for astrocyte activation are not well understood. A recent study from our lab in paclitaxel-treated rats has demonstrated increases in TLR4 and MyD88 in DRG and TLR4 in spinal cord (Li et al., 2014). This suggests that damage-associated molecular patterns from outside of the spinal cord may activate astrocytes. It also strongly suggests increases in proinflammatory cytokines released from astrocytes. This could have a direct impact on glutamate transporter expression, and it could further sensitize surrounding neurons to glutamate signaling directly. Furthermore, TLR4 activation is capable of upregulating connexin 43 (Aguirre et al., 2013), which strongly suggests a possible single site for all of the activity observed in gap junction, glutamate transporter, and cytokine regulation. However, whether or not

TLR4 is activated by chemotherapy treatment as a whole has yet to be verified

outside of the paclitaxel model. Future studies should be conducted to verify whether

this occurs in the bortezomib model, as well. The activity of astrocytes provides a

very promising point for studies to elaborate on an overall pathway for CIPN, as well

as for the development of therapeutic strategies for its prevention.

5.   CONCLUSION

5.1.   General Conclusions

The research encompassed by this dissertation was geared towards an understanding of one possible means by which bortezomib may cause chemotherapy-induced peripheral neuropathy. To provide a true answer to this question is far beyond the scope of what is attainable in a single dissertation, but the present work was sufficient to set a basic framework for future study. Prior research was sufficient to establish a possible link between astrocytes and CIPN in paclitaxel, but these observations had not been generalized to other drugs.

Because of the lack of previous research published on BIPN in animals, it was important to first characterize what behavioral modalities are affected within the rat model and how neuronal responses in the spinal cord may be altered. Without this first step, it would have otherwise been impossible to tie any mechanistic studies back to the overall presentation of BIPN in rats. The summarized findings of this initial study were that sensitivity to mechanical stimuli was increased in bortezomib-treated animals without affecting heat or cold sensation or motor capability, and bortezomib-treated animals showed persistent withdrawal behaviors that paralleled increased activity and persistent after-discharges in spinal wide dynamic range neurons. These findings were distinct from the trend seen in patients, which includes sensitivity to cold stimuli, as well as behaviors seen in other models of CIPN. However, the activity of spinal WDR neurons was in line with previous findings and provided a case for disrupted glutamate transport. Although the stimulus application

in this data was not blind, the activity of neurons in response to venous clip or arterial clip, which are free of observer input, nevertheless provided objective measures of increased and persistent WDR neuron firing.

The second major point of study followed on previous findings within our lab that demonstrated activation of astrocytes in paclitaxel in the absence of microglial activation. In this study, the same general activation profile was found in animals treated with bortezomib or oxaliplatin. The time course of this activation varies from one drug to another, but this study showed a generalized correlation between CIPN and activation of astrocytes. Furthermore, this study demonstrated that behaviors and expression of observed proteins in animals co-treated with minocycline either did not differ from saline-treated controls or showed less of a change than those treated with bortezomib alone. This strongly suggested that proinflammatory signals drive both the behavior and glial activity. Nevertheless, this was not sufficient to establish a causal relationship.

The final study sought to establish a means by which astrocytes may directly contribute to BIPN through mechanisms specific to these cells. The activation profile of connexins and glutamate transporters in this study revealed that connexin 43 and GLAST were affected at the time point corresponding to peak behavioral sensitivity. This evidence favors a glial mechanism for BIPN, as the disruption of glutamate transport and increases in inter-astrocyte signaling could explain enhanced and persistent responses at the behavioral level. This still does not exhaust every possibility for a role for astrocytes, and it does not conclusively explain what happens downstream from connexin upregulation. However, this study established a

high likelihood that the simultaneous changes in behavior and glial activation are directly related.

The findings of these studies support a model of astrocyte involvement in an animal model of BIPN. The observed activation is present in every instance of the disorder, it is not present in the absence of the disorder, and suppression of this change coincides with the suppression of the disorder. However, future studies should focus on establishing upstream and downstream targets to clarify more exactly the role of astrocytes in BIPN. The present studies have not included a survey of proinflammatory cytokines and chemokines induced by BIPN, in spite of the clear activity of minocycline in affecting how bortezomib impacts behavioral and glial changes. However, because of the diverse activity of proinflammatory cytokines and chemokines that may be induced by activation of astrocytes, this could be the subject of a dissertation on its own. Among the possible activities related to proinflammatory messengers, it is possible that their release from astrocytes would be sufficient to lower response thresholds in neurons and drive central sensitization. In combination with the present findings regarding glutamate transport and connexins, such a finding could explain a mechanism by which astrocyte activation contributes to BIPN.

From a therapeutic perspective, it would be extremely important for future studies to investigate the upstream components that are responsible for astrocyte activation. The inability of bortezomib to cross the blood-brain barrier clearly indicates that BIPN begins in the periphery. It is therefore important to investigate how peripheral nerve fibers and dorsal root ganglia may be affected by bortezomib

so that therapeutic strategies may target BIPN at its root. Findings in paclitaxel that heat shock proteins are activated in spinal astrocytes (Li et al., 2014) need to be investigated in bortezomib-treated rats, as well. A translation of these findings to the bortezomib model would suggest a means by which astrocytes may be activated. Heat shock proteins such as HSP90 respond to a diverse array of both pathogen-associated molecular patterns (PAMPs) and damage-associated molecular patterns (DAMPs) (Harris, Andersson, and Pisetsky, 2012; Zhao et al., 2014). In particular, DAMPs like high mobility group box 1 (HMGB1) are released following cellular stress or damage (Harris, Andersson, and Pisetsky, 2012; Keyel 2014). Therefore, if damage at the level of the dorsal root ganglion occurs in response to bortezomib treatment, it is possible that release of HMGB1 could activate astrocytes and potentiate neuronal responses in the dorsal root ganglion. However, this requires extensive investigation in order to be anything more than conjecture and is only one possibility. If the findings related to heat shock proteins in paclitaxel are replicated in bortezomib, then it is possible that a pathway like this one could be at the heart of CIPN as a whole.

In addition to establishing a preclinical model of BIPN, the findings in the present studies must also be translated into clinical studies in order to be effective. While the astrocytes cannot be surveyed directly in living patients, the present studies have provided potential molecular targets and therapeutic agents for investigation in clinical trial. In particular, minocycline has shown great promise. Our lab has been in collaboration with other investigators previously to investigate the effects of minocycline in bortezomib-treated patients, but these efforts were

inconclusive. This trial therefore needs repetition in order to ascertain whether or not minocycline is effective in patients, as well. Even if it is not, there may be other, more specific drugs that may prove to be effective. However, minocycline is already well-established and safe, and it is therefore also desirable from a standpoint of FDA approval. Additional studies will also be necessary to ensure that any possible treatments for the prevention of BIPN do not negatively impact the efficacy of bortezomib as an anti-tumor agent.

The present studies show promise for identifying a cause for bortezomib-induced peripheral neuropathy, as well as potentially chemotherapy-induced peripheral neuropathy as a whole or other neuropathies altogether. It is clear that astrocytes are more intimately involved in such disorders than previously thought, and it is possible that the impact of this work may have ramifications that bleed over into other areas of research in the future.

5.2. Shortcomings of the Animal BIPN Model

The findings of this dissertation have provided several promising targets for future study in characterizing BIPN. However, there are several points at which the animal model does not fully match what is seen in patients. The first of these to address is that the rats used in modeling BIPN do not have cancer. It is entirely possible that some BIPN symptoms in patients may be affected by changes resulting from multiple myeloma in a currently unknown manner. However, the neuropathy as induced by bortezomib itself was the focus of this research, and cancer was not

modeled in the interest of observing the effects of bortezomib isolated from other influences. Second, the dosage used in the current research was equivalent to a single cycle of bortezomib treatment, whereas patients receive multiple cycles of treatment. A dose was selected for rats based on what would induce altered behavioral symptoms without excessive cytotoxicity as a possible confound, and so this dosing schedule was selected. This then identifies another possible confound, in that patients were reported in the introduction to be most likely to develop symptoms between three to five cycles of treatment, whereas a single "cycle" in rats was sufficient to induce behavioral changes. However, it was also noted that a single cycle may in some cases be sufficient for patients to develop CIPN symptoms, so it is possible for animals to show a similar predisposition. Also, 37% of patients were reported to develop BIPN, whereas the animals used uniformly developed behavioral changes when treated with bortezomib. With the Sprague-Dawley strain of lab rats used, there is a high degree of homogeneity among individuals due to large-scale inbreeding, so it is possible that both a predisposition to earlier onset of symptoms and uniformity of symptom development could occur in a set of individuals with uniform genes. Even so, there is little data surrounding what genetic markers may predispose individuals to BIPN, so this cannot be proven either way.

In addition to issues concerning dosing schedules and symptom onset, there is also an issue in the nature of symptoms developed. Patients are scored based on paresthesias in most neuropathy scores, although painful symptoms are also common (Berkowitz and Walker, 2012). These painful symptoms are of greater concern than non-painful symptoms and are more likely to necessitate dose

reduction. Symptoms in patients may also include numbness or lack of sensation in BIPN. On the other hand, rats developed behaviors that are frequently interpreted by investigators as painful and increased, rather than decreased, sensitivity to stimuli. One explanation for why loss of sensation is not observed in animals could be a function of the lower dose used. If the Cavaletti lab is correct in reporting that peripheral nerve damage and axonal degeneration is the initial cause of BIPN, then damage could cause spontaneous or enhanced sensations, and a subsequent complete denervation could then result in loss of sensation. It is therefore possible that the lower dose used in the current model is not sufficient to generate this kind of effect. As for the distinction between painful symptoms and non-painful paresthesias, this is one drawback of using reflexive measures. It is impossible to distinguish between responses to either of these types of stimuli using the present methods. A reflexive withdrawal could indicate either a nocifensive response or increased vigilance to stimuli in response to unpleasant paresthesias. However, either of these sensations would indicate neuropathy in the animal model. Care must therefore be taken that conclusions derived from this model are not dependent on behaviors occurring in response to pain.

Another possible contributing factor to the disparity between patient symptoms and the animal model is the presence of comorbidities and differences in patient demographics. The presence of diabetes is notable among multiple myeloma patients observed within our own clinical data, and it is possible that sub-clinical diabetic neuropathy is present in many of these individuals prior to treatment. This is not the only possible contributor to neuropathy, but is by far the most prevalent.

Furthermore, multiple myeloma patients are generally at least middle-aged, if not older. The rats used in the dissertation research were adolescents. It is possible that the disparity in age could account for part of the mismatch in symptom severity, recovery time, or other differences in observed symptoms. Many patients receiving chemotherapy treatment have also had prior or overlapping radiation treatment that may have a further negative effect on nerve function. It would be an important follow-up study to model comorbidities of diabetes with streptozotocin or radiation treatment by irradiating animals in order to determine if either of these may contribute. Using elderly rats in experiments may also be beneficial.

The fact that affected behaviors in animals were isolated to mechanical stimulation also warrants further discussion. It is possible that there is a subtype of sensory neurons preferentially affected by bortezomib that have a lesser response to thermal stimuli. For example, while IB4+ sensory neurons may still respond to heat stimuli, IB4- sensory neurons respond to heat to a much greater extent (Stucky and Lewin, 1999). It is unknown, however, how or why cells like these would be selectively targeted in rats and not humans. Furthermore, patients show a decrease in motor skill that was not seen in rats (Cata et al., 2007). This may be due in part to the disparity between type of motor skills tested. Whereas patients displayed marked decreases in fine motor skill, rats were tested on coordinated walking ability. There is not a test in the animal model that would directly parallel pegboard completion, so the rotarod was selected on the basis of testing overall motor capability. It is possible that rats also exhibit impaired fine motor skill, but that the current testing methods were not sufficient to detect such a change.

5.3.   Proposed Molecular Pathway of the BIPN Animal Model

The research of this dissertation has been limited to several preliminary

studies aimed at a general mechanistic framework. There is substantial room for

future studies to further investigate the molecular pathway that may be responsible

for BIPN based on the findings in other animal models of neuropathy. From these

findings, it is possible to extrapolate a hypothetical pathway that ties together current

findings in the animal model of BIPN from our lab and others. One such pathway will

be outlined in this section and summarized in Fig. 19.

The primary basis of Cavaletti's work in BIPN centers around damage to

peripheral nerves. The hypothesis is certainly justified, since bortezomib does not

cross the blood-brain barrier. Cavaletti has presented data indicating possible axonal

degeneration (Carozzi et al., 2013) and the involvement of damage-associated

molecules such as TNF-α, CGRP, and substance P in the dorsal root ganglion

(Chiorazzi et al., 2013; Quartu et al., 2014). Satellite glial cells may further contribute

to this, as spontaneous discharges that may be induced by axonal degeneration

cause release of ATP and MMP9 from DRG neurons that triggers the release of

TNF-α and IL-1β from satellite glial cells (Ji, Berta, and Nedergaard, 2013).

Although Cavaletti has not investigated the activity of high-mobility group box

1 (HMGB1) in bortezomib, this is a damage-associated molecular pattern (DAMP)

that could also be involved in a maladaptive signal from the DRG. It is not the only

possibility for DAMP expression in the DRG, but is of particular interest because of

its relationship to TNF-α and activity on astrocytes. The activity of TNF-α has shown to be necessary for the expression of HMGB1 in DRG in a CCI model of neuropathy (Wang et al., 2013), and application of TNF-α has even been shown to induce secretion of HMGB1 in some cell types (Willenbrock et al., 2012). It is unknown at this time whether DAMPs like HMGB1 may be released from the DRG into the spinal cord, but this is one means by which downstream activity could potentially be induced. In favor of this possibility, an SNL model was shown to induce expression of HMGB1 and one of its receptors, the receptor for advanced glycation end products (RAGE), in both DRG and spinal cord (Shibasaki et al., 2010). The expression of these molecules was lower in the spinal cord than in the DRG, but this suggests some kind of communication in HMGB1 and RAGE expression from the DRG into the spinal cord, although how this occurs is unknown. Furthermore, expression of RAGE was limited to the spinal dorsal horn, suggesting a potential role in altered somatosensation.

RAGE is implicated in the activity of toll-like receptors, particularly in potentiating the activity of TLR4. Although TLR4 is often attributed to microglial activity, it is important to note that TLR4, RAGE, and HMGB1 expression are all simultaneously increased in spinal cord astrocytes in models like ALS (Casula et al., 2011). The downstream activity of astrocytic toll-like receptors is then sufficient to explain a variety of the findings of this dissertation. Astrocytic TLR4 activates the MAPK pathways for p38, ERK, and JNK (Liu, Gao, and Ji, 2012), each of which have a possible contributing role to the BIPN model.

The activity of p38 has recently been shown to be necessary for increases of GFAP expression that were used to indicate reactive gliosis (Roy Choudhury et al., 2014). GFAP was selected as a structural marker for its historical use and positive correlation with neuropathy models, but also because there are at this time no known functional markers consistently indicative of reactive astrocytosis (Watkins and Maier, 2003; Cao and Zhang, 2008). GFAP is a protein that composes intermediate filaments in astrocytes that are responsible for a multitude of purposes, including the trafficking of GLAST (Middeldorp and Hol, 2011), and GFAP expression has been shown to be inversely proportional to GLAST expression in neuropathy models (Xin, Weng, and Dougherty, 2009; Gao and Ji, 2010b), but it is unlikely that it has a direct contribution to neuropathy (Watkins and Maier, 2003). However, these changes do occur in parallel to other functional changes proposed.

The p38 pathway has also been shown to induce expression of connexin 43, the major astrocytic gap junction protein (Morioka et al., 2014). Along with glutamate transporters, gap junctions may contribute to persistent synaptic glutamate through increases in astrocyte intracellular calcium, which triggers glutamate release from astrocytes. The data of this dissertation has indicated a possible role for Cx43 and GLAST in this model, lending credence to the possibility of persistent synaptic glutamate. GLAST expression may be decreased by activation of TLR3 (Costello and Lynch, 2013). Although it has not been investigated in the context of TLR4, decreases in GLAST expression coincide with increased phosphorylation of ERK, which is common to both TLR3 and TLR4 (Zamoner, Heimfarth, and Pessoa-Pureur, 2008).

In addition to p38 and ERK, TLR4 may also activate the JNK MAPK pathway. This activation may result in the increased production and release of proinflammatory MCP-1, IL-1β, and others (Liu, Gao, and Ji, 2012). Although the receptor for MCP-1, CCR2, is not normally expressed on spinal neurons, it may be expressed in DRG neurons following paclitaxel treatment (Zhang et al., 2013). This change was not observed in the spinal cord in this model, although it did occur in the spinal cord in a lumbar disc herniation model of neuropathy (Zhu et al., 2014). The binding of cytokines and chemokines onto neuronal receptors may then sensitize them to further stimuli. The proposed model therefore provides a twofold means by which neurons in the spinal cord may be affected by astrocytes: first, by an increase in synaptic neurotransmitter that may increase EPSPs and sensitize neurons, and second, by further neuronal sensitization through cytokine and chemokine release.

To summarize the pathway that has been proposed, bortezomib first induces damage within the peripheral nerve and DRG. HMGB1 from the DRG then signals into the spinal cord and triggers a TLR4-mediated signal cascade that is potentiated by binding to RAGE. MAPK pathways then alter the expression of several astrocytic proteins. ERK decreases the expression of glutamate transporters, p38 increases the expression of GFAP and Cx43, and JNK increases the expression of MCP-1 and IL-1β. The changes in glutamate transporter and gap junction expression then increase synaptic glutamate, which increases the likelihood of EPSPs in the neuron. The parallel activity of cytokines and chemokines further sensitizes neurons, increasing the likelihood of a response.

There are several points along the proposed pathway in which alternative signaling molecules may serve a similar role. Instead of the activity of HMGB1, it is possible that MCP-1 or TNF-α may enter the spinal cord directly from the DRG. It is also possible that excessive presynaptic activity in DRG neurons may trigger downstream changes in the spinal cord, instead of the release of DAMPs or cytokines. The proposed model is just one possibility that may explain the observed phenomena in this dissertation, and further research is necessary to verify or disprove this pathway.
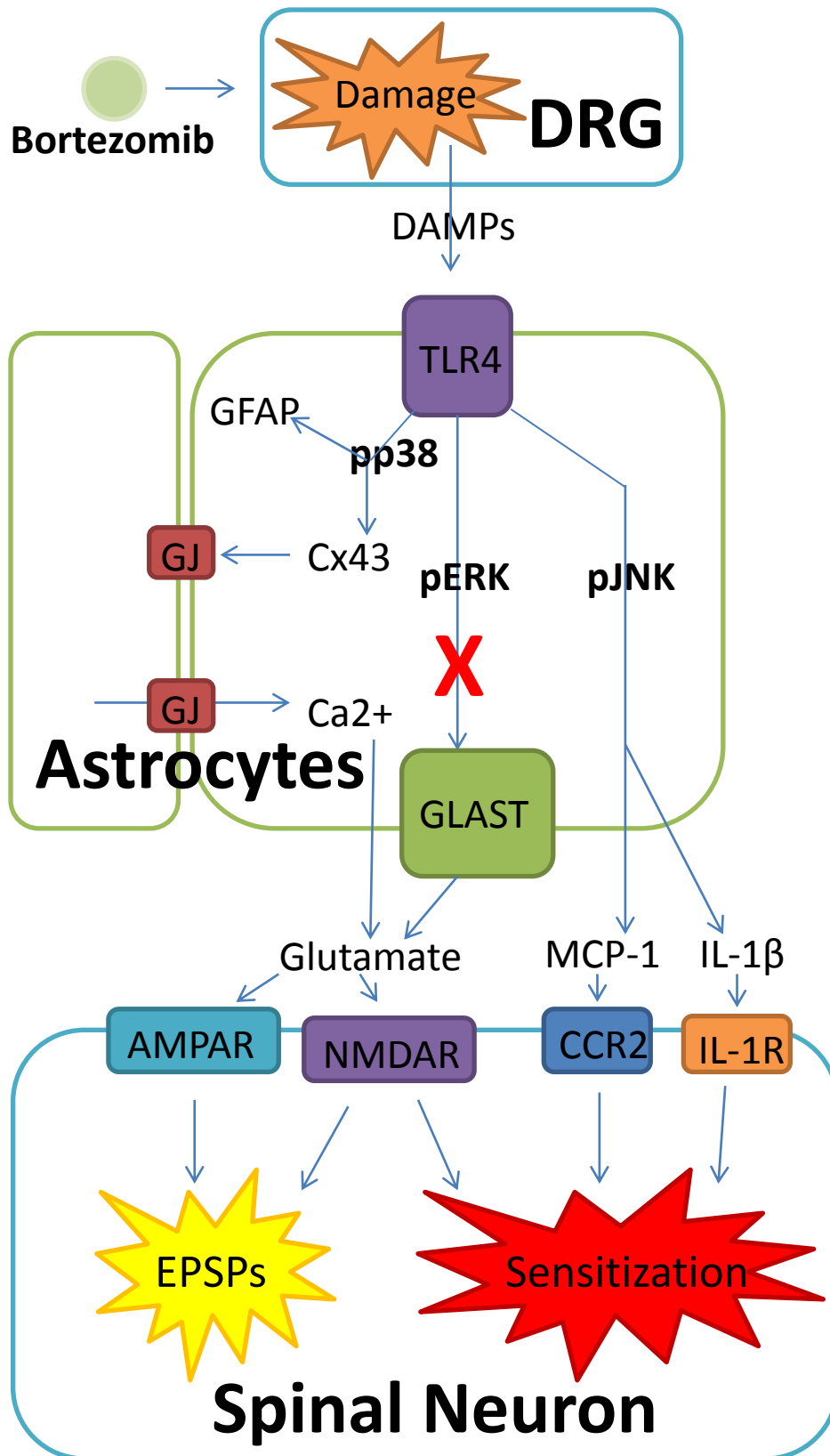
Figure 19. Proposed pathway for induction of BIPN model.

6. APPENDIX: Early Expression of GFAP and OX-42

As a follow-up on observed changes in glial surface markers in bortezomib-treated animals (see chapter 3), it was deemed necessary to examine possible glial activation at an earlier time point. One possibility of the lack of an observed change in microglial activity was that there could be a transient activation of microglia that returned to baseline activity by the 7-day time point that was observed. In order to address this possibility, animals were treated with a single injection of 0.15mg/kg bortezomib or an equivalent volume of saline and sacrificed 24 hours later for immunohistochemistry (for full methods, see chapter 3).

The expression of GFAP and OX-42 at this time point did not differ significantly between treatment groups (Fig. 20). GFAP expression was 97.1 ± 7.3% of control, and OX-42 expression was 100.3 ± 7.1% of control. It is important to note that, as previously mentioned, bortezomib has a half-life of 24 hours, and proteasome activity does not return to basal levels until 72 to 96 hours following bortezomib treatment. It is therefore unlikely that time points earlier than 24 hours would show any different effect.
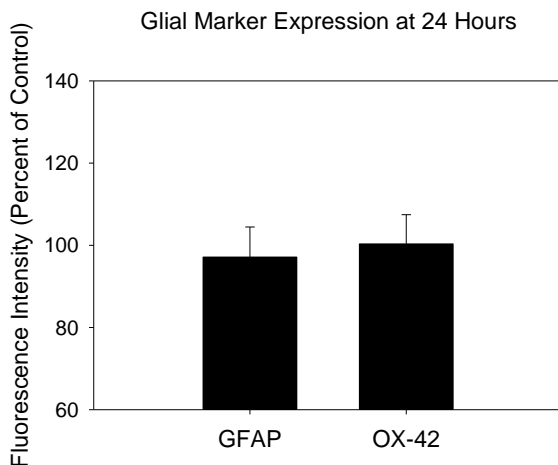
Figure 20. GFAP and OX-42 expression at 24 hours following bortezomib treatment. Animals treated with a single injection of bortezomib (n=6) did not show significantly different expression of GFAP or OX-42 24 hours later versus saline-treated controls (n=6).

119

BIBLIOGRAPHY

1. Adams J, Palombella VJ, Sausville EA, Johnson J, Destree A, Lazarus DD, Maas J, Pien CS, Prakash S, Elliott PJ (1999) Proteasome Inhibitors: a novel class of potent and effective antitumor agents. Cancer Res 59: 2615-2622.

2. Adams J (2001) Proteasome inhibition in cancer: development of PS-341. Semin Oncol 28:613-619.

3. Adams J (2002) Development of the proteasome inhibitor PS-341. Oncologist 7: 9-16.

4. Adams J, Kauffman M (2004) Development of the proteasome inhibitor Velcade (Bortezomib). Cancer Invest 22: 304-311.

5. Aghajanian C, Soignet S, Dizon DS, Pien CS, Adams J, Elliott PJ, Sabbatini P, Miller V, Hensley ML, Pezzulli S, Canales C, Daud A, Spriggs DR (2002) A phase I trial of the novel proteasome inhibitor PS341 in advanced solid tumor malignancies. Clin Cancer Res 8: 2505-2511.

6. Aguirre A, Maturana CJ, Harcha PA, Sáez JC (2013) Possible involvement of TLRs and hemichannels in stress-induced CNS dysfunction via mastocytes, and glia activation. Mediators Inflamm 2013:893521.

7. Alé A, Bruna J, Morell M, Van de Velde H, Monbaliu J, Navarro X, Udina E (2014) Treatment with anti-TNF alpha protects against the neuropathy induced by the proteasome inhibitor bortezomib in a mouse model. Exp Neurol 253:165-173.

8. Araque A, Navarrete A (2010) Glial cells in neuronal network function. Philos Trans R Soc Lond B Biol Sci 365:2375-2381.

9. Argyriou AA, Iconomou G, Kalofonos HP (2008) Bortezomib-induced peripheral neuropathy in multiple myeloma: a comprehensive review of the literature. Blood 112:1593-1599.

10. Argyriou AA, Bruna J, Marmiroli P, Cavaletti G (2012) Chemotherapy-induced peripheral neurotoxicity (CIPN): an update. Crit Rev Oncol Hematol 82:51-77.

11. Argyriou AA, Kyritsis AP, Makatsoris T, Kalofonos HP (2014) Chemotherapy-induced peripheral neuropathy in adults: a comprehensive update of the literature. Cancer Manag Res 6:135-147.

12. Arnulf B, Pylypenko H, Grosicki S, Karamanesht I, Leleu X, van de Velde H, Feng H, Cakana A, Deraedt W, Moreau P (2012) Updated survival analysis of a randomized phase III study of subcutaneous versus intravenous bortezomib in patients with relapsed multiple myeloma. Haematologica 97:1925-1928.

13. Attal N (2012) Neuropathic pain: mechanisms, therapeutic approach, and interpretation of clinical trials. Continuum (Minneap Minn) 18:161-175.

14. Azoulay D, Lavie D, Horowitz N, Suriu C, Gatt ME, Akira L, Perlman R, Braester A, Ben-Yehuda D (2014) Bortezomib-induced peripheral neuropathy is related to altered levels of brain-derived neurotrophic factor in the peripheral blood of patients with multiple myeloma. Br J Haematol. 164:454-456.

15. Bang SM, Lee JH, Yoon SS, Park S, Min CK, Kim CC, Suh C, Sohn SK, Min YH, Lee JJ, Kim K, Seong CM, Yoon HJ, Cho KS, Jo DY, Lee KH, Lee NR, Kim CS

(2006) A multicenter retrospective analysis of adverse events in Korean patients using bortezomib for multiple myeloma. Int J Hematol 97:485-490.

16. Baron R, Binder A, Wasner G (2010) Neuropathic pain: diagnosis, pathophysiological mechanisms, and treatment. Lancet Neurol 9:807-819.

17. Beattie MS (2004) Inflammation and apoptosis: linked therapeutic targets in spinal cord injury. Trends Mol Med 10:580-583.

18. Bennett GJ, Xie YK (1988) A peripheral mononeuropathy in rat that produces disorders of pain sensation like those seen in man. Pain 33:87-107.

19. Berenson JR, Ma HM, Vescio R (2001) The role of nuclear factor-kappaB in the biology and treatment of multiple myeloma. Semin Oncol 28:626-633.

20. Berkowitz A, Walker S (2012) Bortezomib-induced peripheral neuropathy in patients with multiple myeloma. Clin J Oncol Nurs 16:86-89.

21. Bhattacharyya S, Yu H, Mim C, Matouschek A (2014) Regulated protein turnover: snapshots of the proteasome in action. Nat Rev Mol Cell Biol 15:122-133.

22. Boche D, Perry VH, Nicoll JA (2013) Review: activation patterns of microglia and their identification in the human brain. Neuropathol Appl Neurobiol 39:3-18.

23. Boyette-Davis J, Dougherty PM (2011) Protection against oxaliplatin-induced mechanical hyperalgesia and intraepidermal nerve fiber loss by minocycline. Exp Neurol 229: 353-357.

24. Boyette-Davis JA, Cata JP, Zhang H, Driver LC, Wendelschafer-Crabb G, Kennedy WR, Dougherty PM (2011) Follow-up psychophysical studies in bortezomib-related chemoneuropathy patients. J Pain 12: 1017-1024.

25. Boyette-Davis J, Xin W, Zhang H, Dougherty PM (2011) Intraepidermal nerve fiber loss corresponds to the development of taxol-induced hyperalgesia and can be prevented by treatment with minocycline. Pain 152:308-313.

26. Boyette-Davis JA, Cata JP, Driver LC, Novy DM, Bruel BM, Mooring DL, Wendelschafer-Crabb G, Kennedy WR, Dougherty PM (2012) Persistent chemoneuropathy in patients receiving the plant alkaloids paclitaxel and vincristine. Cancer Chemother Pharmacol 71: 619-626.

27. Bradesi S (2010) Role of spinal cord glia in the central processing of peripheral pain perception. Neurogastroenterol Motil 22:499-511.

28. Brix Finnerup N, Hein Sindrup S, Staehelin Jensen T (2013) Management of painful neuropathies. Handb Clin Neurol 115:279-290.

29. Broyl A, Corthals SL, Jongen JL, van der Holt B, Kuiper R, de Knegt Y, van Duin M, el Jarari L, Bertsch U, Lokhorst HM, Durie BG, Goldschmidt H, Sonneveld P (2010) Mechanisms of peripheral neuropathy associated with bortezomib and vincristine in patients with newly diagnosed multiple myeloma: a prospective analysis of data from the HOVON-65/GMMG-HD4 trial. Lancet Oncol 11:1057-1065.

30. Broyl A, Jongen JLM, Sonneveld P (2012) General aspects and mechanisms of peripheral neuropathy associated with bortezomib in patients with newly diagnosed multiple myeloma. Semin Hematol 49: 249-257.

31. Brush DE (2012) Complications of long-term opioid therapy for management of chronic pain: the paradox of opioid-induced hyperalgesia. J Med Toxicol 8:387-392.

32. Campbell SL, Hablitz JJ (2004) Glutamate transporters regulate excitability in local networks in rat neocortex. Neuroscience 127:625-635.

33. Cao H, Zhang Y-Q (2008) Spinal glial activation contributes to pathological pain states. Neurosci Behav Rev 32:972-983.

34. Carozzi VA, Renn CL, Bardini M, Fazio G, Ciorazzi A, Meregalli C, Oggioni N, Shanks K, Quartu M, Serra MP, Sala B, Cavaletti G, Dorsey SG (2013) Bortezomib-induced painful peripheral neuropathy: an electrophysiological, behavioral, morphological and mechanistic study in the mouse. PLoS One 8:e72995.

35. Casellini CM, Vinik AI (2007) Clinical manifestations and current treatment options for diabetic neuropathies. Endocr Pract 13:550-566.

36. Casha S, Zygun D, McGowan MD, Bains I, Yong VW, Hurlbert RJ (2012) Results of a phase II placebo-controlled randomized trial of minocycline in acute spinal cord injury. Brain 135:1224-1236.

37. Casula M, Iyer AM, Spliet WG, Anink JJ, Steentjes K, Sta M, Troost D, Aronica E (2011) Toll-like receptor signaling in amyotrophic lateral sclerosis spinal cord tissue. Neuroscience 179:233-243.

38. Cata JP, Weng HR, Chen JH, Dougherty PM (2006) Altered discharges of spinal wide dynamic range neurons and down-regulation of glutamate transporter expression in rats with paclitaxel-induced hyperalgesia. Neuroscience 138: 329-338.

39. Cata JP, Weng HR, Lee BN, Reuben JM, Dougherty PM (2006) Clinical and experimental findings in humans and animals with chemotherapy-induced peripheral neuropathy. Minerva Anestesiol 72:151-169.

40. Cata JP, Weng HR, Burton AW, Villareal H, Giralt S, Dougherty PM (2007) Quantitative sensory findings in patients with bortezomib-induced pain. J Pain 8: 296-306.

41. Cata JP, Weng HR, Dougherty PM (2008) Behavioral and electrophysiological studies in rats with cisplatin-induced chemoneuropathy. Brain Res 1230: 91-98.

42. Cata JP, Weng HR, Dougherty PM (2008) The effects of thalidomide and minocycline on taxon-induced hyperalgesia in rats. Brain Res 1229: 100-110.

43. Cavaletti G, Gilardini A, Canta A, Rigamonti L, Rodriguez-Menendez V, Ceresa C, Marmiroli P, Bossi M, Oggioni N, D'Incalci M, De Coster R (2007) Bortezomib-induced peripheral neurotoxicity: a neurophysiological and pathological study in the rat. Exp Neurol 204:317-325.

44. Cavaletti G, Marmiroli P (2010) Chemotherapy-induced peripheral neurotoxicity. Nat Rev Neurol 6:657-666.

45. Cavaletti G, Jakubowiak AJ (2010) Peripheral neuropathy during bortezomib treatment of multiple myeloma: a review of recent studies. Leuk Lymphoma 51: 1178-1187.

46. Cavo M (2006) Proteasome inhibitor bortezomib for the treatment of multiple myeloma. Leukemia 20:1341-1352.

47. Cavo M, Tacchetti P, Patriarca F, Petrucci MT, Pantani L, Galli M, Di Raimondo F, Crippa C, Zamagni E, Palumbo A, Offidani M, Corradini P, Narni F, Spadano

A, Pescosta N, Deliliers GL, Ledda A, Cellini C, Caravita T, Tosi P, Baccarani M, GIMEMA Italian Myeloma Network (2010) Bortezomib with thalidomide plus dexamethasone compared with thalidomide plus dexamethasone as induction therapy before, and consolidation therapy after, double autologous stem-cell transplantation in newly diagnosed multiple myeloma: a randomized phase 3 study. Lancet 376:2075-2085.

48. Chen G, Park CK, Xie RG, Berta T, Nedergaard M, Ji RR (2014) Connexin-43 induces chemokine release from spinal cord astrocytes to maintain late-phase neuropathic pain in mice. Brain pii: awu140.

49. Chen MJ, Kress B, Han X, Moll K, Peng W, Ji RR, Nedergaard M (2012) Astrocytic CX43 hemichannels and gap junctions play a crucial role in development of chronic neuropathic pain following spinal cord injury. Glia 60:1660-1670.

50. Chew SS, Johnson CS, Green CR, Danesh-Meyer HV (2010) Role of connexin43 in central nervous system injury. Exp Neurol 225:250-261.

51. Chiang CY, Li Z, Dostrovsky JO, Sessle BJ (2010) Central sensitization in medullary dorsal horn involves gap junctions and hemichannels. Neuroreport 21:233-237.

52. Chiorazzi A, Canta A, Meregalli C, Carozzi V, Sala B, Oggioni N, Monbaliu J, Van de Velde H, Cavaletti G (2013) Antibody against tumor necrosis factor-α reduces bortezomib-induced allodynia in a rat model. Anticancer Res 33:5453-5459.

53. Christensen MD, Everhart AW, Pickelman JT, Hulsebosch CE (1996) Mechanical and thermal allodynia in chronic pain following spinal cord injury. Pain 68:97-107.

54. Clark AK, Old EA, Malcangio M (2013) Neuropathic pain and cytokines: current perspectives. J Pain Res 6: 803-814.

55. Corthals SL, Kuiper R, Johnson DC, Sonneveld P, Hajek R, van der Holt B, Magrangeas F, Goldschmidt H, Morgan GJ, Avet-Loiseau H (2011) Genetic factors underlying the risk of bortezomib induced peripheral neuropathy in multiple myeloma patients. Haematologica 96:1728-1732.

56. Costello DA, Lynch MA (2013) Toll-like receptor 3 activation modulates hippocampal network excitability, via glial production of interferon-β. Hippocampus 23:696-707.

57. Costigan M, Scholz J, Woolf CJ (2009) Neuropathic pain: a maladaptive response of the nervous system to damage. Annu Rev Neurosci 32:1-32.

58. D'Angelo R, Morreale A, Donadio V, Boriani S, Maraldi N, Piazzi G, Liquori R (2013) Neuropathic pain following spinal cord injury: what we know about mechanisms, assessment, and management. Eur Rev Med Pharmacol Sci 17:3257-3261.

59. Decosterd I, Woolf CJ (2000) Spared nerve injury: an animal model of persistent peripheral neuropathic pain. Pain 87:149-158.

60. Devinsky O, Vessani A, Najjar S, De Lanerolle NC, Rogawski MA (2013) Glia and epilepsy: excitability and inflammation. Trends Neurosci 36:174-184.

61. Di Cesare Mannelli L, Pacini A, Bonaccini L, Zanardelli M, Mello T, Ghelardini C (2013) Morphologic features and glial activation in rat oxaliplatin-dependent neuropathic pain. J Pain 14:1585-1600.

62. Dina OA, Chen X, Reichling D, Levine JD (2001) Role of protein kinase Cepsilon and protein kinase A in a model of paclitaxel-induced painful peripheral neuropathy in the rat. Neuroscience 108: 507-515.

63. Dodd S, Maes M, Anderson G, Dean OM, Moylan S, Berk M (2013) Putative neuroprotective agents in neuropsychiatric disorders. Prog Neuropsychopharmacol Biol Psychiatry 42:135-145.

64. Dougherty PM, Cata JP, Burton AW, Vu K, Weng HR (2007) Dysfunction in multiple primary afferent fiber subtypes revealed by quantitative sensory testing in patients with chronic vincristine-induced pain. J Pain Symptom Manage 33: 166-179.

65. Ducourneau VR, Dolique T, Hachem-Delaunay S, Miraucourt LS, Amadio A, Blaszczyk L, Jacquot F, Ly J, Devoize L, Oliet SH, Dallel R, Mothet JP, Nagy F, Fenelon VS, Voisin DL (2014) Cancer pain is not necessarily correlated with spinal overexpression of reactive glia markers. Pain 155:275-291.

66. Eyo UB, Dailey ME (2013) Microglia: key elements in neural development, plasticity, and pathology. J Neuroimmune Pharmacol 8:494-509.

67. Favis R, Sun Y, van de Velde H, Broderick E, Levey L, Meyers M, Mulligan G, Harousseau JL, Richardson PG, Ricci DS (2011) Genetic variation associated with bortezomib-induced peripheral neuropathy. Pharmacogenet Genomics 21:121-129.

68. Ferri KF, Kroemer G (2001) Organelle-specific initiation of cell death pathways. Nat Cell Biol 3:E255-E263.

69. Ferrier J, Pereira V, Busserolles J, Authier N, Balayssac D (2013) Emerging trends in understanding chemotherapy-induced peripheral neuropathy. Curr Pain Headache Rep 17:364.

70. Festoff BW, Ameenuddin S, Arnold PM, Wong A, Santacruz KS, Citron BA (2006) Minocycline neuroprotects, reduces microgliosis, and inhibits caspase protease expression early after spinal cord injury. J Neurochem 97:1314-1326.

71. Freynhagen R, Bennett MI (2009) Diagnosis and management of neuropathic pain. BMJ 339:b3002.

72. Gao YJ, Ji RR (2010) Chemokines, neuronal-glial interactions, and central processing of neuropathic pain. Pharmacol Ther 126:56-68.

73. Gao YJ, Ji RR (2010) Targeting astrocyte signaling for chronic pain. Neurotherapeutics 7:482-493.

74. Garner SE, Eady A, Bennett C, Newton JN, Thomas K, Popescu CM (2012) Minocycline for acne vulgaris: efficacy and safety. Cochrane Database Syst Rev 8.

75. Garrido-Mesa N, Zarzuelo A, Gálvez J (2013) Minocycline: far beyond an antibiotic. Br J Pharmacol 169:337-352.

76. Garrison CJ, Dougherty PM, Kajander KC, Carlton SM (1991) Staining of glial fibrillary acidic protein (GFAP) in lumbar spinal cord increases following a sciatic nerve constriction injury. Brain Res 565:1-7.

77. Giaume C, Liu X (2012) From a glial syncytium to a more restricted and specific glial networking. J Physiol Paris 106:34-39.

78. Giaume C, Venance L (1998) Intercellular calcium signaling and gap junctional communication in astrocytes. Glia 24:50-64.

79. Gilardini A, Avila RL, Oggioni N, Rodriguez-Menendez V, Bossi M, Canta A, Cavaletti G, Kirschner DA (2012) Myelin structure is unaltered in chemotherapy-induced peripheral neuropathy. Neurotoxicology 33:1-7.

80. Gonzalez JC, Egea J, Del Carmen GM, Fernandez-Gomez FJ,Sanchez-Prieto J, Gandia L, Garcia AG, Jordan J, Hernandez-Guijo JM (2007) Neuroprotectant minocycline depresses glutamatergic neurotransmission and Ca(2+) signaling in hippocampal neurons. Eur J Neurosci 26:2481–2495.

81. Graeber MB (2010) Changing face of microglia. Science 330:783-788.

82. Gregory NS, Harris AL, Robinson CR, Dougherty PM, Fuchs PN, Sluka KA (2013) An overview of animal models of pain: disease models and outcome measures. J Pain 14:1255-1269.

83. Gruner JA (1992) A monitored contusion model of spinal cord injury in the rat. J Neurotrauma 9:123-128.

84. Guasti L, Richardson D, Jhaveri M, Eldeeb K, Barrett D, Elphick MR, Alexander SP, Kendall D, Michael GJ, Chapman V (2009) Minocycline treatment inhibits microglial activation and alters spinal levels of endocannabinoids in a rat model of neuropathic pain. Mol Pain 5:35.

85. Guerrero AR, Uchida K, Nakajima H, Watanabe S, Nakamura M, Johnson WE, Baba H (2012) Blockade of interleukin-6 signaling inhibits the classic pathway

and promotes an alternative pathway of macrophage activation after spinal cord injury in mice. J Neuroinflammation 9:40.

86. Hailer NP (2008) Immunosuppression after traumatic or ischemic CNS damage: it is neuroprotective and illuminates the role of microglial cells. Prog Neurobiol 84:211-233.

87. Hald A (2009) Spinal astrogliosis in pain models: cause and effects. Cell Mol Neurobiol, 29:609-619.

88. Hansen RR, Malcangio M (2013) Astrocytes—multitaskers in chronic pain. Eur J Pharmacol 716:120-128.

89. Hao JX, Xu XJ, Aldskogius H, Seiger A, Weisenfeld-Hallin Z (1991) Allodynia-like effects in rat after ischaemic spinal cord injury photochemically induced by laser irradiation. Pain 45:175-185.

90. Harris HE, Andersson U, Pisetsky DS (2012) HMGB1: a multifunctional alarmin driving autoimmune and inflammatory disease. Nat Rev Rheumatol 8:195-202.

91. Haydon PG (2001) Glia: listening and talking to the synapse. Nat Rev Neurosci 2:185-193.

92. Henry CJ, Huang Y, Wynne A, Hanke M, Himler J, Bailey MT, Sheridan JF, Godbout JP (2008) Minocycline attenuates lipopolysaccharide (LPS)-induced neuroinflammation, sickness behavior, and anhedonia. J Neuroinflammation 5:15.

93. Hideshima T, Richardson P, Chauhan D, Palombella VJ, Elliott PJ, Adams J, Anderson KC (2001) The proteasome inhibitor PS-341 inhibits growth, induces

apoptosis, and overcomes drug resistance in human multiple myeloma cells. Cancer Res 61: 3071-3076.

94. Hideshima T, Mitsiades C, Akiyama M, Hayashi T, Chauhan D, Richardson P, Schlossman R, Podar K, Munshi NC, Mitsiades N, Anderson KC (2003) Molecular mechanisms mediating antimyeloma activity of proteasome inhibitor PS-341. Blood 101: 1530-1534.

95. Homkajorn B, Sims NR, Muyderman H (2010) Connexin 43 regulates astrocytic migration and proliferation in response to injury. Neurosci Lett 486:197-201.

96. Hu X, Li P, Guo Y, Wang H, Leak RK, Chen S, Gao Y, Chen J (2012) Microglia/macrophage polarization dynamics reveal novel mechanism of injury expansion after focal cerebral ischemia. Stroke 43:3063-3070.

97. Hua XY, Svensson CI, Matsui T, Fitzsimmons B, Yaksh TL, Webb M (2005) Intrathecal minocycline attenuates peripheral inflammation-induced hyperalgesia by inhibiting p38 MAPK in spinal microglia. Eur J Neurosci 22:2431-2440.

98. Huang CY, Chen YL, Li AH, Lu JC, Wang HL (2014) Minocycline, a microglial inhibitor, blocks spinal CCL2-induced heat hyperalgesia and augmentation of glutamatergic transmission in substantia gelatinosa neurons. J Neuroinflammation 11:7.

99. Jagannath S, Richardson PG, Barlogie B, Berenson JR, Singhal S, Irwin D, Srkalovic G, Schenkein DP, Esseltine DL, Anderson KC, SUMMIT/CREST Investigators (2006) Bortezomib in combination with dexamethasone for the treatment of patients with relapsed and/or refractory multiple myeloma with less than optimal response to bortezomib alone. Haematologica 91:929-934.

100.   Jagannath S, Durie BG, Wolf JL, Camacho ES, Irwin D, Lutzky J, McKinley M, Potts P, Gabayan AE, Mazumder A, Crowley J, Vescio R (2009) Extended follow-up of a phase 2 trial of bortezomib alone and in combination with dexamethasone for the frontline treatment of multiple myeloma. Br J Haematol 146:619-626.

101.   Jay GW, Barkin RL (2014) Neuropathic pain: etiology, pathophysiology, mechanisms, and evaluations. Dis Mon 60:6-14.

102.   Ji RR, Kohno T, Moore KA, Woolf CJ (2003) Central sensitization and LTP: do pain and memory share similar mechanisms? Trends Neurosci 26: 696-705.

103.   Ji RR, Suter MR (2007) P38 MAPK, microglial signaling, and neuropathic pain. Mol Pain 3:33.

104.   Ji RR, Berta T, Nedergaard M (2013) Glia and pain: is chronic pain a gliopathy? Pain 154 Suppl 1: S10-28.

105.   Joseph EK, Levine JD (2009) Comparison of oxaliplatin- and cisplatin-induced painful peripheral neuropathy in the rat. J Pain 10: 534-541.

106.   Juntunen J, Teräväinen H, Eriksson K, Panula P, Larsen A (1978) Experimental alcoholic neuropathy in the rat: histological and electrophysiological study on the myoneural junctions and the peripheral nerves. Acta Neuropathol 41:131-137.

107.   Juszczak GR, Swiergiel AH (2009) Properties of gap junction blockers and their behavioral, cognitive and electrophysiological effects: animal and human studies. Prog Neuropsychopharmacol Biol Psychiatry 33:181-198.

108. Kandhare AD, Raygude KS, Ghosh P, Ghule AE, Bodhankar SL (2012) Therapeutic role of curcumin in prevention of biochemical aberration induced by alcoholic neuropathy in laboratory animals. Neurosci Lett 511:18-22.

109. Kane RC, Farrell AT, Sridhara R, Pazdur R (2006) United States Food and Drug Administration approval summary: bortezomib for the treatment of progressive multiple myeloma after one prior therapy. Clin Cancer Res 12: 2955-2960.

110. Kaufman JL, Nooka A, Vrana M, Gleason C, Heffner LT, Lonial S (2010) Bortezomib, thalidomide, and dexamethasone as induction therapy for patients with symptomatic multiple myeloma: a retrospective study. Cancer 116: 3143-3151.

111. Keyel PA (2014) How is inflammation initiated? Individual influences of IL-1, IL-18 and HMGB1. Cytokine pii: S1043-4666(14)00075-1.

112. Kielian T, Esen N, Liu S, Phulwani NK, Syed MM, Phillips N, Nishina K, Cheung AL, Schwartzman JD, Ruhe JJ (2007) Minocycline modulates neuroinflammation independently of its antimicrobial activity in staphylococcus aureus-induced brain abscess. Am J Pathol 171:1199-1214.

113. Kim K, Lee SG, Kegelman TP, Su ZZ, Das SK, Dash R, Dasgupta S, Barral PM, Hedvat M, Diaz P, Reed JC, Stebbins JL (2011) Role of excitatory amino acid transporter-2 (EAAT2) and glutamate in neurodegeneration: opportunities for developing novel therapeutics. J Cell Physiol 226:2484-2493.

114. Kim NH, Kim DH (2012) Ulnar neuropathy at the wrist in a patient with carpal tunnel syndrome after open carpal tunnel release. Ann Rehabil Med 36:291-296.

115. Kim SH, Chung JM (1992) An experimental model for peripheral neuropathy produced by segmental spinal nerve ligation in the rat. Pain 50:355-363.

116. Landowski TH, Megli CJ, Nullmeyer KD, Lynch RM, Dorr RT (2005) Mitochondrial-mediated dysregulation of Ca2+ is a critical determinant of Velcade (PS-341/Bortezomib) cytotoxicity in myeloma cell lines. Cancer Res 65: 3828-3836.

117. Lau JTC, Stavrou P (2004) Posterior tibial nerve—primary. Foot Ankle Clin 9:271-285.

118. Ledeboer A, Sloane EM, Milligan ED, Frank MG, Mahony JH, Maier SF, Watkins LR (2005) Minocycline attenuates mechanical allodynia and proinflammatory cytokine expression in rat models of pain facilitation. Pain 115:71-83.

119. Lee SG, Su ZZ, Emdad L, Gupta P, Sarkar D, Borjabad A, Volsky DJ, Fisher PB (2008) Mechanism of ceftriaxone induction of excitatory amino acid transporter-2 expression and glutamate uptake in primary human astrocytes. J Biol Chem 283:13116-13123.

120. Levitt M, Levitt JH (1981) The deafferentation syndrome in monkeys: dysesthesias of spinal origin. Pain 10:129-147.

121. Li Y, Zhang H, Zhang H, Kosturakis AK, Jawad AB, Dougherty PM (2014) Toll-like receptor 4 signaling contributes to paclitaxel-induced peripheral neuropathy. J Pain pii: S1526-5900(14)00678-6.

122. Liaw WJ, Stephens RL Jr, Binns BC, Chu Y, Sepkuty JP, Johns RA, Rothstein JD, Tao YX (2005) Spinal glutamate uptake is critical for maintaining normal sensory transmission in rat spinal cord. Pain 115:60-70.

123. Lightcap ES, McCormack TA, Pien CS, Chau V, Adams J, Elliot PJ (2000) Proteasome inhibition measurements: clinical application. Clin Chem 46:673-683.

124. Liu T, Gao YJ, Ji RR (2012) Emerging role of toll-like receptors in the control of pain and itch. Neurosci Bull 28:131-144.

125. López-Bayghen E, Ortega A (2011) Glial glutamate transporters: new actors in brain signaling. IUBMB Life 63:816-823.

126. Ma MH, Yang HH, Parker K, Manyak S, Friedman JM, Altamirano C, Wu ZQ, Borad MJ, Frantzen M, Roussos E, Neeser J, Mikail A, Adams J, Sjak-Shie N, Vescio RA, Berenson JR (2003) The proteasome inhibitor PS-341 markedly enhances sensitivity of multiple myeloma tumor cells to chemotherapeutic agents. Clin Cancer Res 9:1136-1144.

127. Malarkey EB, Parpura V (2008) Mechanisms of glutamate release from astrocytes. Neurochem Int 52:142-154.

128. Mancini F, Sambo CF, Ramirez JD, Bennett DL, Haggard P, Ianetti GD (2013) A fovea for pain at the fingertips. Curr Biol 23:496-500.

129. Mao-Ying QL, Wang XW, Yang CJ, Li X, Mi WL, Wu GC, Wang YQ (2012) Robust spinal neuroinflammation mediates mechanical allodynia in Walker 256 induced bone cancer rats. Mol Brain 5:16.

130. Marchand F, Perretti M, McMahon SB (2005) Role of the immune system in chronic pain. Nat Rev Neurosci 6:521-532.

131.   Mateos MV, Richardson PG, Schlag R, Khuageva NK, Dimopoulos MA, Shpilberg O, Kropff M, Spicka I, Petrucci MT, Palumbo A, Samoilova OS, Dmoszynska A, Abdulkadyrov KM, Schots R, Jiang B, Esseltine DL, Liu K, Cakana A, van de Velde H, San Miguel JF (2010) Bortezomib plus melphalan and prednisone compared with melphalan and prednisone in previously untreated multiple myeloma: updated follow-up and impact of subsequent therapy in the phase III VISTA trial. J Clin Oncol 28:2259-2266.

132.   Mattern MR, Wu J, Nicholson B (2012) Ubiquitin-based anticancer therapy: carpet bombing with proteasome inhibitors vs surgical strikes with E1, E2, E3, or DUB inhibitors. Biochim Biophys Acta 1823:2014-2021.

133.   Matute C, Domercq M, Sánchez-Gómez MV (2006) Glutamate-mediated glial injury: mechanisms and clinical importance. Glia 53:212-224.

134.   Melvin AT, Woss GS, Park JH, Waters ML, Allbritton NL (2013) Measuring activity in the ubiquitin-proteasome system: from large scale discoveries to single cells analysis. Cell Biochem Biophys 67:75-89.

135.   Merbl Y, Kirschner MW (2009) Large-scale detection of ubiquitination substrates using cell extracts and protein microarrays. Proc Natl Acad Sci U S A 106:2543-2548.

136.   Middeldorp J, Hol EM (2011) GFAP in health and disease. Prog Neurobiol 93:421-443.

137.   Miller RJ, Jung H, Bhangoo SK, White FA (2009) Cytokine and chemokine regulation of sensory neuron function. Handb Exp Pharmacol 419-449.

138.   Milligan ED, Watkins LR (2009) Pathological and protective roles of glia in chronic pain. Nat Rev Neurosci 10:23-36.

139.   Miltenburg NC, Boogerd W (2014) Chemotherapy-induced neuropathy: a comprehensive survey. Cancer Treat Rev 40:872-882.

140.   Mitsiades N, Mitsiades CS, Poulaki V, Chauhan D, Richardson PG, Hideshima T, Munshi N, Treon SP, Anderson KC (2002) Biologic sequelae of nuclear factor-kappaB blockade in multiple myeloma: therapeutic applications. Blood 99:4079-4086.

141.   Morioka N, Suekama K, Zhang FF, Kajitani N, Hisaoka-Nakashima K, Takebayashi M, Nakata Y (2014). Amitriptyline up-regulates connexin43-gap junction in rat cultured cortical astrocytes via activation of the p38 and c-Fos/AP-1 signalling pathway. Br J Pharmacol 171:2854-2867.

142.   Nagy JI, Rash JE (2000) Connexins and gap junctions of astrocytes and oligodendrocytes in the CNS. Brain Res Brain Res Rev 32:29-44.

143.   Nakagawa T, Kaneko S (2010) Spinal astrocytes as therapeutic targets for pathological pain. J Pharmacol Sci 114:347-353.

144.   Nasu S, Misawa S, Nakaseko C, Shibuya K, Isose S, Sekiguchi Y, Mitsuma S, Ohmori S, Iwai Y, Beppu M, Shimizu N, Ohwada C, Takeda Y, Fujimaki Y, Kuwabara S (2014) Bortezomib-induced neuropathy: axonal membrane depolarization precedes development of neuropathy. Clin Neurophysiol 125:381-387.

145. Nicholson KJ, Gilliland TM, Winkelstein BA (2014) Upregulation of GLT-1 by treatment with ceftriaxone alleviates radicular pain by reducing spinal astrocyte activation and neuronal hyperexcitability. J Neurosci Res 92:116-129.

146. Nie H, Zhang H, Weng HR (2010) Bidrectional neuron-glia interactions triggered by deficiency of glutamate uptake at spinal sensory synapses. J Neurophysiol 104:713-725.

147. Pannasch U, Rouach N (2013) Emerging role for astroglial networks in information processing: from synapse to behavior. Trends Neurosci 36:405-417.

148. Parpura V, Basarsky TA, Liu F, Jeftinija K, Jeftinija S, Haydon PG (1994) Glutamate-mediated astrocyte-neuron signaling. Nature 369:744-747.

149. Parpura V, Zorec R (2010) Gliotransmission: exocytotic release from astrocytes. Brain Res Rev 63:83-92.

150. Petersen KL, Fields HL, Brennum J, Sandroni P, Rowbotham MC (2000) Capsaicin evoked pain and allodynia in post-herpetic neuralgia. Pain 88:125-133.

151. Plane JM, Shen Y, Pleasure DE, Deng W (2010) Prospects for minocycline neuroprotection. Arch Neurol 67:1442-1448.

152. Porter JT, McCarthy KD (1997) Astrocytic neurotransmitter receptors *in situ* and *in vivo*. Prog Neurobiol 51:439-455.

153. Postma TJ, Heimans JJ (2000) Grading of chemotherapy-induced peripheral neuropathy. Annals of Oncology 11:509-513.

154. Quartu M, Carozzi VA, Dorsey SG, Serra MP, Poddighe L, Picci C, Boi M, Melis T, Del Fiacco M, Meregalli C, Chiorazzi A, Renn CL, Cavaletti G, Marmiroli P (2014). Bortezomib treatment produces nocifensive behavior and changes in

the expression of TRPV1, CGRP, and substance P in the rat DRG, spinal cord, and sciatic nerve. Biomed Res Int 2014:180428.

155.   Ramesh G, MacLean AG, Phillipp MT (2013) Cytokines and chemokines at the crossroads of inflammation, neurodegeneration, and neuropathic pain. Mediators Inflamm 2013:480739.

156.   Reece D, Imrie K, Stevens A, Smith CA, Hematology Disease Site Group of Cancer Care Ontario's Program in Evidence-based Care (2006) Bortezomib in multiple myeloma and lymphoma: a systematic review and clinical practice guideline. Curr Oncol 13:160-172.

157.   Richardson PG, Hideshima T, Anderson KC (2003) Bortezomib (PS-341): a novel, first-in-class proteasome inhibitor for the treatment of multiple myeloma and other cancers. Cancer Control 10:361-369.

158.   Richardson PG, Barlogie B, Berenson J, Singhal S, Jagannath S, Irwin D, Rajkumar SV, Srkalovic G, Alsina M, Alexanian R, Siegel D, Orlowski RZ, Kuter D, Limentani SA, Lee S, Hideshima T, Esseltine DL, Kauffman M, Adams J, Schenkein DP, Anderson KC (2003) A phase 2 study of bortezomib in relapsed, refractory myeloma. N Engl J Med 348:2609-2617.

159.   Richardson PG, Briemberg H, Jagannath S, Wen PY, Barlogie B, Berenson J, Singhal S, Siegel DS, Irwin D, Schuster M, Srkalovic G, Alexanian R, Rajkumar SV, Limentani S, Alsina M, Orlowski RZ, Najarian K, Esseltine D, Anderson KC, Amato AA (2006) Frequency, characteristics, and reversibility of peripheral neuropathy during treatment of advanced multiple myeloma with bortezomib. J Clin Oncol 24: 3113-3120.

160.   Richardson PG, Sonneveld P, Schuster MW, Stadtmauer EA, Facon T, Harousseau JL, Ben-Yehuda D, Lonial S, Goldschmidt H, Reece D, Bladé J, Boccadoro M, Cavenagh JD, Boral AL, Esseltine DL, Wen PY, Amato AA, Anderson KC, San Miguel J (2009) Reversibility of symptomatic peripheral neuropathy with bortezomib in the phase III APEX trial in relapsed multiple myeloma: impact of a dose-modification guide. Br J Haematol 144:895-903.

161.   Richardson PG, Xie W, Mitsiades C, Chanan-Khan AA, Lonial S, Hassoun H, Avigan DE, Oaklander AL, Kuter DJ, Wen PY, Kesari S, Briemberg HR, Schlossman RL, Munshi NC, Heffner LT, Doss D, Esseltine DL, Weller E, Anderson KC, Amato AA (2009) Single-agent bortezomib in previously untreated multiple myeloma: efficacy, characterization of peripheral neuropathy, and molecular correlations with response and neuropathy. J Clin Oncol 27:3518-3525.

162.   Ringkamp M, Eschenfelder S, Grethel EJ, Häbler HJ, Meyer RA, Jänig W, Raja SN (1999) Lumbar sympathectomy failed to reverse mechanical allodynia- and hyperalgesia-like behavior in rats with L5 spinal nerve injury. Pain 79:143-153.

163.   Robinson CR, Zhang H, Dougherty PM (2014) Astrocytes, but not microglia, are activated in oxaliplatin and bortezomib-induced peripheral neuropathy in the rat. Neuroscience pii: S0306-4522(14)00459-X.

164.   Robinson CR, Zhang H, Dougherty PM (2014) Altered discharges of spinal neurons parallel the behavioral phenotype shown by rats with Bortezomib related

chemotherapy induced peripheral neuropathy. Brain Res pii: S0006-8993(14)00816-6.

165. Roccaro AM, Hideshima T, Raje N, Kumar S, Ishitsuka K, Yasui H, Shiraishi N, Ribatti D, Nico B, Vacca A, Dammacco F, Richardson PG, Anderson KC (2006) Bortezomib mediates antiangiogenesis in multiple myeloma via direct and indirect effects on endothelial cells. Cancer Res 66:184-191.

166. Roy Choudhury G, Ryou MG, Poteet E, Wen Y, He R, Sun F, Yuan F, Jin K, Yang SH (2014) Involvement of p38 MAPK in reactive astrogliosis induced by ischemic stroke. Brain Res 1551:45-58.

167. Rygh LJ, Svendsen F, Hole K, Tjølsen A (1999) Natural noxious stimulation can induce long-term increase of spinal nociceptive responses. Pain 82: 305-310.

168. Ryu JK, Franciosi S, Sattayaprasert P, Kim SU, McLarnon JG (2004) Minocycline inhibits neuronal death and glial activation induced by β-amyloid peptide in rat hippocampus. Glia 48:85-90.

169. Samuelsson C, Kumlien E, Flink R, Lindholm D, Ronne-Engström E (2000) Decreased cortical levels of astrocytic glutamate transport protein GLT-1 in a rat model of posttraumatic epilepsy. Neurosci Lett 289:185-188.

170. San Miguel JF, Schlag R, Khuageva NK, Dimopoulos MA, Shpilberg O, Kropff M, Spicka I, Petrucci MT, Palumbo A, Samoilova OS, Dmoszynska A, Abdulkadyrov KM, Schots R, Jiang B, Mateos MV, Anderson KC, Esseltine DL, Liu K, Cakana A, van de Velde H, Richardson PG, VISTA Trial Investigators

(2008) Bortezomib plus melphalan and prednisone for initial treatment of multiple myeloma. N Engl J Med 359: 906-917.

171.   Schreiber A, Peter M (2014) Substrate recognition in selective autophagy and the ubiquitin-proteasome system. Biochim Biophys Acta 1843:163-181.

172.   Seltzer Z, Dubner R, Shir Y (1990) A novel behavioral model of neuropathic pain disorders produced in rats by partial sciatic nerve injury. Pain 43:205-218.

173.   Shastri A, Bonifati DM, Kishore U (2013) Innate immunity and neuroinflammation. Mediators Inflamm 2013:342931.

174.   Shibasaki M, Sasaki M, Miura M, Mizukoshi K, Ueno H, Hashimoto S, Tanaka Y, Amaya F (2010) Induction of high mobility group box-1 in dorsal root ganglion contributes to pain sensitivity after peripheral nerve injury. Pain 149:514-521.

175.   Sivilotti L, Woolf CJ (1994) The contribution of GABAA and glycine receptors to central sensitization: disinhibition and touch-evoked allodynia in the spinal cord. J Neurophysiol 72:169-179.

176.   Smith C (2013) Review: the long-term consequences of microglial activation following acute traumatic brain injury. Neuropathol Appl Neurobiol 39:35-44.

177.   Solan JL, Lampe PD (2007) Key connexin43 phosphorylation events regulate the gap junction life cycle. J Membr Biol 217:35-41.

178.   Sotgiu ML, Biella G (2000) Contribution of central sensitization to the pain-related abnormal activity in neuropathic rats. Somatosens Mot Res 17:32-38.

179.   Spataro LE, Sloane EM, Milligan ED, Wieseler-Frank J, Schoeniger D, Jekich BM, Barrientos RM, Maier SF, Watkins LR (2004) Spinal gap junctions: potential involvement in pain facilitation. J Pain 5:392-405.

180. Stucky CL, Lewin GR (1999) Isolectin B(4)-positive and –negative nociceptors are functionally distinct. J Neurosci 19:6497-6505.

181. Sullivan KA, Lentz SI, Roberts JL Jr., Feldman EL (2008) Criteria for creating and assessing mouse models of diabetic neuropathy. Curr Drug Targets 9:3-13.

182. Sung B, Lim G, Mao J (2003) Altered expression and uptake activity of spinal glutamate transporters after nerve injury contribute to the pathogenesis of neuropathic pain rats. J Neurosci 23:2899-2910.

183. Sung CS, Cherng CH, Wen ZH, Chang WK, Huang SY, Lin SL, Chan KH, Wong CS (2012) Minocycline and fluorocitrate suppress spinal nociceptive signaling in intrathecal IL-1β-induced thermal hyperalgesic rats. Glia 60:2004-2017.

184. Tabernero A, Medina JM, Giaume C (2006) Glucose metabolism and proliferation in glia: role of astrocytic gap junctions. J Neurochem 99:1049-1061.

185. Teng YD, Choi H, Onario RC, Zhu S, Desilets FC, Lan S, Woodard EJ, Snyder EY, Eichler ME, Friedlander RM (2004) Minocycline inhibits contusion-triggered mitochondrial cytochrome c release and mitigates functional deficits after spinal cord injury. Proc Natl Acad Sci USA, 101:3071-3076.

186. Theis M, Giaume C (2012) Connexin-based intercellular communication and astrocyte heterogeneity. Brain Res 1487:88-98.

187. Thompson WL, Van Eldik LJ (2009) Inflammatory cytokines stimulate the chemokines CCL2/MCP-1 and CCL7/MCP-3 through NFkB and MAPK dependent pathways in rat astrocytes [corrected]. Brain Res 287:47-57.

188.   Treede RD, Jensen TS, Campbell JN, Cruccu G, Dostrovsky JO, Griffin JW, Hansson P, Hughes R, Nurmikko T, Serra J (2008) Neuropathic pain: redefinition and a grading system for clinical and research purposes. Neurology 70:1630-1635.

189.   Trevisan G, Materazzi S, Fusi C, Altomare A, Aldini G, Lodovici M, Patacchini R, Geppetti P, Nassini R (2013) Novel therapeutic strategy to prevent chemotherapy-induced persistent sensory neuropathy by TRPA1 blockade. Cancer Res 73:3120-3131.

190.   Vandenberg RJ, Ryan RM (2013) Mechanisms of glutamate transport. Physiol Rev 93:1621-1657.

191.   Vierck CJ Jr., Hamilton DM, Thornby JL (1971) Pain reactivity of monkeys after lesions to the dorsal and lateral columns of the spinal cord. Exp Brain Res 13:140-158.

192.   Voorhees PM, Dees EC, O'Neil B, Orlowski RZ (2003) The proteasome as a target for cancer therapy. Clin Cancer Res 9: 6316-6325.

193.   Wang RK, Zhang QQ, Pan YD, Guo QL (2013) Etanercept decreases HMGB1 expression in dorsal root ganglion neuron cells in a rat chronic constriction injury model. Exp Ther Med 5:581-585.

194.   Watkins LR, Milligan ED, Maier SF (2001) Spinal cord glia: new players in pain. Pain 93:201-205.

195.   Watkins LR, Maier SF (2003) Glia: a novel drug discovery target for clinical pain. Nat Rev Drug Discov 2:973-985.

196. Weng HR, Cordella JV, Dougherty PM (2003) Changes in sensory processing in the spinal dorsal horn accompany vincristine-induced hyperalgesia and allodynia. Pain 103:131-138.

197. Weng HR, Aravindan N, Cata JP, Chen JH, Shaw AD, Dougherty PM (2005) Spinal glial glutamate transporters downregulate in rats with taxol-induced hyperalgesia. Neurosci Lett 386:18-22.

198. Willenbrock S, Braun O, Baumgart J, Lange S, Junghanss C, Heisterkamp A, Nolte I, Bullerdiek J, Murua Escobar H (2012) TNF-α induced secretion of HMGB1 from non-immune canine mammary epithelial cells (MTH53A). Cytokine 57:210-220.

199. Wu A, Green CR, Rupenthal ID, Moalem-Taylor G (2012) Role of gap junctions in chronic pain. J Neurosci Res 90:337-345.

200. Wu XF, Liu WT, Liu YP, Huang ZJ, Zhang YK, Song XJ (2011) Reopening of ATP-sensitive potassium channels reduces neuropathic pain and regulates astroglial gap junctions in the rat spinal cord. Pain 152:2605-2615.

201. Xiao WH, Zheng H, Bennett GJ (2012) Characterization of oxaliplatin-induced chronic painful peripheral neuropathy in the rat and comparison with the neuropathy induced by paclitaxel. Neuroscience 203: 194-206.

202. Xin WJ, Weng HR, Dougherty PM (2009) Plasticity in expression of the glutamate transporters GLT-1 and GLAST in spinal dorsal horn glial cells following partial sciatic nerve ligation. Mol Pain 5:15.

203. Yakhnitsa V, Linderoth B, Meyerson BA (1999) Spinal cord stimulation attenuates dorsal horn neuronal hyperexcitability in a rat model of neuropathy. Pain 79:223-233.

204. Yezierski RP, Santana M, Park SH, Madsen PW (1993) Neuronal degeneration and spinal cavitation following intraspinal injections of quisqualic acid in the rat. J Neurotrauma 10:445-456.

205. Yi JH, Hazell AS (2006) Excitotoxic mechanisms and the role of astrocytic glutamate transporters in traumatic brain injury. Neurochem Int 48:394-403.

206. Yong VW, Wells J, Giuliani F, Casha S, Power C, Metz LM (2004) The promise of minocycline in neurology. Lancet Neurol 3:744-751.

207. Yoon SY, Robinson CR, Zhang H, Dougherty PM (2013) Spinal astrocyte gap junctions contribute to oxaliplatin-induced mechanical hypersensitivity. J Pain 14: 205-214.

208. Yrjänheikki J, Tikka T, Keinänen R, Goldsteins G, Chan PH, Koistinaho J (1999) A tetracycline derivative, minocycline, reduces inflammation and protects against focal cerebral ischemia with a wide therapeutic window. Proc Natl Acad Sci USA 96:13496-13500.

209. Zamoner A, Heimfarth L, Pessoa-Pureur R (2008) Congenital hypothyroidism is associated with intermediate filament misregulation, glutamate transporters down-regulation and MAPK activation in developing rat brain. Neurotoxicology 29:1092-1099.

210. Zemke D, Majid A (2004) The potential of minocycline for neuroprotection in human neurologic disease. Clin Neuropharmacol 27:293-298.

211.   Zeng Z, Lin J, Chen J (2013) Bortezomib for patients with previously untreated multiple myeloma: a systematic review and meta-analysis of randomized controlled trials. Ann Hematol 92:935-943.

212.   Zhang D, Hu X, Qian L, O'Callaghan JP, Hong JS (2010) Astrogliosis in CNS pathologies: is there a role for microglia? Mol Neurobiol 41:232-241.

213.   Zhang H, Xin W, Dougherty PM (2009) Synaptically evoked glutamate transporter currents in Spinal Dorsal Horn Astrocytes. Mol Pain 5:36.

214.   Zhang H, Yoon SY, Zhang H, Dougherty PM (2012) Evidence that spinal astrocytes but not microglia contribute to the pathogenesis of paclitaxel-induced painful neuropathy. J Pain 13: 293-393.

215.   Zhang H, Boyette-Davis JA, Kosturakis AK, Li Y, Yoon SY, Walters ET, Dougherty PM (2013) Induction of monocyte chemoattractant protein-1 (MCP-1) and its receptor CCR2 in primary sensory neurons contributes to paclitaxel-induced peripheral neuropathy. J Pain 14:1031-1044.

216.   Zhao H, Perez JS, Lu K, George AJ, Ma D (2014) Role of toll-like receptor-4 in renal graft ischemia-reperfusion injury. Am J Physiol Renal Physiol 306:F801-F811.

217.   Zheng FY, Xiao WH, Bennett GJ (2011) The response of spinal microglia to chemotherapy-evoked painful peripheral neropathies is distinct from that evoked by traumatic nerve injuries. Neuroscience 176:447-454.

218.   Zheng H, Xiao WH, and Bennett GJ (2012) Mitotoxicity and bortezomib-induced chronic painful peripheral neuropathy. Exp Neurol 238:225-234.

219.   Zhu X, Cao S, Zhu MD, Liu JQ, Chen JJ, Gao YJ (2014) Contribution of
       chemokine CCL2/CCR2 signaling in the dorsal root ganglion and spinal cord to
       the maintenance of neuropathic pain in a rat model of lumbar disc herniation. J
       Pain 15:516-526.

220.   Zhuang ZY, Kawasaki Y, Tan PH, Wen YR, Huang J, Ji RR (2007) Role of
       the CX3CR1/p38 MAPK pathway in spinal microglia for the development of
       neuropathic pain following nerve injury-induced cleavage of fractalkine. Brain
       Behav Immun 21:642-651.

VITA

Caleb Robert Robinson was born in Plano, TX on January 30, 1987 to Robert McCollum Robinson, Jr. and Pamela Jo Robinson. He and his older sister, Morgan, grew up in Katy, TX, where a majority of his family continues to reside. After graduating from James E. Taylor High School in 2005, he enrolled at Abilene Christian University the following fall. He graduated with his Bachelor of Science degree in 2009 with a major in Biology and minors in Chemistry and Bible, Missions, and Ministry. He then entered into his graduate studies at the University of Texas Graduate School of Biomedical Sciences in January of 2010. He currently resides in Katy, TX with his wife, Melissa Elizabeth Robinson.

Permanent Address:

1503 Leatherwood Dr.
Katy, TX 77450